frontiers | Research Topics

Genetic and environmental factors in the occurrence of paediatric disorders – volume II

Edited by
Wenhao Zhou, Maria Elisabetta Baldassarre and Mingbang Wang

Published in
Frontiers in Genetics
Frontiers in Pediatrics

ISSN 1664-8714
ISBN 978-2-8325-2806-8
DOI 10.3389/978-2-8325-2806-8

About Frontiers

Frontiers is more than just an open access publisher of scholarly articles: it is a pioneering approach to the world of academia, radically improving the way scholarly research is managed. The grand vision of Frontiers is a world where all people have an equal opportunity to seek, share and generate knowledge. Frontiers provides immediate and permanent online open access to all its publications, but this alone is not enough to realize our grand goals.

Frontiers journal series

The Frontiers journal series is a multi-tier and interdisciplinary set of open-access, online journals, promising a paradigm shift from the current review, selection and dissemination processes in academic publishing. All Frontiers journals are driven by researchers for researchers; therefore, they constitute a service to the scholarly community. At the same time, the *Frontiers journal series* operates on a revolutionary invention, the tiered publishing system, initially addressing specific communities of scholars, and gradually climbing up to broader public understanding, thus serving the interests of the lay society, too.

Dedication to quality

Each Frontiers article is a landmark of the highest quality, thanks to genuinely collaborative interactions between authors and review editors, who include some of the world's best academicians. Research must be certified by peers before entering a stream of knowledge that may eventually reach the public - and shape society; therefore, Frontiers only applies the most rigorous and unbiased reviews. Frontiers revolutionizes research publishing by freely delivering the most outstanding research, evaluated with no bias from both the academic and social point of view. By applying the most advanced information technologies, Frontiers is catapulting scholarly publishing into a new generation.

What are Frontiers Research Topics?

Frontiers Research Topics are very popular trademarks of the *Frontiers journals series*: they are collections of at least ten articles, all centered on a particular subject. With their unique mix of varied contributions from Original Research to Review Articles, Frontiers Research Topics unify the most influential researchers, the latest key findings and historical advances in a hot research area.

Find out more on how to host your own Frontiers Research Topic or contribute to one as an author by contacting the Frontiers editorial office: frontiersin.org/about/contact

Genetic and environmental factors in the occurrence of paediatric disorders – volume II

Topic editors

Wenhao Zhou — Fudan University, China

Maria Elisabetta Baldassarre — University of Bari Aldo Moro, Italy

Mingbang Wang — South China Hospital of Shenzhen University, China

Citation

Zhou, W., Baldassarre, M. E., Wang, M., eds. (2023). *Genetic and environmental factors in the occurrence of paediatric disorders – volume II*. Lausanne: Frontiers Media SA. doi: 10.3389/978-2-8325-2806-8

Table of contents

frontiers in Genetics

CASE REPORT
published: 24 February 2022
doi: 10.3389/fgene.2022.821226

Case Report: Biventricular Noncompaction Cardiomyopathy With Pulmonary Stenosis and Bradycardia in a Fetus With KCNH2 Mutation

Hairui Sun[1†], Xiaowei Liu[1†], Xiaoyan Hao[1†], Xiaoxue Zhou[1], Jingyi Wang[1], Jiancheng Han[1], Mengmeng Liang[2], Hongjia Zhang[3†] and Yihua He[1*]*

[1]Department of Echocardiography, Beijing Anzhen Hospital, Capital Medical University, Beijing, China, [2]Cipher Gene LLC, Beijing, China, [3]Department of Cardiac Surgery, Beijing Anzhen Hospital, Capital Medical University, Beijing, China

Background: Left ventricular noncompaction (LVNC) is a rare cardiomyopathy, long QT syndrome (LQTS) is a rare ion channel disease, and simultaneous occurrence of both is even rarer. Further clinical reports and studies are needed to identify the association between LVNC and LQTS and the underlying mechanism.

Methods and Results: A 26-year-old primigravida was referred at 25 weeks gestation for prenatal echocardiography due to fetal bradycardia detected during the routine ultrasound examination. The echocardiographic findings were consistent with biventricular noncompaction cardiomyopathy (BVNC) with pulmonary stenosis and suspected LQTS. After detailed counseling, the couple decided to terminate the pregnancy, and subsequent postmortem examination confirmed BVNC and pulmonary stenosis. Then, A trio (fetus and the parents) whole-exome sequencing (WES) and copy number variation sequencing (CNV-seq) were performed. CNV-seq identified no aneuploidy or pathogenic CNV. A *de novo* missense variant in KCNH2 (NM_000238.3:c.1847A > G,p.Tyr616Cys) was identified by WES. This KCNH2 missense mutation was classified as pathogenic according to the American College of Medical Genetics and Genomics and the Association for Molecular Pathology variant interpretation guidelines.

Conclusion: We report the first prenatal case of KCNH2 mutation presenting with LVNC combined with bradycardia and second-degree 2:1 atrioventricular block. Importantly, this case reminds clinicians to systematically search ion channel gene mutations in patients with LVNC and arrhythmia.

Keywords: left ventricular noncompaction, long QT syndrome, congenital heart disease, prenatal diagnosis, KCNH2 gene mutation

OPEN ACCESS

Edited by:
Rita Selvatici,
University of Ferrara, Italy

Reviewed by:
Seiko Ohno,
National Cerebral and Cardiovascular Center, Japan
Maria Paola Lombardi,
University of Amsterdam, Netherlands

***Correspondence:**
Hongjia Zhang
zhanghongjia722@hotmail.com
Yihua He
heyihuaecho@hotmail.com

[†]These authors have contributed equally to this work

Specialty section:
This article was submitted to Genetics of Common and Rare Diseases, a section of the journal Frontiers in Genetics

Received: *24 November 2021*
Accepted: *10 February 2022*
Published: *24 February 2022*

Citation:
Sun H, Liu X, Hao X, Zhou X, Wang J, Han J, Liang M, Zhang H and He Y (2022) Case Report: Biventricular Noncompaction Cardiomyopathy With Pulmonary Stenosis and Bradycardia in a Fetus With KCNH2 Mutation. Front. Genet. 13:821226. doi: 10.3389/fgene.2022.821226

INTRODUCTION

Left ventricular noncompaction (LVNC) is rare genetic cardiomyopathy (Towbin et al., 2015). Genes associated with LVNC usually include those encoding sarcomere, ion channels, nuclear envelope, and chaperone proteins. Many ion-channel genes, such as SCN5A, RYR2, KCNQ1, and HCN4, have been associated with LVNC, but the underlying molecular mechanisms are unknown (Milano et al., 2014; Nakashima et al., 2013; Schweizer et al., 2014; Towbin, 2014). KCNH2, and an ion-channel

gene, encodes the pore-forming subunit of a rapidly activating-delayed rectifier potassium channel that plays a critical role in the final repolarization of the ventricular action potential (Gianulis and Trudeau, 2011). Mutations in the KCNH2 gene cause long QT syndrome type 2 (LQTS2, MIM:613688) (Amin et al., 2008). The combination of LVNC with LQTS is scarce, and clinical reports of KCNH2 variants in such cases are even rarer. Due to the scarcity of clinical reports, LVNC has not been recognized as a feature of LQTS2. Here we report the first fetal case, to our knowledge, with KCNH2 mutation presenting with LVNC, LQTS, and sinus bradycardia. We also reviewed the literature to identify additional cases of KCNH2 mutation with LVNC-LQTS combined phenotype.

MATERIALS AND METHODS

Editorial Policies and Ethical Considerations

This study was approved by the Ethics Committee of Beijing Anzhen Hospital, Capital Medical University and adhered to the tenets of the Declaration of Helsinki. Informed written consent was obtained from the parents of the fetus.

Fetal Ultrasound and Echocardiography Examination

A complete fetal echocardiographic examination, including twodimensional (2D), M-mode, color, and pulse Doppler echocardiography, was performed using the General Electric Voluson E8 ultrasound system with transabdominal 2- to 4-MHz curvilinear transducers (GE Healthcare Ultrasound, Milwaukee, WI, United States) according to the American Society of Echocardiography guidelines and standards for performance of the fetal echocardiogram (Rychik et al., 2004).

Copy Number Variation Sequencing (CNV-Seq) and Whole-Exome Sequencing (WES)

Both CNV-seq and WES were done in the setting of a purely research-based protocol, and performed using methods as previously described on genomic DNA from the deceased fetus and the parents (Sun et al., 2019). Briefly, genomic DNA was extracted, hybridized and enriched for whole-exome sequencing. The captured libraries were sequenced using Illumina NovaSeq 6,000 (Illumina, Inc., San Diego, CA, United States). Then, the sequencing data were aligned to the human reference genome (hg38/GRCh38) using BWA (http://bio-bwa.sourceforge.net/) and PCR duplicates were removed by using Picard v1.57 (http://picard.sourceforge.net/). GATK (https://software.broadinstitute.org/gatk/) was applied for variant calling. ANNOVAR (http://wannovar.wglab.org/) was used for variant annotation and interpretation. We determined the frequency of each variant in the dbSNP150 (https://www.ncbi.nlm.nih.gov/snp/), 1,000 Genomes Project (http://www.internationalgenome.org/) and gnomAD (https://gnomad.broadinstitute.org/) to remove common SNPs (minor allele frequency >0.1%). Then, non-synonymous, splicing, frameshift and non-frameshift variants, as well as variants located in splice sites within 20 base pairs of an exon, were prioritized for evaluation. SIFT (http://sift.jcvi.org), PolyPhen-2 (http://genetics.bwh. harvard. edu/pph2), MutationTaster (http://www.mutation taster.org) and CADD (http://cadd.gs.washington.edu) were used to predict the pathogenicity of missense variants, while HSF (http://www.umd.be/HSF3/), and MatEntScan (Yeo and Burge, 2004) were used to evaluate the effects on splicing. Missense variants not presenting damaging results in any protein function prediction from SIFT, Polyphen2, MutationTaster, and CADD were excluded. Intronic variants not presenting damaging results in any prediction from HSF and MatEntScan were excluded. Pathogenicity of variants was determined according to current ACMG guidelines that recommend classifying variants into five categories: pathogenic, likely pathogenic, uncertain significance, likely benign or benign (Richards et al., 2015). Sanger sequencing was used to validate the presence of positive genetic results.

RESULTS

Clinical Phenotypes

A 26-year-old primigravida was referred at 25 weeks' gestation for prenatal echocardiography due to fetal bradycardia detected during the routine ultrasound examination. The woman was healthy with no significant family history and did not take any medication. Her anti-Ro/SSA and anti-La/SSB antibody status were both negative. She and her partner were non-consanguineous.

The fetal echocardiography identified noncompacted layers in both ventricles. An extensive trabeculated layer, with multiple deep intratrabecular recesses filled with blood directly from the ventricular cavity, was seen (**Figure 1A**). Moreover, a thickened, stenotic pulmonary valve was noted with a peak velocity of 158 cm/s shown by spectral Doppler (**Figure 1B**). There was fetal bradycardia; second-degree 2:1 atrioventricular block was seen by spectral Doppler and M-mode Echocardiography (**Figures 1C,D**). The fetal echocardiographic findings were consistent with biventricular noncompaction cardiomyopathy (BVNC) with pulmonary stenosis, second-degree 2:1 atrioventricular block, and sinus bradycardia.

At the time of the fetal diagnosis, the family was counseled about the potential overall poor prognosis for this fetus related to the BVNC with the second-degree atrioventricular block and pulmonary stenosis. Finally, the family decided to terminate the pregnancy and undergo genetic testing. The pregnancy was terminated at 26 weeks' gestation. Subsequent postmortem examination confirmed BVNC and pulmonary stenosis (**Figure 1E**).

Molecular Findings

A trio (fetus and the parents) CNV-seq and WES were performed to determine the underlying genetic cause of the fetal cardiac

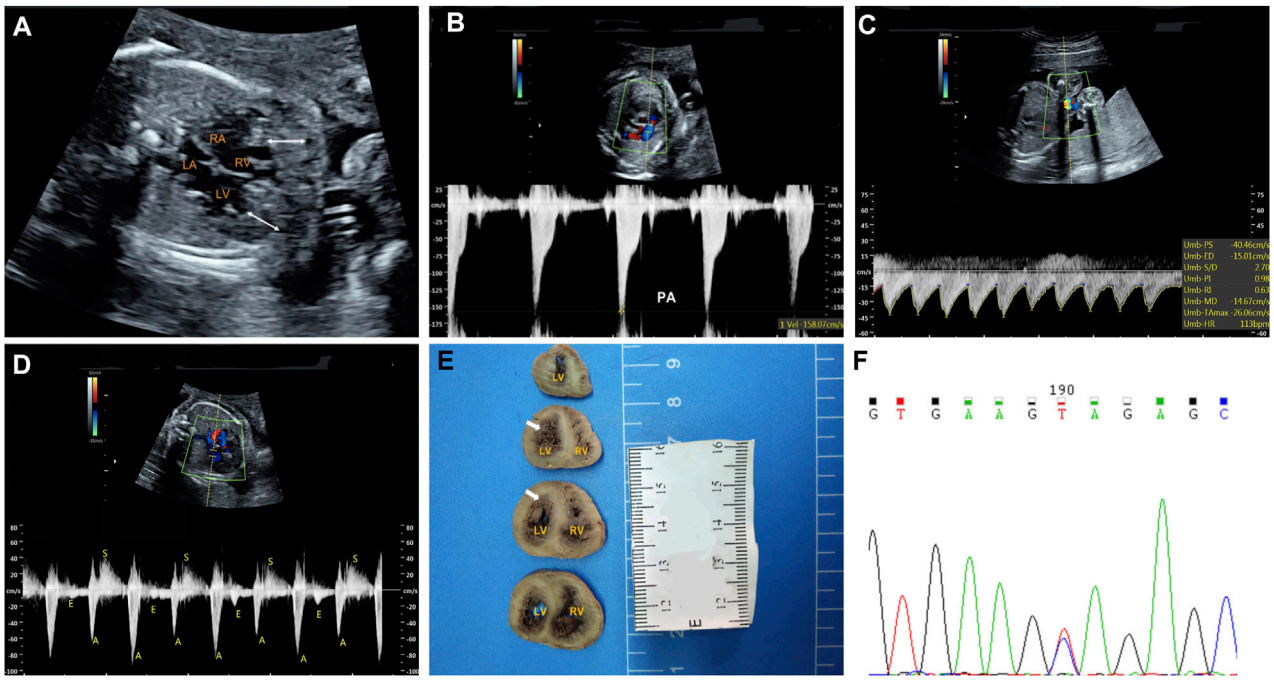

FIGURE 1 | Clinical phenotypes and molecular findings of the fetus. (**A–D**): Echocardiography of the fetus at 25 weeks' gestation. The phenotype includes biventricular noncompaction cardiomyopathy **(A)**, pulmonary stenosis **(B)**, sinus bradycardia **(C)** and second-degree 2:1 atrioventricular block (D). A. The area between the white arrows indicate numerous ventricular trabeculae **(C)**. Sinus bradycardia was seen with ventricular rate of 113 bpm by umbilical artery blood flow spectrum **(D)**. Mitral inflow and left ventricular outflow spectrum shows a 2:1 second-degree atrioventricular block **(E)**: Pathological anatomy shows that the noncompaction myocardium below the level of the left ventricular papillary muscle is obvious. The white arrows indicate the noncompaction myocardium **(F)**: Sanger sequencing shows that the mutation is heterozygous in the fetus. LA: left atrium; LV: left ventricle; RA: right atrium; RV: right ventricle.

phenotype. CNV-seq analysis identified no chromosomal abnormalities. The WES analysis initially identified 83,186 initial variants. The filtering cascades for WES data are listed in **Supplementary Table S1**. After four filters of the variants data for WES data, 91 variants were kept (**Supplementary Table S2**). Finally, we identified a *de novo* missense variant in KCNH2 (NM_000238.3:c.1847A > G,p.Tyr616Cys) in the fetus (**Figure 1F**), while no pathogenic variants in other known genes associated with cardiomyopathy or arrhythmias were identified. This KCHN2 variant was not found in the biggest general population database (gnomAD, https://gnomad.broadinstitute.org) and in-house control database and showed a deleterious effect by multiple in silico algorithms. The variant has been reported previously in several individuals with LQTS (Kapplinger et al., 2009; Ware et al., 2012), and ClinVar database (http://www.ncbi.nlm.nih.gov/clinvar) contains an entry for this variant (Variation ID: 67295). In addition, the Tyr616 is located in the intramembrane pore-forming H5 domain of KCNH2, and mutations at surrounding codons (Leu615Phe, Leu615Val, Ala614Val, and Thr613Met) have also been reported in association with LQTS, supporting the functional importance of this region of the protein. Furthermore, functional studies carried out by Anderson et al. (2014) demonstrate Tyr616Cys generated minimal current, suggesting altered channel permeability as a mechanism that leads to Prolonged QT interval. In conclusion, the variant is classified as pathogenic according to the 2015 American College of Medical Genetics and Genomics guidelines (Richards et al., 2015).

DISCUSSION

In this report we present the first fetal case with KCNH2 mutation presenting with BVNC, pulmonary stenosis, second-degree 2:1 atrioventricular block, and sinus bradycardia. LVNC is an increasingly recognized type of cardiomyopathy characterized by excessive trabeculation of the ventricles with deep intertrabecular recesses. While LVNC was classified as distinct cardiomyopathy by the American Heart Association (Maron et al., 2006), the European Society of Cardiology categorizes it as unclassified cardiomyopathy (Elliott et al., 2007). In the early fetal period, about 12 weeks, the myocardium is widely formed by trabeculae. These trabeculations undergo a compaction process, mainly finished before the 16–18 weeks of pregnancy (Faber et al., 2021; Finsterer et al., 2017). According to the non-compaction theory, LVNC results from the arrest of endomyocardial morphogenesis, leading to trabecular compaction failure (Hussein et al., 2015).

In the absence of a known family history, the diagnosis of fetal LQTS is based on the correct recognize of the signature rhythms, such as second-degree AVB, and sinus bradycardia. Second-degree AVB is the signature rhythm of LQTS in the perinatal period, and have been reported in about 25% of fetal LQTS cases (Horigome

et al., 2010; Mitchell et al., 2012). Sinus bradycardia is also a common manifestation of fetal LQTS, and has been reported in as many as 44–66% of fetuses diagnosed with LQTS (Cuneo et al., 2013; Greene et al., 2013; Horigome et al., 2010; Mitchell et al., 2012). In this fetus, a prenatal LQTS was highly suspected based on the following: second-degree AVB(Cuneo et al., 2013; Greene et al., 2013), sinus bradycardia (Cuneo et al., 2013; Greene et al., 2013; Mitchell et al., 2012), and the report of the same KCNH2 in several individuals with LQTS (Kapplinger et al., 2009; Ware et al., 2012). However, we were unable to make a definitive diagnosis because a QT prolongation was not proven.

Through systematic literature review, we identified several additional cases of KCNH2 mutation with LVNC-LQTS combined phenotype (AlSenaidi et al., 2014; Ogawa et al., 2009; Rammes et al., 2017). The first association between LVNC and KCNH2 mutations was described by Ogawa et al. (2009) reporting 2 unrelated individuals with isolated LVNC and LQTS carrying missense mutations in KCNH2. Subsequent AlSenaidi et al. (2014) reported a 5-year-old girl of consanguineous Oman parents carrying a KCNH2 homozygous frameshift mutation in association with phenotypes including LVNC, dilated ascending aorta and LQTS. Interestingly, both the parents of the girl carried this KCNH2 heterozygous mutation but neither presented with LVNC, indicating that LVNC is incomplete in LQTS patients with KCNH2 mutations. Recently, Rammes et al. (2017) also reported a familial case, in which both the proband and her son presented with LVNC, and LQTS carrying a published pathogenic variant in KCNH2. These increasing reports suggest that the coexistence of LVNC and arrhythmia may not be rare, significantly, as the detection rate of LVNC is gradually increasing with the advances of echocardiography and MRI.

Interestingly, KCNH2 mutations have also been reported in patients with isolated LVNC. Recent works of LVNC by the groups of Miszalski-Jamka and Wang have reported several individuals carrying KCNH2 mutations in association with LVNC(Miszalski-Jamka et al., 2017; Wang et al., 2017). Notably, no arrhythmia has been reported in these subjects. In addition, in the study by Wang et al. (2017), the number of rare variants in KCNH2 was significantly enriched in LVNC patients compared with the control group, further supporting the association between LVNC and KCNH2 mutation. In several recent independent LVNC cohorts, the variation burden of ion channel genes were as high as 8.8–14.7 (Hirono et al., 2020; Cambon-Viala et al., 2021; Miszalski-Jamka et al., 2017; Wang et al., 2017), significantly higher than in the general population. This suggests that ion-channel dysfunction may play a role in the pathogenesis of LVNC(Milano et al., 2014; Nakashima et al., 2013; Shan et al., 2008; Towbin, 2014). Although the exact mechanism is unclear, several hypotheses have been proposed. They suggest that direct protein-protein interaction between the ion channel gene products and the sarcomere may induce ventricular noncompaction or that ventricular noncompaction is an acquired adaptive remodeling feature in response to impaired conduction (Ergul et al., 2011; Brescia et al., 2013; Caliskan et al., 2012; Steffel and Duru, 2011; Zhang et al., 2013).

CONCLUSION

In summary, we present the first fetus with LVNC-LQTS combined phenotype and KCNH2 mutation. This case reminds clinicians that ion channel gene variants should be searched systematically in LVNC patients, especially in the arrhythmia phenotype.

DATA AVAILABILITY STATEMENT

The datasets for this article are not publicly available due to concerns regarding participant/patient anonymity. Requests to access the datasets should be directed to the corresponding author.

ETHICS STATEMENT

The studies involving human participants were reviewed and approved by the Ethics Committee of Beijing Anzhen Hospital, Capital Medical University. Written informed consent to participate in this study was provided by the participants' legal guardian/next of kin. Written informed consent was obtained from the individual(s), and minor(s)' legal guardian/next of kin, for the publication of any potentially identifiable images or data included in this article.

AUTHOR CONTRIBUTIONS

HZ and YH designed the study. XH, XZ, and JH collected the clinical data and samples from the family. HS and ML completed the experiments. HS and XL analyzed and interpreted the data. HS and XL wrote the manuscript. HS and XL contributed equally to this work. All authors read and approved the final manuscript.

FUNDING

This work was supported by the National Natural Science Foundation of China (No. 82170301 to YH), Beijing Advanced Innovation Center for Big Data-based Precision Medicine, Capital Medical University, Beijing, 100069, China (No. PXM 2021_014226_000026 to HZ) and Beijing Lab for Cardiovascular Precision Medicine, Beijing, China (No. PXM 2020_014226_000017_00377132_FCG to HZ).

SUPPLEMENTARY MATERIAL

The Supplementary Material for this article can be found online at: https://www.frontiersin.org/articles/10.3389/fgene.2022.821226/full#supplementary-material

REFERENCES

AlSenaidi, K. S., Wang, G., Zhang, L., Beer, D. A., AlFarqani, A. M., AlMaskaryi, S. N., et al. (2014). Long QT Syndrome, Cardiovascular Anomaly and Findings in ECG-Guided Genetic Testing. *IJC Heart & Vessels* 4, 122–128. doi:10.1016/j.ijchv.2014.06.001

Amin, A. S., Herfst, L. J., Delisle, B. P., Klemens, C. A., Rook, M. B., Bezzina, C. R., et al. (2008). Fever-induced QTc Prolongation and Ventricular Arrhythmias in Individuals with Type 2 Congenital Long QT Syndrome. *J. Clin. Invest.* 118 (7), 2552–2561. doi:10.1172/JCI35337

Anderson, C. L., Kuzmicki, C. E., Childs, R. R., Hintz, C. J., Delisle, B. P., and January, C. T. (2014). Large-scale Mutational Analysis of Kv11.1 Reveals Molecular Insights into Type 2 Long QT Syndrome. *Nat. Commun.* 5 (1), 5535. [Journal Article; Research Support, N.I.H., Extramural; Research Support, Non-U.S. Gov't]. doi:10.1038/ncomms6535

Brescia, S. T., Rossano, J. W., Pignatelli, R., Jefferies, J. L., Price, J. F., Decker, J. A., et al. (2013). Mortality and Sudden Death in Pediatric Left Ventricular Noncompaction in a Tertiary Referral center. *Circulation* 127 (22), 2202–2208. doi:10.1161/CIRCULATIONAHA.113.002511

Caliskan, K., Ujvari, B., Bauernfeind, T., Theuns, A.M.J. D., Akca, F., Akca, F, et al. (2012). The Prevalence of Early Repolarization in Patients with Noncompaction Cardiomyopathy Presenting with Malignant Ventricular Arrhythmias. *J. Cardiovasc. Electr.* 23 (9), 938–944. doi:10.1111/j.1540-8167.2012.02325.x

Cambon-Viala, M., Gerard, H., Nguyen, K., Richard, P., Ader, F., Pruny, J.-F., et al. (2021). Phenotype/Genotype Relationship in Left Ventricular Noncompaction: Ion Channel Gene Mutations Are Associated with Preserved Left Ventricular Systolic Function and Biventricular Noncompaction. *J. Card. Fail.* 27 (6), 677–681. doi:10.1016/j.cardfail.2021.01.007

Cuneo, B. F., Etheridge, S. P., Horigome, H., Sallee, D., Moon-Grady, A., Weng, H.-Y., et al. (2013). Arrhythmia Phenotype during Fetal Life Suggests Long-QT Syndrome Genotype. *Circ. Arrhythm Electrophysiol.* 6 (5), 946–951. doi:10.1161/CIRCEP.113.000618

Elliott, P., Andersson, B., Arbustini, E., Bilinska, Z., Cecchi, F., Charron, P., et al. (2007). Classification of the Cardiomyopathies: a Position Statement from the European Society of Cardiology Working Group on Myocardial and Pericardial Diseases. *Eur. Heart J.* 29 (2), 270–276. doi:10.1093/eurheartj/ehm342

Ergul, Y., Nisli, K., Varkal, M. A., Oner, N., Dursun, M., Dindar, A., et al. (2011). Electrocardiographic Findings at Initial Diagnosis in Children with Isolated Left Ventricular Noncompaction. *Ann. Noninvas. Electro.* 16 (2), 184–191. doi:10.1111/j.1542-474X.2011.00428.x

Faber, J. W., D'Silva, A., Christoffels, V. M., and Jensen, B. (2021). Lack of Morphometric Evidence for Ventricular Compaction in Humans. *J. Cardiol.* 78 (5), 397–405. doi:10.1016/j.jjcc.2021.03.006

Finsterer, J., Stöllberger, C., and Towbin, J. A. (2017). Left Ventricular Noncompaction Cardiomyopathy: Cardiac, Neuromuscular, and Genetic Factors. *Nat. Rev. Cardiol.* 14 (4), 224–237. doi:10.1038/nrcardio.2016.207

Gianulis, E. C., and Trudeau, M. C. (2011). Rescue of Aberrant Gating by a Genetically Encoded PAS (Per-Arnt-Sim) Domain in Several Long QT Syndrome Mutant Human Ether-Á-Go-Go-Related Gene Potassium Channels. *J. Biol. Chem.* 286 (25), 22160–22169. [Journal Article; Research Support, N.I.H., Extramural; Research Support, Non-U.S. Gov't]. doi:10.1074/jbc.M110.205948

Greene, E. A., Berul, C. I., and Donofrio, M. T. (2013). Prenatal Diagnosis of Long QT Syndrome: Implications for Delivery Room and Neonatal Management. *Cardiol. Young* 23 (1), 141–145. doi:10.1017/S1047951112000583

Hirono, K., Hata, Y., Miyao, N., Okabe, M., Takarada, S., Nakaoka, H., et al. (2020). Increased burden of Ion Channel Gene Variants Is Related to Distinct Phenotypes in Pediatric Patients with Left Ventricular Noncompaction. *Circ. Genom Precis Med.* 13 (4), e002940. doi:10.1161/CIRCGEN.119.002940

Horigome, H., Nagashima, M., Sumitomo, N., Yoshinaga, M., Ushinohama, H., Iwamoto, M., et al. (2010). Clinical Characteristics and Genetic Background of Congenital Long-QT Syndrome Diagnosed in Fetal, Neonatal, and Infantile Life. *Circ. Arrhythm Electrophysiol.* 3 (1), 10–17. doi:10.1161/CIRCEP.109.882159

Hussein, A., Karimianpour, A., Collier, P., and Krasuski, R. A. (2015). Isolated Noncompaction of the Left Ventricle in Adults. *J. Am. Coll. Cardiol.* 66 (5), 578–585. doi:10.1016/j.jacc.2015.06.017

Kapplinger, J. D., Tester, D. J., Salisbury, B. A., Carr, J. L., Harris-Kerr, C., Pollevick, G. D., et al. (2009). Spectrum and Prevalence of Mutations from the First 2,500 Consecutive Unrelated Patients Referred for the FAMILION Long QT Syndrome Genetic testResearch Support, Non-U.S. Gov't]. *[Journal ArticleHeart Rhythm* 6 (9), 1297–1303. doi:10.1016/j.hrthm.2009.05.021

Maron, B. J., Towbin, J. A., Thiene, G., Antzelevitch, C., Corrado, D., Arnett, D., et al. (2006). Contemporary Definitions and Classification of the Cardiomyopathies. *Circulation* 113 (14), 1807–1816. doi:10.1161/CIRCULATIONAHA.106.174287

Milano, A., Vermeer, A. M. C., Lodder, E. M., Barc, J., Verkerk, A. O., Postma, A. V., et al. (2014). HCN4 Mutations in Multiple Families with Bradycardia and Left Ventricular Noncompaction cardiomyopathyResearch Support, Non-U.S. Gov't]. *J. Am. Coll. CardiologyJ. Am. Coll. Cardiol.* 64 (8), 745–756. doi:10.1016/j.jacc.2014.05.045

Miszalski-Jamka, K., Jefferies, J. L., Mazur, W., Głowacki, J., Hu, J., Lazar, M., et al. (2017). Novel Genetic Triggers and Genotype-Phenotype Correlations in Patients with Left Ventricular Noncompaction. *Circ. Cardiovasc. Genetcirculation: Cardiovasc. Genet.* 10 (4). doi:10.1161/CIRCGENETICS.117.001763

Mitchell, J. L., Cuneo, B. F., Etheridge, S. P., Horigome, H., Weng, H.-Y., and Benson, D. W. (2012). Fetal Heart Rate Predictors of Long QT Syndrome. *Circulation* 126 (23), 2688–2695. doi:10.1161/CIRCULATIONAHA.112.114132

Nakashima, K., Kusakawa, I., Yamamoto, T., Hirabayashi, S., Hosoya, R., Shimizu, W., et al. (2013). A Left Ventricular Noncompaction in a Patient with Long QT Syndrome Caused by a KCNQ1 Mutation: A Case Report. *[Journal Article] Heart Vessels* 28 (1), 126–129. doi:10.1007/s00380-012-0235-8

Ogawa, K., Nakamura, Y., Terano, K., Ando, T., Hishitani, T., and Hoshino, K. (2009). Isolated Non-compaction of the Ventricular Myocardium Associated with Long QT Syndrome A Report of 2 Cases. *Circ. J.* 73 (11), 2169–2172. doi:10.1253/circj.cj-08-0339

Rammes, S., Farr, M., Laser, T., and Dubowy, K. O. (2017). Left Ventricular Noncompaction Cardiomyopathy and Long QT Syndrome, a Common Cause? A Case Report. *Thorac. Cardiovasc. Surg.* 65 (S 02), S111–S142. doi:10.1055/s-0037-1598992

Richards, S., Aziz, N., Bale, S., Bick, D., Das, S., Gastier-Foster, J., et al. (2015). Standards and Guidelines for the Interpretation of Sequence Variants: a Joint Consensus Recommendation of the American College of Medical Genetics and Genomics and the Association for Molecular Pathology. *Genet. Med.* 17 (5), 405–424. doi:10.1038/gim.2015.30

Rychik, J., Ayres, N., Cuneo, B., Gotteiner, N., Hornberger, L., Spevak, P. J., et al. (2004). American Society of Echocardiography Guidelines and Standards for Performance of the Fetal Echocardiogram. *J. Am. Soc. Echocardiography* 17 (7), 803–810. doi:10.1016/j.echo.2004.04.011

Schweizer, P. A., Schröter, J., Greiner, S., Haas, J., Yampolsky, P., Mereles, D., et al. (2014). The Symptom Complex of Familial Sinus Node Dysfunction and Myocardial Noncompaction Is Associated with Mutations in the HCN4 channelResearch Support, Non-U.S. Gov't]. *J. Am. Coll. CardiologyJ. Am. Coll. Cardiol.* 64 (8), 757–767. doi:10.1016/j.jacc.2014.06.1155

Shan, L., Makita, N., Xing, Y., Watanabe, S., Futatani, T., Ye, F., et al. (2008). SCN5A Variants in Japanese Patients with Left Ventricular Noncompaction and Arrhythmia. *Mol. Genet. Metab.* 93 (4), 468–474. doi:10.1016/j.ymgme.2007.10.009

Steffel, J., and Duru, F. (2011). Rhythm Disorders in Isolated Left Ventricular Noncompaction. *Ann. Med.* 44 (2), 101–108. doi:10.3109/07853890.2011.554427

Sun, H., Yi, T., Hao, X., Yan, H., Wang, J., Li, Q., et al. (2020). Contribution of Single-gene Defects to Congenital Cardiac Left-sided Lesions in the Prenatal Setting. *Ultrasound Obstet. Gynecol.* 56, 225–232. doi:10.1002/uog.21883

Towbin, J. A. (2014). Ion Channel Dysfunction Associated with Arrhythmia, Ventricular Noncompaction, and Mitral Valve Prolapse. *J. Am. Coll. Cardiol.* 64 (8), 768–771. doi:10.1016/j.jacc.2014.06.1154

Towbin, J. A., Lorts, A., and Jefferies, J. L. (2015). Left Ventricular Non-compaction Cardiomyopathy. *The Lancet* 386 (9995), 813–825. doi:10.1016/S0140-6736(14)61282-4

Wang, C., Hata, Y., Hirono, K., Takasaki, A., Ozawa, S. W., Nakaoka, H., et al. (2017). A Wide and Specific Spectrum of Genetic Variants and Genotype-Phenotype Correlations Revealed by Next-Generation Sequencing in Patients

with Left Ventricular Noncompaction. *Jaha* 6 (9). doi:10.1161/JAHA.117.006210

Ware, J. S., Walsh, R., Cunningham, F., Birney, E., and Cook, S. A. (2012). Paralogous Annotation of Disease-Causing Variants in Long QT Syndrome Genes. *Hum. Mutat.* 33 (8), 1188–1191. doi:10.1002/humu.22114

Yeo, G., and Burge, C. B. (2004). Maximum Entropy Modeling of Short Sequence Motifs with Applications to RNA Splicing Signals. *J. Comput. Biol.* 11 (2-3), 377–394. [Journal Article; Research Support, Non-U.S. Gov't; Research Support, U.S. Gov't, Non-P.H.S.; Research Support, U.S. Gov't, P.H.S.]. doi:10.1089/1066527041410418

Zhang, W., Chen, H., Qu, X., Chang, C.-P., and Shou, W. (2013). Molecular Mechanism of Ventricular Trabeculation/compaction and the Pathogenesis of the Left Ventricular Noncompaction Cardiomyopathy (LVNC). *Am. J. Med. Genet.* 163 (3), 144–156. Research Support, N.I.H., Extramural; Research Support, Non-U.S. Gov't; Review]. doi:10.1002/ajmg.c.31369

Conflict of Interest: Author ML was employed by Cipher Gene LLC.

The remaining authors declare that the research was conducted in the absence of any commercial or financial relationships that could be construed as a potential conflict of interest.

Publisher's Note: All claims expressed in this article are solely those of the authors and do not necessarily represent those of their affiliated organizations, or those of the publisher, the editors and the reviewers. Any product that may be evaluated in this article, or claim that may be made by its manufacturer, is not guaranteed or endorsed by the publisher.

frontiers | Frontiers in Genetics

CASE REPORT
published: 05 July 2022
doi: 10.3389/fgene.2022.924573

Case Report: Prenatal Whole-Exome Sequencing Identified a Novel Nonsense Mutation of the *KCNH2* Gene in a Fetus With Familial 2q14.2 Duplication

Jianlong Zhuang[1†], Chunnuan Chen[2†], Yuanbai Wang[1], Shuhong Zeng[1], Yu'e Chen[3], Yuying Jiang[1], Yingjun Xie[4,5] and Gaoxiong Wang[6]**

[1]Prenatal Diagnosis Center, Quanzhou Women's and Children's Hospital, Quanzhou, China, [2]Department of Neurology, The Second Affiliated Hospital of Fujian Medical University, Quanzhou, China, [3]Ultrasonography, Quanzhou Women's and Children's Hospital, Quanzhou, China, [4]Department of Obstetrics and Gynecology, Guangdong Provincial Key Laboratory of Major Obstetric Diseases, The Third Affiliated Hospital of Guangzhou Medical University, Guangzhou, China, [5]Key Laboratory of Reproduction and Genetics of Guangdong Higher Education Institutes, The Third Affiliated Hospital of Guangzhou Medical University, Guangzhou, China, [6]Quanzhou Women's and Children's Hospital, Quanzhou, China

OPEN ACCESS

Edited by:
Oscar Campuzano,
University of Girona, Spain

Reviewed by:
Ru Li,
Guangzhou Medical University, China
Monica Coll,
Institute of Biomedical Research of Girona, Spain

***Correspondence:**
Gaoxiong Wang
wanggaoxiong2013@163.com
Yingjun Xie
xieyjun@mail2.sysu.edu.cn

[†]These authors contributed equally to this work

Specialty section:
This article was submitted to Genetics of Common and Rare Diseases, a section of the journal Frontiers in Genetics

Received: 20 April 2022
Accepted: 24 May 2022
Published: 05 July 2022

Citation:
Zhuang J, Chen C, Wang Y, Zeng S, Chen Y, Jiang Y, Xie Y and Wang G (2022) Case Report: Prenatal Whole-Exome Sequencing Identified a Novel Nonsense Mutation of the KCNH2 Gene in a Fetus With Familial 2q14.2 Duplication. Front. Genet. 13:924573. doi: 10.3389/fgene.2022.924573

Background: Pathogenic mutations in the *KCNH2* gene were associated with long QT syndrome 2 (LQT2), which typically manifest in a prolonged QT interval and may lead to recurrent syncopes, seizure, or sudden death. Limited reports indicated that the *KCNH2* mutations would result in LQT2 combined with tetralogy of fallot. Our goal was to present an additional case of LQT2 combined with the tetralogy of fallot in a fetus with a novel *KCNH2* mutation.

Case presentation: Enrolled in this study was a 23-year-old pregnant woman from Quanzhou Fujian province, China. In her pregnancy, fetal ultrasound anomalies were identified, including tetralogy of fallot, coronary sinus enlargement, and persistent left superior vena cava. No chromosomal abnormality was detected by fetal karyotype analysis. However, 238.1-kb duplication in the 2q14.2 region containing the *GLI2* gene was observed in the fetus by chromosomal array analysis, which was inherited from the mother with normal clinical features and interpreted as a variant of uncertain significance (VOUS). Furthermore, whole-exome sequencing (WES) detection identified a novel nonsense c.1907C > G (p.S636*) mutation in the *KCNH2* gene in the fetus, and it was classified as a likely pathogenic variant, according to the ACMG guidelines. Parental verification analysis indicated that c.1907C > G (p.S636*) mutation was inherited from the mother.

Conclusion: In this study, we believe that 2q14.2 duplication may not be the reason for fetal heart defects; moreover, we described an additional case with *KCNH2* gene mutation, which may lead to LQTS and be associated with congenital heart defects. In addition, our study further confirms the application value of the WES technology in prenatal genetic etiology diagnosis of fetuses with structural anomalies and unexplained structural variants.

Keywords: chromosomal array analysis, *KCNH2*, tetralogy of fallot, LQTS, whole-exome sequencing

INTRODUCTION

Background

Microdeletions or microduplications in the 2q14.2 region are extremely rare variants, with approximately 10 case reports being available in the literature. The 2q14.2 microscopic deletions usually manifest phenotypic variability and incomplete penetrance; the clinical phenotypes are typically characterized as holoprosencephaly, abnormal pituitary gland formation and/or function, craniofacial dysmorphisms, branchial arch anomalies, and polydactyly (Kevelam et al., 2012; Kordaß et al., 2015; Elizabeth et al., 2020). Isolated 2q14.2 duplications are rarer with no defined specific syndrome. To the best of our knowledge, only one report was referred to 2q14.2 duplication, and it demonstrated that it may be responsible for microphthalmia/microcornea and congenital cataracts in an affected family (Schilter et al., 2013).

Congenital long QT syndrome (LQTS) is a genetic disorder that typically manifests arrhythmia of a prolonged QT interval and a risk of recurrent syncopes, seizures, or sudden death (Crotti et al., 2008; Hedley et al., 2009; Christiansen et al., 2014). A previous study indicated that LQTS showed a high incidence of approximately 1/2,500 in healthy live births (Schwartz et al., 2009). Among them, *KCNQ1*, *KCNH2* (*HERG*), and *SCN5A* are the three most frequently affected genes, which would lead to LQT1, LQT2, and LQT3, respectively. The main mutation types in LQT2 are nonsense mutation and missense mutation, with more than half of them being nonsense mutations and predict to result in haploinsufficiency through nonsense-mediated RNA decay (Ono et al., 2020). At present, no specific forms of congenital heart defects (CHD) have been reported to associate with LQT2, while several cases with *KCNH2* mutations showed coexistence of CHD (Bhuiyan et al., 2014; Ebrahim et al., 2017; Song et al., 2018).

In this study, the whole-exome sequencing (WES) technology was first employed for further prenatal diagnosis in a fetus who harbored familial 2q14.2 duplication and exhibited fetal congenital heart defects including tetralogy of fallot. In addition, our study further strengthened the application value of the WES technology in genetic etiology of fetuses with structural anomalies and unexplained copy number variants.

CASE PRESENTATION

A 23-year-old Chinese pregnant woman, gravida 1, para 0, from Quanzhou Fujian province, was enrolled in this study. Her husband was 29 years old, and they denied consanguinity marriage and had a family history of inherited disease. In this pregnancy, low progesterone was observed in the first trimester and was treated with didroxyprogesterone. No obvious abnormality was found by ultrasound examination during her first-trimester pregnancy, with a normal nuchal translucency (0.7 mm). In the second trimester, a low-risk screening result was detected by Down's screening. However, at the gestational age of 23^{+2} weeks, three-level color Doppler ultrasound examination results revealed abnormal heart defects in the fetus, including tetralogy of fallot (ventricular septal defect, overriding aorta, and pulmonary artery stenosis), coronary sinus enlargement, and persistent left superior vena cava (**Figure 1**). Amniocentesis was performed at the gestational age of 25^{+5} weeks, after sufficient genetic consultation.

No obvious chromosomal abnormality was detected in the fetus by karyotype analysis, and her parents showed normal karyotypes as well. However, chromosomal array analysis (CMA) results demonstrated a 238.1-kb duplication in the 2q14.2 region ([GRCh37]2q14.2 (121,477,769–121,715,896)x3) in the fetus containing the *GLI2* gene (OMIM:165230). According to the ACMG guidelines, the 2q14.2 duplication was interpreted as variants of uncertain significance. Parental CMA verification demonstrated that the 2q14.2 duplication was inherited from the mother who exhibited normal clinical features.

WES technology was carried out to look for additional variants in the fetus with unexplained structural variants of 2q14.2 duplication. A novel nonsense mutation of c.1907C > G (p.S636*) in the *KCNH2* gene was identified in the fetus by WES technology, which was inherited from the mother and further confirmed by Sanger sequencing (**Figure 2**). No frequency was found in the databases of gnomAD, 1,000 genomes, dbSNP, and ExAC. In addition, several computer-aided analysis software applications predicted that this variation may affect the protein structure/function (MetaSVM_score: 0.717; GERP++_RS: 5.14; dbscSNV_ADA: 0; dbscSNV_RF: 0). According to the ACMG Guidelines (Richards et al., 2015), the nonsense mutation was interpreted as a likely pathogenic variant (PVS1, PM2_Supporting). At present, no obvious cardiac abnormality was observed in the pregnant woman by electrocardiogram and echocardiography. Finally, the family chose to terminate her pregnancy at a gestational age of 30 weeks.

DISCUSSION AND CONCLUSION

With the advanced application of the CMA technology, an increasing rate of variants of uncertain significance (VOUS) and variants with phenotypical diversity may be followed, which will result in a big challenge for genetic consultation. The WES technology showed a great effectiveness in genetic etiology diagnosis in patients at the single-gene level, while few studies were available to further reveal the phenotypical diversity of unexplained structure variants using WES technology. Additional mutations besides the structural variants were identified by WES detection in patients with familial 1q21.1 microduplication/microdeletion, duplication of Xp22.31, and 16p11.2 duplication who exhibited phenotypical variability (Dastan et al., 2016; Qiao et al., 2017; Qiao et al., 2019). In addition, a recent study conducted by Granata et al. (2022) identified variants in *CECR2*, *MTOR*, *RICTOR,* and *LRRK2* genes by WES detection in the affected patients who also had a 16p13.11 microdeletion and proposed that WES technology could be used as a fundamental tool to identify additional mutations in patients with a predisposing variant. In this study, the WES technology was employed to further

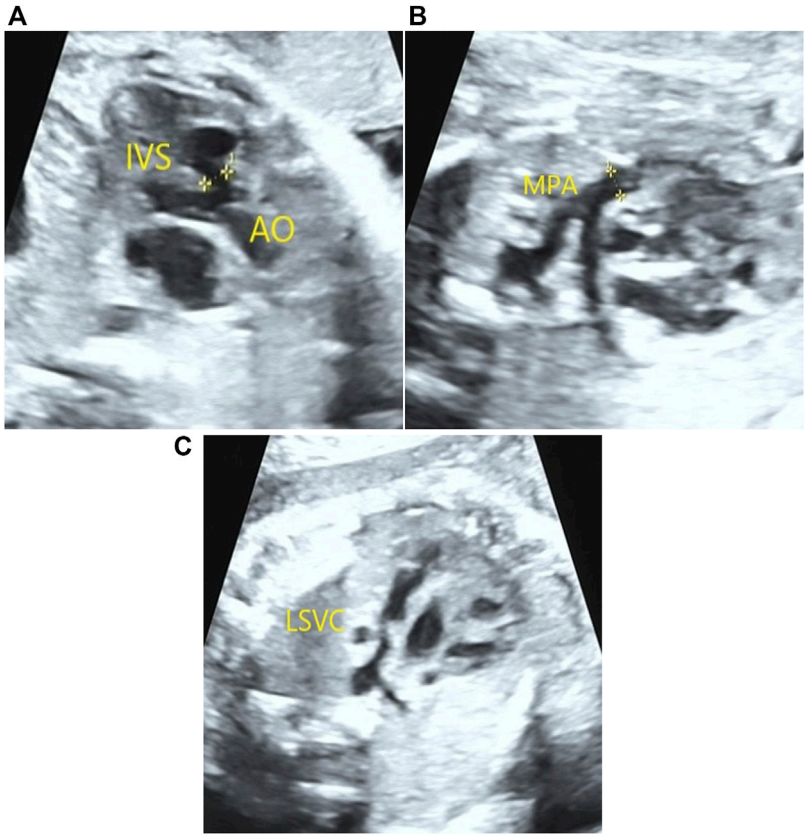

FIGURE 1 | Congenital heart defects detected in the fetus by prenatal ultrasound examination. A 0.41-cm ventricular septal defect and overriding aorta **(A)** were detected in the fetus by prenatal ultrasound examination. In addition, pulmonary artery stenosis **(B)** and persistent left superior vena cava **(C)** were also observed.

investigate the genetic etiology in a fetus with familial 2q14.2 duplication who had more severe phenotypes.

In the present study, a 238.1-kb duplication in the 2q14.2 region was identified in the fetus, which was inherited from her mother with a normal phenotype. As shown in the DECIPHER database and listed in **Table 1**, all small fragments of 2q14.2 duplication were interpreted as VOUS without specific syndrome. In addition, as elicited in the ClinGen database, the dosage sensitivity of *GLI2* gene indicated sufficient evidence of haploinsufficiency (3) but without triplosensitivity evidence (0). In addition, a patient harbored both 2q14.1q14.2 duplication and 2q37.3 deletion and exhibited autism, while the authors believed that the clinical phenotype may ascribe to 2q37.3 deletion (Devillard et al., 2010). In this study, we believe that the 2q14.2 duplication may not contribute to the ultrasonic abnormalities in the fetus. However, a previous study indicated that 2q14.2 duplication was co-segregated with microphthalmia/microcornea and congenital cataracts in an affected family and suggested that the 2q14.2 duplication may be the reason for the clinical features (Schilter et al., 2013). Nevertheless, no obvious ocular abnormalities were observed in our study, and the congenital heart defects including tetralogy of fallot in the fetus were hard to be explained by 2q14.2 duplication.

Further WES detection revealed a novel nonsense mutation of c.1907C > G (p.S636*) in the *KCNH2* gene in the fetus, which was interpreted as a likely pathogenic variant. In addition, no pathogenic or uncertain variants in the known genes that referred to CHD features were identified in the fetus. *KCNH2* encodes the pore-forming subunit of a rapidly activating delayed rectifier potassium channel; loss-of-function mutations in the *KCHN2* gene would lead to LQT2 (Gianulis and Trudeau, 2011). As delineated by previous studies, several patients diagnosed with long QT syndrome are also accompanied by congenital heart defects (Massin et al., 2010; Hsiao et al., 2007; Wu et al., 1999). The study conducted by Murugan et al. (2005) presented a family with LQTS and coexisting persistent patency of the arterial duct, and they proposed that it may not be a coincidence, and hypothesis about a possible genetic mechanism may exist. In addition, a new form of LQTS was indicated in three patients who also had LQTS and associated with structural heart disease and syndactyly (Marks et al., 1995). Moreover, a previous study (Ebrahim et al., 2017) presented 11 patients who harbored single-gene mutations that resulted in long QT syndrome, combined with congenital heart defects. Among them, four patients carried *KCNQ1* gene mutation, and one patient had a *KCNQ1* mutation associated with *KCNH2* mutation. Most of them (six cases) had *KCNH2* mutations, of which two cases had

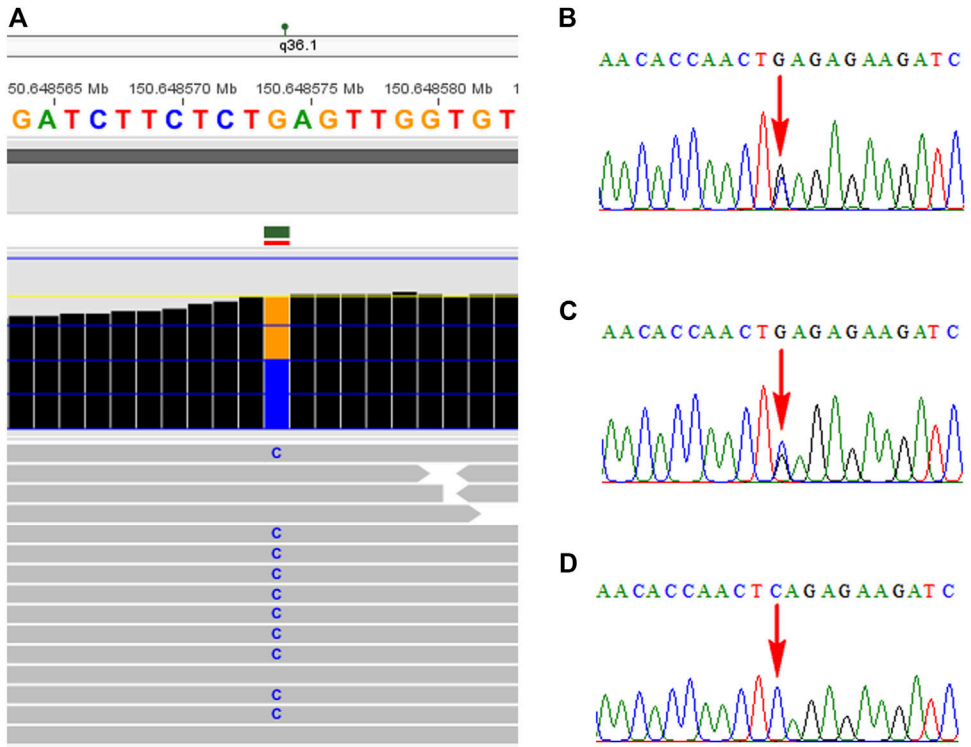

FIGURE 2 | Identification of the *KCNH2* mutation in the family using the WES technology and Sanger sequencing. **(A)** Novel nonsense mutation in the *KCNH2* gene was identified in the fetus by WES. **(B)** Mutation of c.1907C > G was confirmed by Sanger sequencing. Parental Sanger sequencing revealed that her mother carried the same mutation **(C),** while the mutation was not found in her father **(D)**.

TABLE 1 | Cases with less than 1.0-Mb duplications in the 2q14.2 region are presented in the DECIPHER database.

DECIPHER Patients	Sex	Location (GRCh38)	Size (kb)	Inheritance	Pathogenicity	Phenotype
404183	46,XX	2: 120793535–120842777	49.24	Unknown	Uncertain	NM
300369	NM	2: 120842718–121028767	186.05	Maternally	Uncertain	Cognitive impairment and generalized hypotonia
383370	46,XX	2: 120102148–120751795	649.65	Unknown	Uncertain	Abnormal lateral ventricle morphology, abnormal third ventricle morphology, autism, delayed speech and language development, scoliosis, and thick corpus callosum
384452	46,XY	2: 120113202–120975414	862.21	Unknown	Uncertain	Behavioral abnormality
Our case	46,XX	2: 120720193–120958320	238.1	Maternally	Uncertain	Tetralogy of fallot, coronary sinus enlargement, and persistent left superior vena cava

NM: not mentioned.

tetralogy of fallot (TOF) (Ebrahim et al., 2017). In addition, patients with *KCNH2* mutations who had LQTS combined with tetralogy of fallot (TOF) are summarized in **Table 2**. In the present study, the fetus had a novel *KCNH2* mutation and manifested congenital heart defects including TOF, which further enhanced the genotype–phenotype correlation.

In addition, the *KCNH2* mutation in the fetus was inherited from her mother, who had no obvious cardiac phenotype. Similar to a previous study (Bhuiyan et al., 2014), two sisters in a close relative married family were found to carry the *KCNH2* mutation, which was also inherited from their normal mother, which suggests incomplete penetrance of *KCNH2*, although it cannot be ruled out that the phenotype may appear in her mother in the future. Therefore, our study indicated that the additional variant in the *KCNH2* gene identified in the fetus may be responsible for fetal ultrasound anomalies, rather than the 2q14.2 duplication. The fetus is likely to harbor a LQT2; unfortunately, a fetal electrocardiogram *in utero* was not available in this study, and whether the fetus has a prolonged QT interval is unknown. Moreover, the nonsense mutation of the *KCNH2* gene

TABLE 2 | *KCNH2* mutations in patients who had LQTS combined with tetralogy of fallot in the literature.

	(Ebrahim et al., 2017)		(Bhuiyan et al., 2014)		(Chiu et al., 2012)		Our case
	Patient 3	Patient 11	Sister 1	Sister 2	Case 1	Case 2	
Sex/Age	NA	NA	F/13	F/11	M/NA	F/NA	F/Fetus
Genes	KCNH2	KCNH2	KCNH2	KCNH2	KCNH2/SCN5A	KCNH2/SCN5A	KCNH2
Mutations	G1036_ L1042del	G572S	p.[(V172M); (R293C)]	p.[(V172M); (R293C)]	p.M645R/p.R1193Q	p.M645R/p.R1193Q	p.S636*
CHD	TOF	TOF	TOF	TOF	TOF	TOF	TOF
QTc (ms)	635	510	450	NA	581	641	NA
Inheritance	NA	NA	Maternal	Maternal	NA	NA	Maternal

NA: not available; F: female; M: male; CHD: congenital heart defects; TOF: tetralogy of fallot.

identified in the fetus is classified as a secondary finding, according to the ACMG secondary finding v3.0 list; no sufficient evidence was available to reveal the causal relationship between *KCNH2* mutations and CHD so far. Thus, more work needs to be conducted to clarify the existence of a genetic mechanism or if it was just a coincidence between *KCNH2* mutations and CHD.

In conclusion, our study described an additional case of LQT2 combined with tetralogy of fallot in a fetus with a *KCNH2* mutation. In addition, our study enriched the mutation spectrum of the *KCNH2* gene and further indicated the application value of WES in prenatal diagnosis in fetuses with familial uncertain copy number variants.

DATA AVAILABILITY STATEMENT

The datasets for this article are not publicly available due to concerns regarding participant/patient anonymity. Requests to access the datasets should be directed to the corresponding author.

ETHICS STATEMENT

The studies involving human participants were reviewed and approved by Ethics Committee, and the approval was obtained from the Institutional Ethics Committee of Quanzhou women's and children's hospital to the commencement of the study (2020No.31). The patients/participants provided their written informed consent to participate in this study. Written informed consent was obtained from the individual(s) for the publication of any potentially identifiable images or data included in this article.

AUTHOR CONTRIBUTIONS

JZ designed the article; JZ and CC wrote the article; YC and YJ recruited the participants and performed clinical consultation; YW and SZ performed the karyotype analysis and analyzed the data; GW, and YX revised and published the article. All authors approved the final article.

FUNDING

This research was supported by the Fujian Provincial Health Commission Youth Science and Technology Program (2020QNB045) and the Quanzhou City Science and Technology Program (2020C026R).

ACKNOWLEDGMENTS

We wish to express our appreciation to the Fujian Provincial Health Commission and Quanzhou Science and Technology Bureau for funding this work. We also express our appreciation to the patients who participated in this study.

REFERENCES

Bhuiyan, Z. A., Alswaid, A., Belfiore, M., Al-Ghamdi, S. S., Liang, J., and Schlaepffer, J. (2014). Not all Pathogenic Mutations Are Pathogenic: KCNH2 Mutations in Two Sisters with Tetralogy of Fallot. *Int. J. Cardiol.* 172 (1), 276–277. doi:10.1016/j.ijcard.2013.12.242

Chiu, S.-N., Wu, M.-H., Su, M.-J., Wang, J.-K., Lin, M.-T., Chang, C.-C., et al. (2012). Coexisting Mutations/polymorphisms of the Long QT Syndrome Genes in Patients with Repaired Tetralogy of Fallot Are Associated with the Risks of Life-Threatening Events. *Hum. Genet.* 131 (8), 1295–1304. doi:10.1007/s00439-012-1156-4

Christiansen, M., Hedley, P. L., Theilade, J., Stoevring, B., Leren, T. P., Eschen, O., et al. (2014). Mutations in Danish Patients with Long QT Syndrome and the Identification of a Large Founder Family with p.F29L in KCNH2. *BMC Med. Genet.* 15, 31. doi:10.1186/1471-2350-15-31

Crotti, L., Celano, G., Dagradi, F., and Schwartz, P. J. (2008). Congenital Long QT Syndrome. *Orphanet J. Rare Dis.* 3, 18. doi:10.1186/1750-1172-3-18

Dastan, J., Chijiwa, C., Tang, F., Martell, S., Qiao, Y., Rajcan-Separovic, E., et al. (2016). Exome Sequencing Identifies Pathogenic Variants of VPS13B in a Patient with Familial 16p11.2 Duplication. *BMC Med. Genet.* 17 (1), 78. doi:10.1186/s12881-016-0340-0

Devillard, F., Guinchat, V., Moreno-De-Luca, D., Tabet, A.-C., Gruchy, N., Guillem, P., et al. (2010). Paracentric Inversion of Chromosome 2 Associated with Cryptic Duplication of 2q14 and Deletion of 2q37 in a Patient with Autism. *Am. J. Med. Genet.* 152A (9), 2346–2354. doi:10.1002/ajmg.a.33601

Ebrahim, M. A., Williams, M. R., Shepard, S., and Perry, J. C. (2017). Genotype Positive Long QT Syndrome in Patients with Coexisting Congenital Heart Disease. *Am. J. Cardiol.* 120 (2), 256–261. doi:10.1016/j.amjcard.2017.04.018

Elizabeth, M. S. M., Verkerk, A. J. M. H., Hokken-Koelega, A. C. S., Verlouw, J. A. M., Argente, J., Pfaeffle, R., et al. (2020). Unique Near-Complete Deletion of GLI2 in a

Patient with Combined Pituitary Hormone Deficiency and Post-axial Polydactyly. *Growth Hormone IGF Res.* 50, 35–41. doi:10.1016/j.ghir.2019.10.002

Gianulis, E. C., and Trudeau, M. C. (2011). Rescue of Aberrant Gating by a Genetically Encoded PAS (Per-Arnt-Sim) Domain in Several Long QT Syndrome Mutant Human Ether-Á-Go-Go-Related Gene Potassium Channels. *J. Biol. Chem.* 286 (25), 22160–22169. doi:10.1074/jbc.m110.205948

Granata, P., Cocciadiferro, D., Zito, A., Pessina, C., Bassani, A., Zambonin, F., et al. (2022). Whole Exome Sequencing in 16p13.11 Microdeletion Patients Reveals New Variants through Deductive and Systems Medicine Approaches. *Front. Genet.* 13, 798607. doi:10.3389/fgene.2022.798607

Hedley, P. L., Jørgensen, P., Schlamowitz, S., Wangari, R., Moolman-Smook, J., Brink, P. A., et al. (2009). The Genetic Basis of Long QT and Short QT Syndromes: a Mutation Update. *Hum. Mutat.* 30 (11), 1486–1511. doi:10.1002/humu.21106

Hsiao, S.-M., Wu, M.-H., Jou, H.-J., Lee, C.-N., Shyu, M.-K., Shih, J.-C., et al. (2007). Outcome for Fetuses with Prenatally Detected Congenital Heart Disease and Cardiac Arrhythmias in Taiwan. *J. Formos. Med. Assoc.* 106 (6), 423–431. doi:10.1016/s0929-6646(09)60291-6

Kevelam, S. H. G., van Harssel, J. J. T., van der Zwaag, B., Smeets, H. J. M., Paulussen, A. D. C., and Lichtenbelt, K. D. (2012). A Patient with a Mild Holoprosencephaly Spectrum Phenotype and Heterotaxy and a 1.3 Mb Deletion Encompassing GLI2. *Am. J. Med. Genet.* 158A (1), 166–173. doi:10.1002/ajmg.a.34350

Kordaß, U., Schröder, C., Elbracht, M., Soellner, L., and Eggermann, T. (2015). A familialGLI2deletion (2q14.2) Not Associated with the Holoprosencephaly Syndrome Phenotype. *Am. J. Med. Genet.* 167 (5), 1121–1124. doi:10.1002/ajmg.a.36972

Marks, M. L., Whisler, S. L., Clericuzio, C., and Keating, M. (1995). A New Form of Long QT Syndrome Associated with Syndactyly. *J. Am. Coll. Cardiol.* 25 (1), 59–64. doi:10.1016/0735-1097(94)00318-k

Massin, M. M., Dessy, H., Malekzadeh-Milani, S. G., Van Aerschot, I., and Verbeet, T. (2010). Prevalence of Preoperative Arrhythmias in Children with Delayed Treatment of Severe Congenital Heart Disease. *Acta Cardiol.* 65 (1), 37–42. doi:10.2143/ac.65.1.2045887

Murugan, S. J., Parsons, J. M., and Bennett, C. (2005). A Case of Long QT Syndrome Associated with Familial Occurrence of Persistent Patency of the Arterial Duct. *Cardiol. Young* 15 (3), 309–311. doi:10.1017/s1047951105000648

Ono, M., Burgess, D. E., Schroder, E. A., Elayi, C. S., Anderson, C. L., January, C. T., et al. (2020). Long QT Syndrome Type 2: Emerging Strategies for Correcting Class 2 *KCNH2* (*hERG*) Mutations and Identifying New Patients. *Biomolecules* 10 (8), 1144. doi:10.3390/biom10081144

Qiao, Y., Badduke, C., Tang, F., Cowieson, D., Martell, S., Lewis, S. M. E., et al. (2017). Whole Exome Sequencing of Families with 1q21.1 Microdeletion or Microduplication. *Am. J. Med. Genet.* 173 (7), 1782–1791. doi:10.1002/ajmg.a.38247

Qiao, Y., Bagheri, H., Tang, F., Badduke, C., Martell, S., Lewis, S. M. E., et al. (2019). Exome Sequencing Identified a De Novo Mutation of PURA Gene in a Patient with Familial Xp22.31 Microduplication. *Eur. J. Med. Genet.* 62 (2), 103–108. doi:10.1016/j.ejmg.2018.06.010

Richards, S., Aziz, N., Bale, S., Bick, D., Das, S., Gastier-Foster, J., et al. (2015). Standards and Guidelines for the Interpretation of Sequence Variants: a Joint Consensus Recommendation of the American College of Medical Genetics and Genomics and the Association for Molecular Pathology. *Genet. Med.* 17 (5), 405–424. doi:10.1038/gim.2015.30

Schilter, K., Reis, L., Schneider, A., Bardakjian, T., Abdul-Rahman, O., Kozel, B., et al. (2013). Whole-genome Copy Number Variation Analysis in Anophthalmia and Microphthalmia. *Clin. Genet.* 84 (5), 473–481. doi:10.1111/cge.12202

Schwartz, P. J., Stramba-Badiale, M., Crotti, L., Pedrazzini, M., Besana, A., Bosi, G., et al. (2009). Prevalence of the Congenital Long-QT Syndrome. *Circulation* 120 (18), 1761–1767. doi:10.1161/circulationaha.109.863209

Song, M. K., Bae, E. J., Kim, G. B., An, H. S., Ahn, K. J., Seong, M.-W., et al. (2018). Patients Diagnosed with Long QT Syndrome after Repair of Congenital Heart Disease. *Pacing Clin. Electrophysiol.* 41 (11), 1435–1440. doi:10.1111/pace.13512

Wu, M.-H., Hsieh, F.-C., Wang, J.-K., and Kau, M.-L. (1999). A Variant of Long QT Syndrome Manifested as Fetal Tachycardia and Associated with Ventricular Septal Defect. *Heart* 82 (3), 386–388. doi:10.1136/hrt.82.3.386

Conflict of Interest: The authors declare that the research was conducted in the absence of any commercial or financial relationships that could be construed as a potential conflict of interest.

The reviewer RL declared a shared parent affiliation with the author YX to the handling editor at the time of review.

Publisher's Note: All claims expressed in this article are solely those of the authors and do not necessarily represent those of their affiliated organizations, or those of the publisher, the editors, and the reviewers. Any product that may be evaluated in this article, or claim that may be made by its manufacturer, is not guaranteed or endorsed by the publisher.

frontiers | Frontiers in Genetics

CASE REPORT
published: 08 July 2022
doi: 10.3389/fgene.2022.920950

Perthes Disease in a Child With Osteogenesis Imperfecta From a Rare Genetic Variant: A Case Report

Pan Hong[1†], Xiaolong Zhao[2†], Ruikang Liu[3†], Saroj Rai[4], Yingying Song[5], Ruijing Xu[1] and Jin Li[1]**

[1]Department of Orthopaedic Surgery, Union Hospital, Tongji Medical College, Huazhong University of Science and Technology, Wuhan, China, [2]Department of Orthopaedics, First Hospital of Wuhan, Wuhan, China, [3]Department of Endocrinology, Union Hospital, Tongji Medical College, Huazhong University of Science and Technology, Wuhan, China, [4]Department of Orthopaedics and Trauma Surgery, Karama Medical Center, Dubai, United Arab Emirates, [5]Medical Department of Hubei University of Science and Technology, Xianning, China

OPEN ACCESS

Edited by:
Fan Jin,
Zhejiang University, China

Reviewed by:
Silvia Izquierdo Alvarez,
Hospital Universitario Miguel Servet, Spain
Hao Zhang,
Shanghai Jiao Tong University, China

***Correspondence:**
Ruijing Xu
xuruijing99@163.com
Jin Li
lijin2003whxh@foxmail.com

†These authors have contributed equally to this work and share first authorship

Specialty section:
This article was submitted to Genetics of Common and Rare Diseases, a section of the journal Frontiers in Genetics

Received: 15 April 2022
Accepted: 06 June 2022
Published: 08 July 2022

Citation:
Hong P, Zhao X, Liu R, Rai S, Song Y, Xu R and Li J (2022) Perthes Disease in a Child With Osteogenesis Imperfecta From a Rare Genetic Variant: A Case Report. Front. Genet. 13:920950. doi: 10.3389/fgene.2022.920950

Background: Although certain genetic components have been reported as contributing factors for Perthes disease, its etiology remains unclear. We present a rare case of Perthes disease in a child with osteogenesis imperfecta (OI) caused by a mutation in the *COL1A1* gene *(NM_000088):exon25:c.1726C>T, (p.Gln576X)*.

Case presentations: A 7-year-old boy was initially treated at our medical facility in March 2016 with a history of chronic pain in right hip joint and limping for a year. He was diagnosed as Perthes disease in the right hip joint. He underwent acetabular osteotomy and ipsilateral proximal femoral varus osteotomy for better containment. During the follow-ups, the right hip demonstrated a normal range of motion without pain, and the pelvic X-ray demonstrated Stulberg Type II hip joint with a round femoral head. In the latest admission in 2022, he suffered from a right femoral shaft fracture after petty violence. After reviewing his medical history, he was suspected of having OI. The whole exome sequencing demonstrated a gene mutation in *COL1A1* (OMIM 166200) and confirmed the diagnosis of OI. Telescopic nailing was used to treat the femoral shaft fracture. After the nailing of the right femur, the appearance of the lower extremity seemed normal and symmetrical.

Conclusion: This study revealed that there might be an association between OI and Perthes disease. Our case report enriches the phenotypes of osteogenesis imperfecta and provides insight into the pathogenesis of LCPD.

Keywords: osteogenesis imperfecta, Perthes disease, Legg-Calve-Perthes Disease, *COL1A1* gene, case report

BACKGROUND

Osteogenesis imperfecta (OI) is a rare disease which is characterized by brittle bone, blue sclerae and short stature (Schindeler et al., 2022). Most of the OIs result from mutations in the COL1A1 and COL1A2 genes (Chen et al., 2022). Type I collagen is widely present in the bone, skin and tendon tissue, and nowadays, OI is recognized as a collagen-related disorder (Kaneto et al., 2014; Li et al., 2019).

Perthes disease, also known as Legg-Calve-Perthes disease (LCPD), is characterized by necrosis of the femoral head which results from interruption of blood supply to the femoral

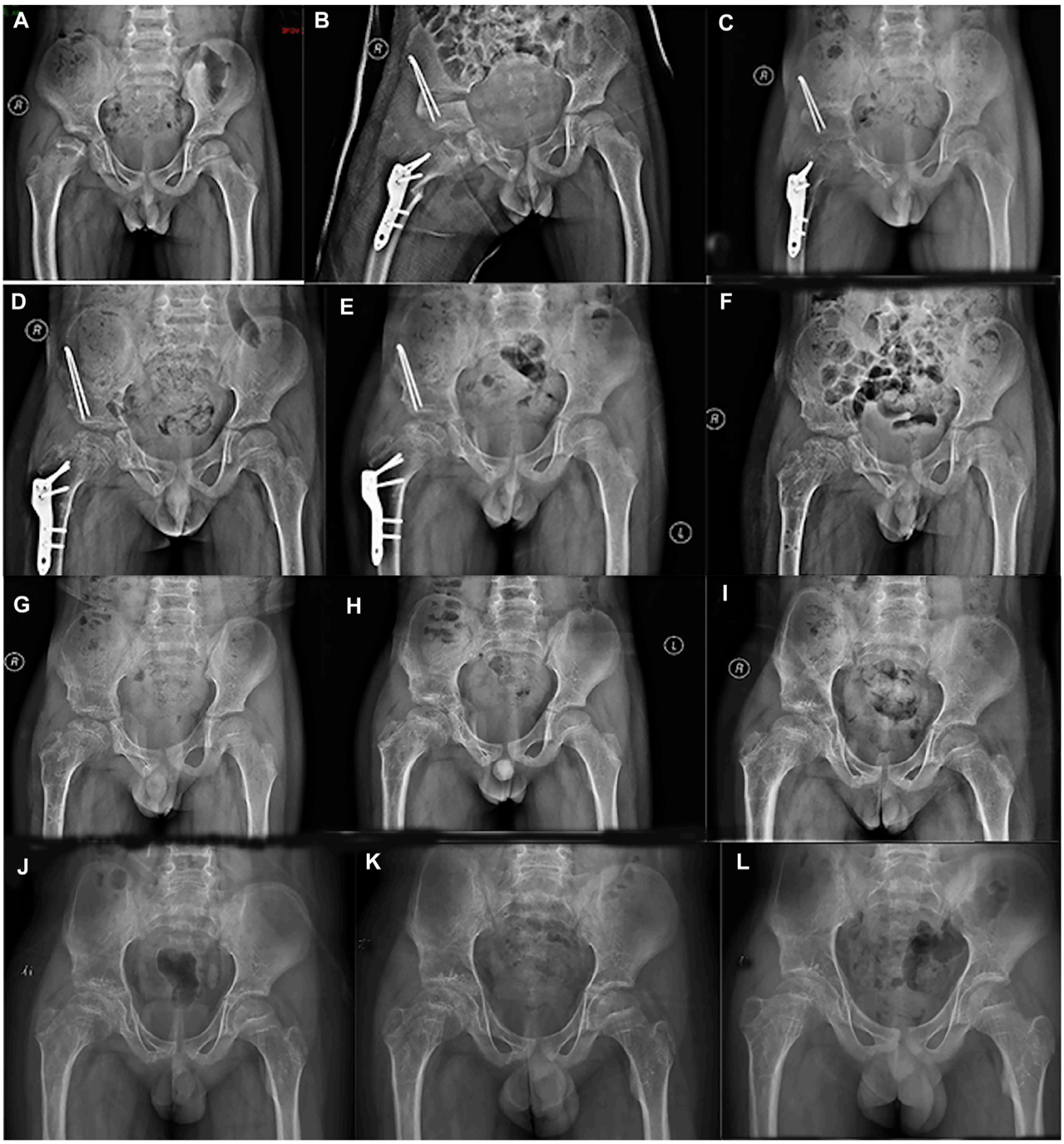

FIGURE 1 | Series radiographs of pelvis from a boy with Perthes disease presentation. **(A)** Pelvic radiograph of a 7.5 years old boy (March 2016). **(B)** Postoperative pelvic radiograph (March 2016). **(C)**. 4 months after operation (July 2016). **(D)**. 7 months after operation (October 2016). **(E)** 11 months after operation (February 2017). **(F)**. 12 months after primary operation, and 1 month after implant removal (March 2017). **(G)** 3 months after implant removal (April 2017). **(H)** 1 year after implant removal (March 2018). **(I)** 2 years after implant removal (January 2019). **(J)** 3 years after implant removal (November 2019). **(K)** 4 years after implant removal (October 2020). **(L)** 5 years after implant removal (January 2022).

head in the pediatric population (Mörlin and Hailer, 2021). Although certain genetic components have been reported as contributing factors, its etiology remains elusive (Rodríguez-Olivas et al., 2022). Mutation in factor V Leiden, polymorphisms in prothrombin, and methylenetetrahydrofolate reductase have been attributed to increased risk of LCPD (Buendía-Pazarán et al., 2022; Yasa et al., 2007).

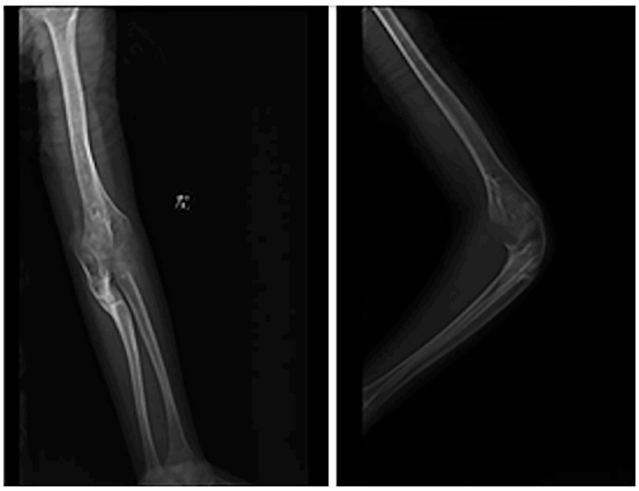

FIGURE 2 | Radiograph of left elbow joint from conservative treatment. **(A)** AP view of elbow joint. **(B)** Latereal view of elbow joint.

Here, We present a rare case of Perthes disease in a child with osteogenesis imperfecta (OI) caused by a mutation in the COL1A1 gene (*NM_000088):exon25:c.1726C>T, (p.Gln576X)*. To the best of our knowledge, this is the first ever reported case genetically confirmed OI patient with Perthes disease. The genetic mutation in COL1A1 might be an underlying genetic cause of Perthes disease.

CASE PRESENTATION

A 7-year-old boy was treated in our hospital in March 2016 with a history of chronic pain in the right hip joint and limping for a year. He was radiologically diagnosed as Perthes disease. He underwent right acetabular osteotomy and ipsilateral proximal femoral varus osteotomy in order to improve the femoral head containment in the acetabulum. Series radiographs in the subsequent follow-ups demonstrated the progression of Perthes disease (see **Figure 1**). In the past few years, he suffered from multiple fractures in his left upper extremity around elbow joint; however, he did not undergo any surgical treatment (see **Figure 2**). He suffered from right tibial shaft fracture in November 2019, and it was treated with closed reduction and elastic stable intramedullary nails (ESINs) at a local hospital. Unfortunately, he was presented to our hospital with his right femoral shaft fracture in February 2022. Prior to the fracture of his right femur, he had a normal range of motion (ROM) of the hip without limping, and the pelvic X-ray demonstrated Stulberg Type II hip joint with a round femoral head.

Despite having multiple fractures over the period of time, he had neither undergone a complete evaluation in order to diagnose OI nor received any pharmacological intervention for fragility fracture. However, the Z-value on the DEXA (Dual Energy X-ray Absorptiometry) scan in the latest admission was -2.8.

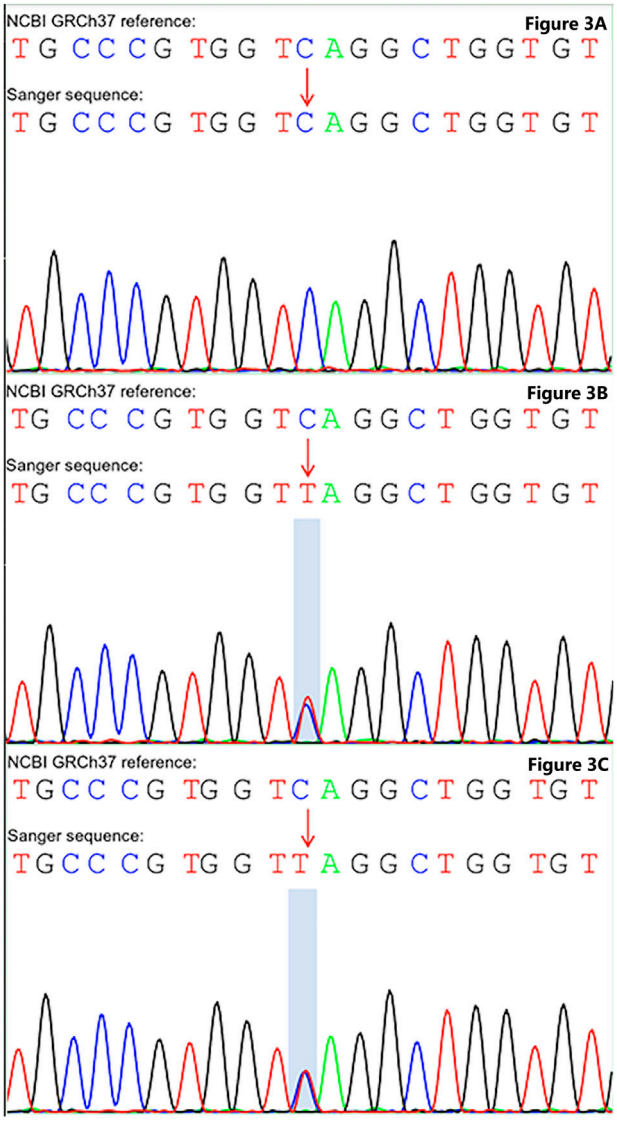

FIGURE 3 | Sanger sequencing unravel gene mutation in COL1A1. **(A)** Wild type was detected in the COL1A1: NM_000088: exon25: c.C1726T: p.Q576X without mutation in the father. **(B)** Heterozygous mutation in the COL1A1: NM_000088: exon25: c.C1726T: p.Q576X of the mother. **(C)** Heterozygous mutation in the COL1A1: NM_000088: exon25: c.C1726T: p.Q576X of the patient.

In the latest admission, the patient's height was 150 cm and body weight was 45 Kg. On inspection, a slightly bluish sclerae were noticed, and an abnormal appearance and limited ROM of the left elbow were evident. After reviewing his medical history, he was suspected of having OI. Subsequently, gene mutation in COL1A1 (OMIM 166200) was unraveled by whole exome sequencing (see **Figure 3**). Therefore, telescopic nailing was used to treat the femoral shaft fracture (see **Figure 4**). After the nailing of the right femur, the appearance of the lower extremity seemed normal and symmetrical.

As for the detailed methodology of genetic analysis, we collected 2 ml of whole blood (EDTA anticoagulation) of the

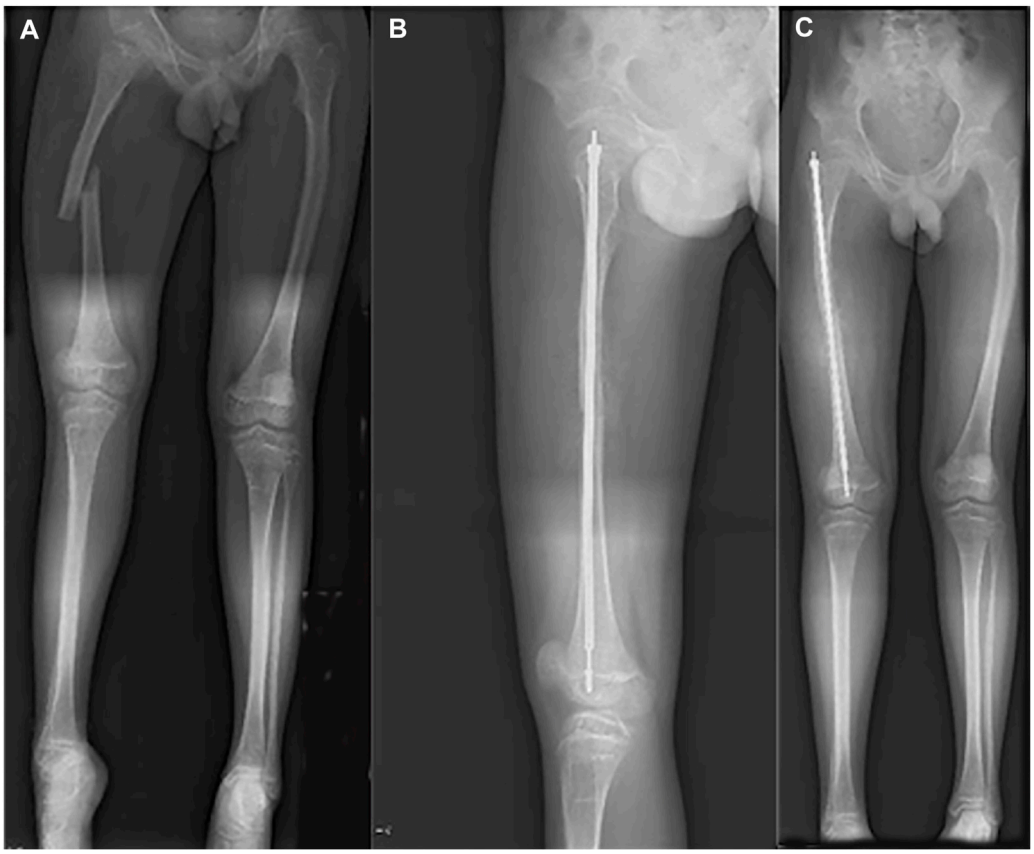

FIGURE 4 | Radiograph of 13-year-old boy with right femoral fracture. **(A)** Full-length AP view of lower extremity before surgery. **(B)** Lateral of femur after surgery. **(C)** Full-length AP view of lower extremity after surgery.

children and their parents, and the samples were sequenced by Xiamen Jiyuan medical laboratory. Subsequently, we extracted the whole genomic DNA of peripheral blood leukocytes, built the DNA library, and carried out 150 bp double terminal sequencing. After analyzing the original data of sequencing by biological information, the detected single nucleotide polymorphism and indel variants were annotated by ANNOVAR software.

The annotation information includes the start and end positions of the chromosome, reference alleles, alternative alleles, gene function, population frequency in the public database (including thousand human genome, ExAC, gnomAD database, etc.), protein function prediction (including revert, ClinPred, SIFT, provian, mutation taster, polyphen2, dbscsnv11, etc.). Furthermore, we followed the classification standards and guidelines of genetic variation of the American College of medical genetics and genomics to evaluate the pathogenicity and genetic interpretation of candidate gene variation.

According to the whole exome sequencing analysis, we found the mutation c.1726C>T: p.Gln576X (NM_000088) in exon 25 of the COL1A1 gene. This was a heterozygous nonsense mutation that base 1726 changed from cytosine C to thymine T, resulting in the mutation of amino acid 576 from glutamine to stop the codon from forming the truncated protein. Besides, the detected variation had been reported in the OI & Ehlers-Danlos syndrome variant databases, but the variation has not been reported in the literature before. The upstream and downstream primers were designed for the candidate ectopic sites, and the polymerase chain reaction was carried out, which was verified by Sanger sequencing. Primer design: COL1A1-F, 5′-CTCCCAAGATGCCCTTCC AG-3’; COL1A1-R, 5′-TCTCCCCAAGTCCCACTCAT-3’. Sanger sequencing was performed on the patient and their parents, suggesting that the variation was inherited from the mother (see **Figure 3**). Combined with the results of whole exome sequencing and Sanger sequencing, the mutation was determined as a gene mutation with possible pathogenicity according to American College of medical genetics and genomics guidelines (the evidence level of pathogenicity was pvs1 + pm2_supporting).

DISCUSSION AND CONCLUSION

We presented a boy with OI caused by a heterozygous mutation in the COL1A1 gene (NM_000088):exon25:c.1726C>T, (p.Gln576X). Series radiographs of the hip joint displayed the characteristics of Perthes disease.

OI is a genetic disorder caused by an abnormal production or structure of collagen type I (Nijhuis et al., 2022). The incidence of this rare condition is 1 in 15,000–20,000 births (Forlino and Marini, 2016). Autosomal dominant, recessive inheritance and X autosomal inheritance patterns have been reported. The severity of symptoms varies widely between different types of OI, ranging from mild symptoms with very few fractures with a normal quality of life to severe symptoms with frequent fractures, severe physical incompetence and decreased life span (Nijhuis et al., 2019; Robinson and Rauch, 2019). The patient had a normal height and relatively normal bone X-ray images in our study. Not only had the boy suffered multiple fractures in the past few years, but his mother, a heterozygous carrier, also experienced one fracture in adolescence and had a mild OI. Therefore, this mutation appeared to be pathogenic, leading to mild type I OI in this pedigree.

Perthes disease has been reported and studied for more than 100 years, but its etiology remains unknown (Pavone et al., 2019). Between 1909 and 1910, LCPD was described almost at the same time by different authors, Arthur Legg, Jacques Calve, Georg Perthes and Henning Waldernstrom (Hailer and Hailer, 2018). Several theories, including environmental, metabolic and genetic predilection, have been proposed as the causative factor for this disease (Leroux et al., 2018; Ibrahim and Little, 2016). Underprivileged social and economic status is associated with the incidence of LCPD in children (Perry et al., 2012a; Perry et al., 2012b), but this is not the scenario for our patient. Obesity has also been identified as a significant risk factor for LCPD (Neal et al., 2016), but this patient presented with average body weight and normal body mass index (BMI).

Presentation of Perthes disease has been reported in certain patients with increased susceptibility (Maleki et al., 2021; Miyamoto et al., 2017). Genetic mutation of COL2A1 has been reported to be involved in the genesis of a type II collagenopathy and a possible cause of LCPD (Kannu et al., 2011; Li et al., 2014). Besides, factor V Leiden has been reported to have an increased risk of Perthes disease, but the result was not significant (Szepesi et al., 2004; Glueck et al., 2007). Moreover, a child with Kienbock's disease and factor V thrombophilia has been reported to develop LCPD (Baltzer et al., 2016). However, the available literature on substantial heterogeneity reached no unanimity on the etiology of LCPD (Woratanarat et al., 2014; Vosmaer et al., 2010; Balasa et al., 2004; Kenet et al., 2003).

The hip disorder has been reported in patients with OI, including hip dysplasia, acetabular protrusio, and pseudo-protrusio acetabular deformity (Kishta et al., 2017; Ahn et al., 2019; Mandel et al., 2020; Song et al., 2021). However, only one study reported a patient with OI associated with Perthes disease in 2003 (Petra and Benson, 2003). However, the follow-up of that patient did not fully demonstrate the progress of Perthes, and the diagnosis of OI was not genetically confirmed. In contrast, the patient in our study demonstrated classic progression of LCPD, and containment surgery was performed to maintain the femoral head within the acetabulum. In the latest follow-up, the radiograph of the hip joint demonstrated Stulberg type II. Moreover, the genetic test unraveled a mutation in the COL1A1 gene (NM_000088):exon25:c.1726C>T, (p.Gln576X), and confirmed the diagnosis of OI. Therefore, our study demonstrated the mutation leading to the abnormal structure or function of collagen type I, resulting in decreased mechanism strength, which should be further studied and clarified in the pathogenesis of the LCPD.

There are certain limitations in our study. Firstly, we did not perform genetic tests for the entire family members, including the grandparents. Besides, future investigations, including animal models, might be warranted to explore the significance of this genetic mutation. Moreover, Perthes disease might be a comorbidity of OI rather than a secondary disease.

In conclusion, we report an OI child with heterozygous c.1726C>T, (p.Gln576X) mutation in the COL1A1 gene who later had been diagnosed as having Perthes disease. This study revealed that there might be an association between OI and Perthes disease. Our case report enriches the phenotypes of osteogenesis imperfecta and provides insight into the pathogenesis of LCPD.

DATA AVAILABILITY STATEMENT

The datasets for this article are not publicly available due to concerns regarding participant/patient anonymity. Requests to access the datasets should be directed to the corresponding authors.

ETHICS STATEMENT

The studies involving human participants were reviewed and approved by Ethics Committee of Tongji Medical College, Huazhong University of Science and Technology (IORG No: IORG0003571) gave a final approval on 20 November 2019. Written consents were obtained from the legal guardians of patient for publication of this paper. Written informed consent to participate in this study was provided by the participants' legal guardian/next of kin. Written informed consent was obtained from the individual(s), and minor(s)' legal guardian/next of kin, for the publication of any potentially identifiable images or data included in this article.

AUTHOR CONTRIBUTIONS

JL and RX are in charge of the main idea and is the guarantor of integrity of the entire study; PH, XZ, and RL are in charge of the study concepts, design, manuscript preparation and editing; RL and YS are in charge of data extraction and statistical analysis. PH and SR are in charge of the language polishing and the grammar revision. All authors read and approved the final manuscript.

REFERENCES

Ahn, J., Carter, E., Raggio, C. L., and Green, D. W. (2019). Acetabular Protrusio in Patients with Osteogenesis Imperfecta: Risk Factors and Progression. *J. Pediatr. Orthop.* 39 (10), e750–e754. doi:10.1097/BPO.0000000000001051

Balasa, V. V., Gruppo, R. A., Glueck, C. J., Wang, P., Roy, D. R., Wall, E. J., et al. (2004). Legg-calvé-perthes Disease and Thrombophilia. *J. Bone Jt. Surgery-American* 86 (12), 2642–2647. doi:10.2106/00004623-200412000-00009

Baltzer, H. L., Riester, S., and Moran, S. L. (2016). Bilateral Legg-Calve-Perthes Disease and Kienbock's Disease in a Child with Factor V Leiden Thrombophilia. *Hand (New York, N,Y.)* 11 (3), NP16–NP19. doi:10.1177/1558944715627274

Buendía-Pazarán, J. G., Hernández-Zamora, E., Rodríguez-Olivas, A. O., Casas-Ávila, L., Valdés-Flores, M., and Reyes-Maldonado, E. (2022). Association of MTHFR Rs1801133 and Homocysteine with Legg-Calvé-Perthes Disease in Mexican Patients. *Orphanet. J. Rare Dis.* 17 (1), 123. doi:10.1186/s13023-022-02264-2

Chen, P., Tan, Z., Shek, H. T., Zhang, J.-n., Zhou, Y., Yin, S., et al. (2022). Phenotypic Spectrum and Molecular Basis in a Chinese Cohort of Osteogenesis Imperfecta with Mutations in Type I Collagen. *Front. Genet.* 13, 816078. doi:10.3389/fgene.2022.816078

Forlino, A., and Marini, J. C. (2016). Osteogenesis Imperfecta. *Lancet* 387, 1657–1671. doi:10.1016/S0140-6736(15)00728-X

Glueck, C. J., Tracy, T., and Wang, P. (2007). Legg-Calve-Perthes Disease, Venous and Arterial Thrombi, and the Factor V Leiden Mutation in a Four-Generation Kindred. *J. Pediatr. Orthop.* 27 (7), 834–837. doi:10.1097/BPO.0b013e31815584bf

Hailer, Y. D., and Hailer, N. P. (2018). Is Legg-Calvé-Perthes Disease a Local Manifestation of a Systemic Condition? *Clin. Orthop. Relat. Res.* 476 (5), 1055–1064. doi:10.1007/s11999.0000000000000214

Ibrahim, T., and Little, D. G. (2016). The Pathogenesis and Treatment of Legg-Calvé-Perthes Disease. *JBJS. Rev.* 4 (7), e4. doi:10.2106/JBJS.RVW.15.00063

Kaneto, C. M., Lima, P. S., Zanette, D. L., Prata, K. L., Pina Neto, J. M., de Paula, F. J., et al. (2014). COL1A1and miR-29b Show Lower Expression Levels during Osteoblast Differentiation of Bone Marrow Stromal Cells from Osteogenesis Imperfecta Patients. *Bmc. Med. Genet.* 15, 45. doi:10.1186/1471-2350-15-45

Kannu, P., Irving, M., Aftimos, S., and Savarirayan, R. (2011). Two Novel COL2A1 Mutations Associated with a Legg-Calvé-Perthes Disease-like Presentation. *Clin. Orthop. Relat. Res.* 469 (6), 1785–1790. doi:10.1007/s11999-011-1850-x

Kenet, G., Hayek, S., Mor, M., Lubetsky, A., Miller, L., Rosenberg, N., et al. (2003). The 1226G (N370S) Gaucher Mutation Among Patients with Legg-Calve-Perthes Disease. *Blood Cells, Mol. Dis.* 31 (1), 72–74. doi:10.1016/s1079-9796(03)00121-9

Kishta, W., Abduljabbar, F. H., Gdalevitch, M., Rauch, F., Hamdy, R., and Fassier, F. (2017). Hip Dysplasia in Children with Osteogenesis Imperfecta: Association with Collagen Type I C-Propeptide Mutations. *J. Pediatr. Orthop.* 37 (7), 479–483. doi:10.1097/BPO.0000000000000644

Leroux, J., Abu Amara, S., and Lechevallier, J. (2018). Legg-Calvé-Perthes Disease. *Orthop. Traumatology Surg. Res.* 104 (1S), S107–S112. doi:10.1016/j.otsr.2017.04.012

Li, L., Cao, Y., Zhao, F., Mao, B., Ren, X., Wang, Y., et al. (2019). Validation and Classification of Atypical Splicing Variants Associated with Osteogenesis Imperfecta. *Front. Genet.* 10, 979. doi:10.3389/fgene.2019.00979

Li, N., Yu, J., Cao, X., Wu, Q.-Y., Li, W.-W., Li, T.-F., et al. (2014). A Novel P. Gly630Ser Mutation of COL2A1 in a Chinese Family with Presentations of Legg-Calvé-Perthes Disease or Avascular Necrosis of the Femoral Head. *PLoS. One.* 9 (6), e100505. doi:10.1371/journal.pone.0100505

Maleki, A., Qoreishy, S. M., and Bahrami, M. N. (2021). Surgical Treatments for Legg-Calvé-Perthes Disease: Comprehensive Review. *Interact. J. Med. Res.* 10 (2), e27075. doi:10.2196/27075

Mandel, M., Saloky, K., Mirenda, W., Seeley, A., and Seeley, M. (2020). Hip Dysplasia and Osteogenesis Imperfecta. *JBJS. Case Connect.* 10 (4), e2000369. doi:10.2106/JBJS.CC.20.00369

Miyamoto, Y., Matsuda, T., Kitoh, H., Haga, N., Ohashi, H., Nishimura, G., et al. (2007). A Recurrent Mutation in Type II Collagen Gene Causes Legg-Calvé-Perthes Disease in a Japanese Family. *Hum. Genet.* 121 (5), 625–629. doi:10.1007/s00439-007-0354-y

Mörlin, G. B., and Hailer, Y. D. (2021). High Blood Pressure and Overweight in Children with Legg-Calvé-Perthes Disease: a Nationwide Population-Based Cohort Study. *Bmc. Musculoskelet. Disord.* 22 (1), 32. doi:10.1186/s12891-020-03889-9

Neal, D. C., Alford, T. H., Moualeu, A., Jo, C.-H., Herring, J. A., and Kim, H. K. W. (2016). Prevalence of Obesity in Patients with Legg-Calvé-Perthes Disease. *J. Am. Acad. Orthop. Surg.* 24 (9), 660–665. doi:10.5435/JAAOS-D-16-00120

Nijhuis, W. H., Eastwood, D. M., Allgrove, J., Hvid, I., Weinans, H. H., Bank, R. A., et al. (2019). Current Concepts in Osteogenesis Imperfecta: Bone Structure, Biomechanics and Medical Management. *J. Children's Orthop.* 13, 1–11. doi:10.1302/1863-2548.13.180190

Nijhuis, W., Verhoef, M., van Bergen, C., Weinans, H., and Sakkers, R. (2022). Fractures in Osteogenesis Imperfecta: Pathogenesis, Treatment, Rehabilitation and Prevention. *Children* 9 (2), 268. doi:10.3390/children9020268

Pavone, V., Chisari, E., Vescio, A., Lizzio, C., Sessa, G., and Testa, G. (2019). Aetiology of Legg-Calvé-Perthes Disease: A Systematic Review. *Wjo* 10 (3), 145–165. doi:10.5312/wjo.v10.i3.145

Perry, D. C., Bruce, C. E., Pope, D., Dangerfield, P., Platt, M. J., and Hall, A. J. (2012a). Legg-Calvé-Perthes Disease in the UK: Geographic and Temporal Trends in Incidence Reflecting Differences in Degree of Deprivation in Childhood. *Arthritis & Rheumatism* 64 (5), 1673–1679. doi:10.1002/art.34316

Perry, D. C., Bruce, C. E., Pope, D., Dangerfield, P., Platt, M. J., and Hall, A. J. (2012b). Perthes' Disease of the Hip: Socioeconomic Inequalities and the Urban Environment. *Arch. Dis. Child.* 97 (12), 1053–1057. doi:10.1136/archdischild-2012-302143

Petra, M., and Benson, M. K. D. (2003). Perthes?? Disease Associated with Osteogenesis Imperfecta. *J. Pediatr. Orthop. Part B* 12 (5), 315–318. doi:10.1097/01.bpb.0000060281.96739.be

Robinson, M.-E., and Rauch, F. (2019). Mendelian Bone Fragility Disorders. *Bone* 126, 11–17. doi:10.1016/j.bone.2019.04.021

Rodríguez-Olivas, A. O., Hernández-Zamora, E., and Reyes-Maldonado, E. (2022). Legg-Calvé-Perthes Disease Overview. *Orphanet. J. Rare Dis.* 17 (1), 125. doi:10.1186/s13023-022-02275-z

Schindeler, A., Lee, L. R., O'Donohue, A. K., Ginn, S. L., and Munns, C. F. (2022). Curative Cell and Gene Therapy for Osteogenesis Imperfecta. *J Bone & Mineral Res* 37, 826–836. doi:10.1002/jbmr.4549

Song, M. H., Kamisan, N., Lim, C., Shin, C. H., Yoo, W. J., Song, H.-R., et al. (2021). Pseudo-Protrusio Acetabular Deformity in Osteogenesis Imperfecta Patients. *J. Pediatr. Orthop.* 41 (3), e285–e290. doi:10.1097/BPO.0000000000001739

Szepesi, K., Pòsán, E., Hársfalvi, J., Ajzner, É., Szücs, G., Gáspár, L., et al. (2004). The Most Severe Forms of Perthes' Disease Associated with the Homozygous Factor V Leiden Mutation. *J. Bone Jt. Surg. Br.* 86-B (3), 426–429. doi:10.1302/0301-620x.86b3.13442

Vosmaer, A., Pereira, R. R., Koenderman, J., Rosendaal, F., and Cannegieter, S. (2010). Coagulation Abnormalities in Legg-Calvé-Perthes Disease. *J. Bone Jt. Surgery-American* 92 (1), 121–128. doi:10.2106/JBJS.I.00157

Woratanarat, P., Thaveeratitharm, C., Woratanarat, T., Angsanuntsukh, C., Attia, J., and Thakkinstian, A. (2014). Meta-analysis of Hypercoagulability Genetic Polymorphisms in Perthes Disease. *J. Orthop. Res.* 32 (1), 1–7. doi:10.1002/jor.22473

Yasa, M. H., Bolaman, Z., Yukselen, V., Kadikoylu, G., Karaoglul, A. O., and Batun, S. (2007). Factor V Leiden G1691A, Prothrombin G20210A, and MTHFR C677T Mutations in Turkish Inflammatory Bowel Disease Patients. *Hepatogastroenterology* 54 (77), 1438–1442. doi:10.1136/gut.2004.40139corr1

Conflict of Interest: The authors declare that the research was conducted in the absence of any commercial or financial relationships that could be construed as a potential conflict of interest.

frontiers | Frontiers in Genetics

TYPE Case Report
PUBLISHED 26 August 2022
DOI 10.3389/fgene.2022.964098

OPEN ACCESS

EDITED BY
Muhammad Jawad Hassan,
National University of Medical Sciences (NUMS), Pakistan

REVIEWED BY
Amjad Khan,
Université de Strasbourg, France
Ewelina Bukowska-Olech,
Poznan University of Medical Sciences, Poland

*CORRESPONDENCE
Chunnuan Chen,
chenchunnuan1983@aliyun.com
Gaoxiong Wang,
wanggaoxiong2013@163.com
Yingjun Xie,
xieyjun@mail2.sysu.edu.cn

†These authors have contributed equally to this work

SPECIALTY SECTION
This article was submitted to Genetics of Common and Rare Diseases, a section of the journal Frontiers in Genetics

RECEIVED 08 June 2022
ACCEPTED 02 August 2022
PUBLISHED 26 August 2022

CITATION
Zhuang J, Wang J, Luo Q, Zeng S, Chen Y, Jiang Y, Chen X, Wang Y, Xie Y, Wang G and Chen C (2022), Case Report: Novel compound heterozygous variants in CHRNA1 gene leading to lethal multiple pterygium syndrome: A case report.
Front. Genet. 13:964098.
doi: 10.3389/fgene.2022.964098

Case Report: Novel compound heterozygous variants in *CHRNA1* gene leading to lethal multiple pterygium syndrome: A case report

Jianlong Zhuang[1†], Junyu Wang[1†], Qi Luo[2], Shuhong Zeng[1], Yu'e Chen[3], Yuying Jiang[1], Xinying Chen[1], Yuanbai Wang[1], Yingjun Xie[4,5]*, Gaoxiong Wang[6]* and Chunnuan Chen[7]*

[1]Prenatal Diagnosis Center, Quanzhou Women's and Children's Hospital, Quanzhou, China, [2]Department of Public Health for Women and Children, Quanzhou Women's and Children's Hospital, Quanzhou, China, [3]Ultrasonography, Quanzhou Women's and Children's Hospital, Quanzhou, China, [4]Department of Obstetrics and Gynecology, Guangdong Provincial Key Laboratory of Major Obstetric Diseases, The Third Affiliated Hospital of Guangzhou Medical University, Guangzhou, China, [5]Key Laboratory of Reproduction and Genetics of Guangdong Higher Education Institutes, The Third Affiliated Hospital of Guangzhou Medical University, Guangzhou, China, [6]Quanzhou Women's and Children's Hospital, Quanzhou, China, [7]Department of Neurology, The Second Affiliated Hospital of Fujian Medical University, Quanzhou, China

Background: Lethal multiple pterygium syndrome (LMPS) is a rare autosomal recessive inherited disorder typically characterized by intrauterine growth retardation, multiple pterygia, and flexion contractures.

Case presentation: We herein report a Chinese case with a history of three adverse pregnancies demonstrating the same ultrasonic phenotypes, including increased nuchal translucency, edema, fetal neck cystoma, reduced movement, joint contractures, and other congenital features. Whole-exome sequencing (WES) revealed novel compound heterozygous variants in the *CHRNA1* gene NM_000079.4: c.[1128delG (p.Pro377Leu*fs*Ter10)]; [505T>C (p.Trp169Arg)] in the recruited individual, and subsequent familial segregation showed that both parents transmitted their respective mutation.

Conclusion: For the first time, we identified an association between the *CHRNA1* gene and the recurrent lethal multiple pterygium syndrome (LMPS) in a Chinese family. This finding may also enrich the mutation spectrum of the *CHRNA1* gene and promote the applications of WES technology in etiologic diagnosis of ultrasound anomalies in prenatal examination.

KEYWORDS

whole-exome sequencing, chromosomal microarray analysis, *CHRNA1*, lethal multiple pterygium syndrome, stillbirth

Introduction

The acetylcholine receptor (AChR) is a member of the superfamily of transmitter-gated ion channels and plays a critical role in controlling electrical signals between nerves and skeletal muscle cells. In the embryonic development, AChR consists of one β (*CHRNB*), one δ (*CHRND*), one γ (*CHRNG*), and two α (*CHRNA1*) subunits, but after a gestational age of 33 weeks, the γ subunit is replaced by an ε (*CHRNE*) subunit (Hesselmans et al., 1993). The α subunit of the muscle acetylcholine receptor encoded by *CHRNA1* gene is known as the main target of pathogenic autoantibodies in autoimmune myasthenia gravis.

CHRNA1 (MIM 100690), *CHRND* (MIM 100720), *CHRNG* (MIM 100730), *RAPSN* (MIM 601592), *DOK7* (MIM 610285), *CNTN1* (MIM 600016), and *SYNE1* (MIM 608441) gene mutations would lead to fetal akinesia deformation sequence and/or multiple pterygium syndrome (MPS) (Chen, 2012), a rare autosomal recessive inherited disorder mainly manifested as arthrogryposis multiplex congenita, pterygia of the neck, fingers, and antecubital, popliteal, and intercrural areas, developmental delay, and facial, vertebral, and genital anomalies (Penchaszadeh and Salszberg, 1981; Ramer et al., 1988). The prevalence of MPS remains uncertain and is supposed to be less than 1/100,000, as reported by a previous study (Mohtisham et al., 2019). MPS is typically divided into prenatally lethal and nonlethal types (Barros et al., 2012; Chen, 2012). The nonlethal form of MPS is also known as Escobar syndrome. The lethal multiple pterygium syndrome (LMPS) is a rare autosomal recessive inherited disorder characterized by intrauterine growth retardation, multiple pterygia, and flexion contractures, causing severe arthrogryposis and fetal akinesia (Vogt et al., 2008; Joshi et al., 2016; Mohtisham et al., 2019). In addition, although the most common inheritance model is autosomal recessive, the autosomal dominant and X-linked inheritance has also been reported (Tolmie et al., 1987; Meyer-Cohen et al., 1999; Chong et al., 2015). Usually, fetuses with LMPS would result in spontaneous miscarriage or stillbirth (Nazari et al., 2019).

In this study, we used whole-exome sequencing (WES) to make a diagnosis of genetic etiology diagnosis in a Chinese family with increased nuchal translucency, fetal edema, fetal neck cystoma, reduced movement, and joint contractures and identified two novel compound heterozygous variants in the *CHRNA1* gene in the fetus, which would lead to LMPS. This study may broaden the spectrum of *CHRNA1* gene variants that lead to LMPS and provide valuable data for application of prenatal WES technology and genetic consultation.

Case presentation

Clinical examination

In this study, a Chinese family with a history of three adverse pregnancies was recruited. The couple denied consanguineous marriage and any related inherited history. This study was approved by the ethics committee of Quanzhou Women's and Children's Hospital (2020 No. 31). The three fetuses in this family all had similar ultrasonic abnormalities. Among them, ultrasound of the first pregnancy in the first trimester showed

TABLE 1 Variants of the *CHRNA1* gene and related clinical findings in the ClinVar database.[a]

Variant (NM_000079.4)	Protein	ACMG classification	Clinical phenotype	Mutation type
c.518dup	p.Ser174Leu*fs*Ter194	P/LP	LMPS	Frameshift mutation
c.436_437insTG	p.Ser146Met*fs*Ter20	VUS	NP	Frameshift mutation
c.380_381del	p.Lys127Ser*fs*Ter18	LP	Congenital myasthenic syndrome	Frameshift mutation
c.292dup	p.Ile98Asn*fs*Ter17	P	LMPS	Frameshift mutation
c.779-1_779insA	—	LP	LMPS	Splicing mutation
c.779-2A>C	—	LP	NP	Splicing mutation
c.235-1G>A	—	LP	NP	Splicing mutation
c.1345C>T	p.Arg449Ter	VUS	NP	Nonsense mutation
c.844G>T	p.Glu282Ter	P	LMPS	Nonsense mutation
c.370A>T	p.Lys124Ter	P	LMPS	Nonsense mutation
c.317G>A	p.Trp106Ter	P/LP	NP	Nonsense mutation
c.249C>A	p.Tyr83Ter	P	LMPS	Nonsense mutation
c.175C>T	p.Gln59Ter	P	NP	Nonsense mutation
c.166C>T	p.Gln56Ter	LP	NP	Nonsense mutation
c.1128delG (our study)	p.Pro377Leu*fs*Ter10	LP	LMPS	Frameshift mutation
c.505T>C (our study)	p.Trp169Arg	VUS	LMPS	Missense mutation

[a]As shown in Table 1, the overall frameshift, splicing, and nonsense mutations in the *CHRNA1* gene in the ClinVar database were presented, except for the 153 missense mutations. P: pathogenic; LP: likely pathogenic; VUS: variants of uncertain significance; NP: not provided; LMPS: lethal multiple pterygium syndrome.

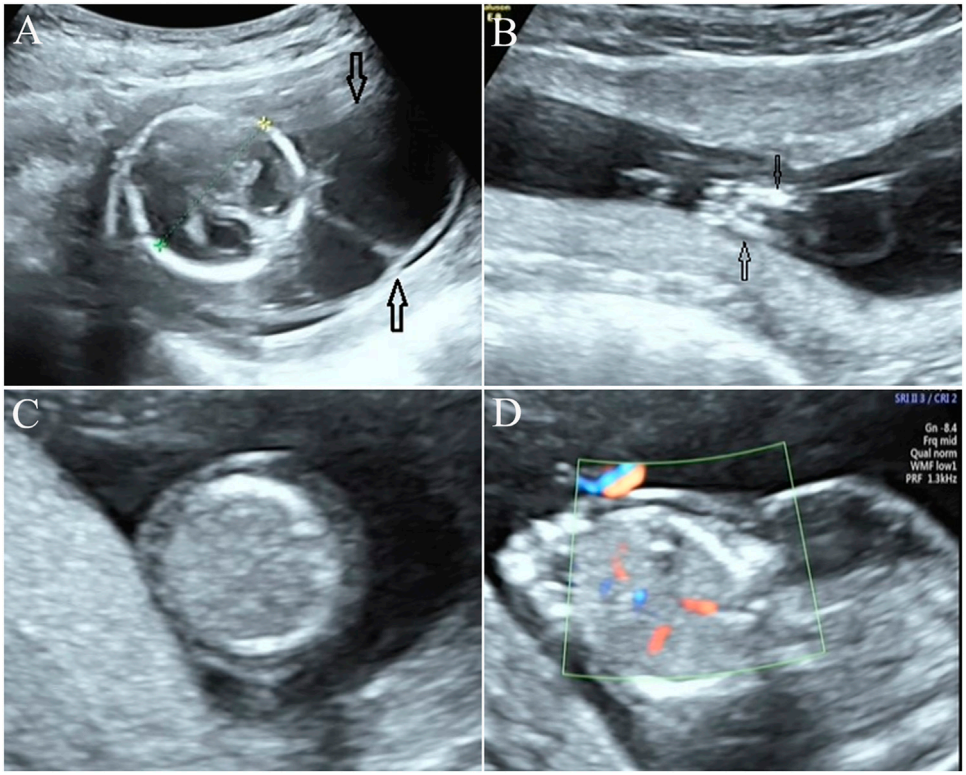

FIGURE 1
Prenatal ultrasonic examination results of the fetus. **(A)** Ultrasound examination elicited neck water sac tumor in the fetus. **(B)** Approach, flexion, and fixation of both lower limbs were observed in the fetus, indicating joint contractures. **(C,D)**: the trunk skin layer is obviously thickened, and the echo is reduced, and diagnosed as fetal edema.

that the fetus had fetal systemic edema, and the pregnant woman and her family chose to terminate the pregnancy without further genetic etiology testing. Subsequently, the woman had the second pregnancy, and ultrasound examination results elicited that the fetus had edema, increased nuchal translucency, neck water sac tumor, reduced movement, and abnormal posture (joint contractures) (Figure 1), and stillbirth occurred at the gestational age of 18^{+5} weeks in the second pregnancy. Upon informed consent from the family, we collected the fetal specimen of the second pregnancy for further cytogenetic and molecular genetic analyses. The third pregnancy of the woman also showed a similar ultrasonic phenotype. Although no stillborn occurred in the second trimester, the family still chose to terminate the pregnancy.

Molecular analysis

No obvious chromosomal abnormalities and copy number variants were detected by karyotype analysis and chromosomal microarray analysis in the fetus of the second pregnancy, as well as their parents who exhibit normal clinical phenotypes.

WES technology was performed for further genetic etiology in the recruited fetus. A novel frameshift variant in exon 8 compound with a novel missense variant in exon 5 in the *CHRNA1* gene NM_000079.4: c.[1128delG (p.Pro377Leu*fs*Ter10)]; [505T>C (p.Trp169Arg)] was detected in the recruited fetus by WES technology detection, which was inherited from their parents, respectively (Figure 2 and Supplementary Table 1). In the third pregnancy, the compound heterozygous variants were also detected by other hospitals using WES technology. At present, the c.1128delG (p.Pro377Leu*fs*Ter10) variant was absent in the gnomAD (http://gnomad-sg.org/, accession date: 28 June 2022), dbSNP (https://www.ncbi.nlm.nih.gov/snp/?term=, accession date: 28 June 2022), 1000 genomes project (http://browser.1000genomes.org/, accession date: 28 June 2022), PubMed (https://pubmed.ncbi.nlm.nih.gov, accession date: 28 June 2022), ClinVar (https://www.ncbi.nlm.nih.gov/clinvar/, accession date: 28 June 2022) (Table 1), and HGMD (http://www.hgmd.cf.ac.uk/ac/index.php, accession date: 28 June 2022) databases and was not found in the local database as well, but it was interpreted as a likely pathogenic variant (PVS1, PM2_Supporting) according to the ACMG (The American College of Medical Genetics and Genomics, ACMG) guidelines (Richards et al., 2015). In

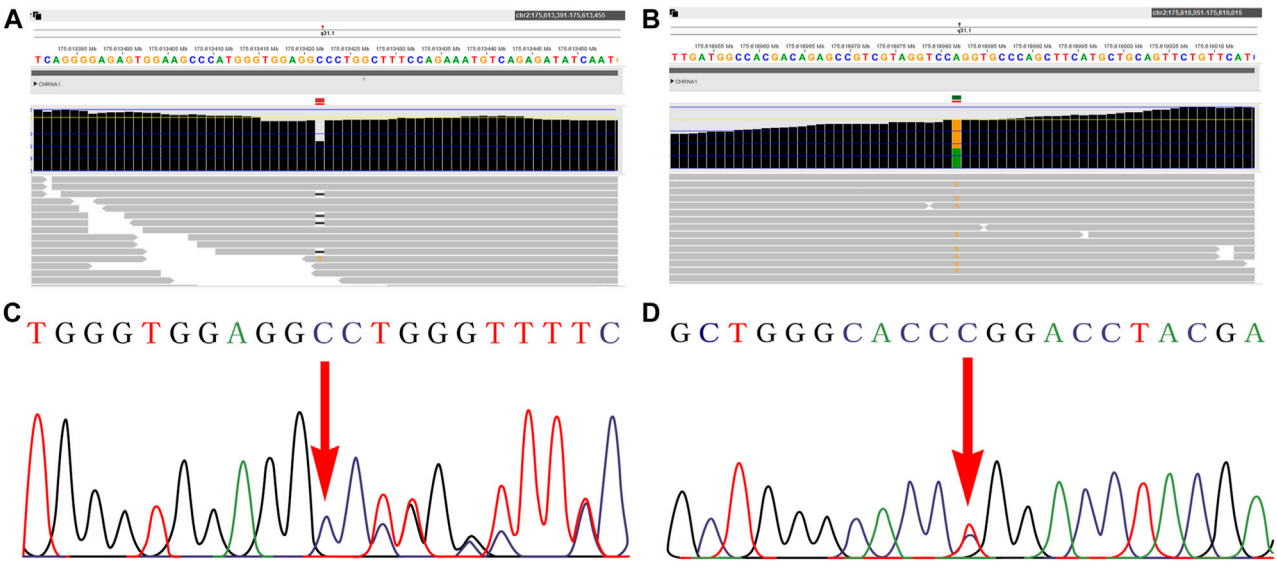

FIGURE 2
Novel variants of the *CHRNA1* gene identified in the fetus. **A–B**: WES detection results demonstrated novel compound heterozyous variants in the *CHRNA1* gene NM_000079.4: c.[1128delG (p.Pro377Leu*fs*Ter10)]; [505T>C (p.Trp169Arg)] in the fetus. **C–D**: both variants were further confirmed by Sanger sequencing.

addition, the c.505T>C (p.Trp169Arg) variant was also absent in the databases mentioned earlier, and online computer-aided analysis predictions (http://159.226.67.237/sun/varcards/welcome/index) suggest that this variant is more likely to affect the protein structure/function (damaging score: 0.87). According to the ACMG guidelines (Richards et al., 2015), the c.505T>C (p.Trp169Arg) variant was interpreted as variant of uncertain significance (PM3, PM2_Supporting, and PP3).

Discussion and conclusion

In the clinical practice, chromosomal microarray analysis (CMA) or copy number variation sequencing has been increasingly used to assess the genetic cause in miscarriage and stillbirth (Sahlin et al., 2014; Martinez-Portilla et al., 2019; Marquès et al., 2020; Zhang et al., 2021). A recent meta-analysis of seven studies involving 903 stillborn fetuses demonstrated a 4% incremental yield of pathogenic copy number variants of CMA over karyotyping, among which 22q11.21 deletion was the most common variant responsible for stillbirth (Martinez-Portilla et al., 2019). However, more than half of them could not get a clear genetic diagnosis. WES has obvious advantages in the detection of monogenic diseases and is, therefore, suggested to be used in prenatal genetic etiology diagnosis in fetuses with ultrasonic structural abnormalities (Lord et al., 2019; Petrovski et al., 2019). In the present study, we detected two novel *CHRNA1* gene mutations in the stillbirth fetus that may result in LMPS by WES.

Previous studies have indicated the application value of WES in identifying the genetic etiology for pregnancy loss or stillbirth (Fu et al., 2018; Demetriou et al., 2019; Zhao et al., 2021). More studies have identified *CHRNA1* mutations in fetuses with recurrent pregnancy loss or stillbirth using WES. A systematic review of 50 studies (Colley et al., 2019) reported a range of candidate genes (*CHRNA1*, *DYNC2H1*, and *RYR1*) that may induce pregnancy loss. In addition, a recent study reviewed 15 articles of 74 families including 279 reported recurrent pregnancy loss, identified 34 candidate pathogenic variants in 19 genes including *CHRNA1* gene by exome sequencing, and recommended that trio-based exome sequencing can be performed in cases with recurrent pregnancy loss and with normal parental karyotypes (Robbins et al., 2019). In addition, a novel mutation in *CHRNA1* was identified by exome sequencing, which was suggested as the cause for recurrent fetal loss, and they hypothesized that exome sequencing could disclose the underlying autosomal recessive mutations in families with recurrent fetal loss (Shamseldin et al., 2013). In the present case study, we identified two compound heterozyous variants in the *CHRNA1* gene, which further confirms the application value of WES in genetic analysis of recurrent pregnancy loss or stillbirth.

The nicotinic acetylcholine receptor (AChR) has five subunits of four different types: two alpha subunits and one each of beta, gamma (or epsilon), and delta subunits, which control electrical signaling between nerve and muscle cells by opening and closing a gate (Miyazawa et al., 2003). Among

them, *CHRNA1* encodes two alpha subunits, playing an important role in maintaining the AChR structure. As exhibited in the OMIM database, heterozygous mutations of *CHRNA1* can cause autosomal dominant congenital slow-channel myasthenic syndrome and congenital fast-channel myasthenic syndrome, while homozygous mutations or compound heterozygous mutations of *CHRNA1* would lead to autosomal recessive LMPS. A previous study identified homozygous mutations in the *CHRNA1* gene in patients from two families with LMPS (Michalk et al., 2008). Among them, the homozygous c.761G>T (p.Arg234Leu) mutation was identified in both fetuses in family 1 with similar prenatal ultrasonic features including growth delay, edema, cystic hygroma, decreased movements, and joint contractures. They observed that the first fetus of family 1 was a stillbirth at a gestational age of 24 weeks, and the second fetus was terminated at a gestational age of 20 weeks. Like family 1, similar intrauterine problems were displayed in both fetuses of family 2, who carried the homozygous mutation of c.117-133dup17 (p.His25Arg*fs*X19) in the *CHRNA1* gene. In addition, a study conducted by Dickinson et al. (2016) found that homozygous lethal mutation was observed in the *CHRNA1*-knockout mice. In the present study, compound heterozygous variants of NM_000079.4: c.[1128delG (p.Pro377Leu*fs*Ter10)]; [505T>C (p.Trp169Arg)] in the fetuses were detected, who manifested intrauterine edema, increased nuchal translucency, neck water sac tumor, and joint contractures, which are consistent with the intrauterine clinical features of LMPS.

At present, neither of two novel *CHRNA1* variants identified in this study has been reported in the databases or the literature. Among them, the missense variant was classified as the variant of uncertain significance according to the ACMG guidelines. Given the consistence of the clinical phenotypes in the fetuses with LMPS and the genotype–phenotype segregation present in the family, we believe that both variants detected in *CHRNA1* could be pathogenic variants and may lead to LMPS. However, future functional studies are required to clarify the molecular mechanism.

In conclusion, an etiologic diagnosis was conducted successfully in a Chinese family with recurrent fetal edema, fetal neck cystoma, and joint contractures by WES. This is the first study reporting the identification of two novel compound heterozyous variants in the *CHRNA1* gene that may lead to LMPS. Our findings may broaden the spectrum of *CHRNA1* gene mutations that result in LMPS and provide valuable data for the application of the prenatal WES technology and genetic consultation.

Data availability statement

The datasets for this article are not publicly available due to concerns regarding participant/patient anonymity. Requests to access the datasets should be directed to the corresponding authors.

Ethics statement

The studies involving human participants were reviewed and approved by the Institutional Ethics Committee of Quanzhou women's and children's hospital to the commencement of the study (2020No. 31). The patients/participants provided their written informed consent to participate in this study. Written informed consent was obtained from the individual(s) for the publication of any potentially identifiable images or data included in this article.

Author contributions

JZ and JW wrote the article; XC, YC, and YJ recruited the participants and performed clinical consultation; YW, QL, and SZ performed the karyotype analysis and analyzed the data; GW, CC, and YX revised and polished the article. All authors approved the final article.

Funding

This research was sponsored by Fujian Provincial Health Technology Project (2020QNB045) and Quanzhou City Science and Technology Program of China (2020C026R).

Acknowledgments

The authors wish to express our appreciation to the Fujian Provincial Health Commission and Quanzhou Science and Technology Bureau for funding this work. They also express their appreciation to the patient who participated in this study.

Conflict of interest

The authors declare that the research was conducted in the absence of any commercial or financial relationships that could be construed as a potential conflict of interest.

Publisher's note

All claims expressed in this article are solely those of the authors and do not necessarily represent those of their

affiliated organizations, or those of the publisher, the editors, and the reviewers. Any product that may be evaluated in this article, or claim that may be made by its manufacturer, is not guaranteed or endorsed by the publisher.

Supplementary material

The Supplementary Material for this article can be found online at: https://www.frontiersin.org/articles/10.3389/fgene.2022.964098/full#supplementary-material

References

Barros, F. S., Araujo Júnior, E., Rolo, L. C., and Nardozza, L. M. (2012). Prenatal diagnosis of lethal multiple pterygium syndrome using two-and three-dimensional ultrasonography. *J. Clin. Imaging Sci.* 2, 65. doi:10.4103/2156-7514.103055

Chen, C. P. (2012). Prenatal diagnosis and genetic analysis of fetal akinesia deformation sequence and multiple pterygium syndrome associated with neuromuscular junction disorders: a review. *Taiwan. J. Obstet. Gynecol.* 51 (1), 12–17. doi:10.1016/j.tjog.2012.01.004

Chong, J. X., Burrage, L. C., Beck, A. E., Marvin, C. T., McMillin, M. J., Shively, K. M., et al. (2015). Autosomal-dominant multiple pterygium syndrome is caused by mutations in MYH3. *Am. J. Hum. Genet.* 96 (5), 841–849. doi:10.1016/j.ajhg.2015.04.004

Colley, E., Hamilton, S., Smith, P., Morgan, N. V., Coomarasamy, A., and Allen, S. (2019). Potential genetic causes of miscarriage in euploid pregnancies: a systematic review. *Hum. Reprod. Update* 25 (4), 452–472. doi:10.1093/humupd/dmz015

Demetriou, C., Chanudet, E., GOSgeneTopf, M., Thomas, A. C., Bitner-Glindzicz, M., et al. (2019). Exome sequencing identifies variants in FKBP4 that are associated with recurrent fetal loss in humans. *Hum. Mol. Genet.* 28 (20), 3466–3474. doi:10.1093/hmg/ddz203

Dickinson, M. E., Flenniken, A. M., Ji, X., Teboul, L., Wong, M. D., White, J. K., et al. (2016). High-throughput discovery of novel developmental phenotypes. *Nature* 537 (7621), 508–514. doi:10.1038/nature19356

Fu, M., Mu, S., Wen, C., Jiang, S., Li, L., Meng, Y., et al. (2018). Whole-exome sequencing analysis of products of conception identifies novel mutations associated with missed abortion. *Mol. Med. Rep.* 18 (2), 2027–2032. doi:10.3892/mmr.2018.9201

Hesselmans, L. F., Jennekens, F. G., Van den Oord, C. J., Veldman, H., and Vincent, A. (1993). Development of innervation of skeletal muscle fibers in man: relation to acetylcholine receptors. *Anat. Rec.* 236 (3), 553–562. doi:10.1002/ar.1092360315

Joshi, T., Noor, N. N., Kural, M., and Tripathi, A. (2016). Lethal multiple pterygium syndrome. *J. Fam. Med. Prim. Care* 5 (2), 477–478. doi:10.4103/2249-4863.192361

Lord, J., McMullan, D. J., Eberhardt, R. Y., Rinck, G., Hamilton, S. J., Quinlan-Jones, E., et al. (2019). Prenatal exome sequencing analysis in fetal structural anomalies detected by ultrasonography (PAGE): a cohort study. *Lancet* 393 (10173), 747–757. doi:10.1016/S0140-6736(18)31940-8

Marquès, B., Benitez, L., Peguero, A., Madrigal, I., Gomez, O., Figueras, F., et al. (2020). Cytogenetic investigation in 136 consecutive stillbirths: Does the tissue type Affect the success rate of chromosomal microarray analysis and karyotype? *Fetal diagn. Ther.* 47 (4), 315–320. doi:10.1159/000505399

Martinez-Portilla, R. J., Pauta, M., Hawkins-Villarreal, A., Rial-Crestelo, M., Paz Y Mino, F., Madrigal, I., et al. (2019). Added value of chromosomal microarray analysis over conventional karyotyping in stillbirth work-up: Systematic review and meta-analysis. *Ultrasound Obstet. Gynecol.* 53 (5), 590–597. doi:10.1002/uog.20198

Meyer-Cohen, J., Dillon, A., Pai, G. S., and Conradi, S. (1999). Lethal multiple pterygium syndrome in four male fetuses in a family: evidence for an X-linked recessive subtype? *Am. J. Med. Genet.* 82 (1), 97–99. doi:10.1002/(sici)1096-8628(19990101)82:1<97::aid-ajmg22>3.0.co;2-g

Michalk, A., Stricker, S., Becker, J., Rupps, R., Pantzar, T., Miertus, J., et al. (2008). Acetylcholine receptor pathway mutations explain various fetal akinesia deformation sequence disorders. *Am. J. Hum. Genet.* 82 (2), 464–476. doi:10.1016/j.ajhg.2007.11.006

Miyazawa, A., Fujiyoshi, Y., and Unwin, N. (2003). Structure and gating mechanism of the acetylcholine receptor pore. *Nature* 423 (6943), 949–955. doi:10.1038/nature01748

Mohtisham, F. S., Sallam, A., and Shawli, A. (2019). Lethal multiple pterygium syndrome. *BMJ Case Rep.* 12 (5), e229045. doi:10.1136/bcr-2018-229045

Nazari, T., Rashidi-Nezhad, A., Ganji, M., Rezaei, Z., Talebi, S., Ghasemi, N., et al. (2019). Utilization of Whole exome sequencing in lethal form of multiple pterygium syndrome: identification of mutations in embryonal subunit of acetylcholine receptor. *Int. J. Mol. Cell. Med.* 8 (4), 258–269. doi:10.22088/IJMCM.BUMS.8.4.258

Penchaszadeh, V. B., and Salszberg, B. (1981). Multiple pterygium syndrome. *J. Med. Genet.* 18 (6), 451–455. doi:10.1136/jmg.18.6.451

Petrovski, S., Aggarwal, V., Giordano, J. L., Stosic, M., Wou, K., Bier, L., et al. (2019). Whole-exome sequencing in the evaluation of fetal structural anomalies: a prospective cohort study. *Lancet* 393 (10173), 758–767. doi:10.1016/S0140-6736(18)32042-7

Ramer, J. C., Ladda, R. L., and Demuth, W. W. (1988). Multiple pterygium syndrome. an overview. *Am. J. Dis. Child.* 142 (7), 794–798. doi:10.1001/archpedi.1988.02150070108039

Richards, S., Aziz, N., Bale, S., Bick, D., Das, S., Gastier-Foster, J., et al. (2015). Standards and guidelines for the interpretation of sequence variants: a joint consensus recommendation of the American College of medical genetics and genomics and the association for molecular pathology. *Genet. Med.* 17 (5), 405–424. doi:10.1038/gim.2015.30

Robbins, S. M., Thimm, M. A., Valle, D., and Jelin, A. C. (2019). Genetic diagnosis in first or second trimester pregnancy loss using exome sequencing: a systematic review of human essential genes. *J. Assist. Reprod. Genet.* 36 (8), 1539–1548. doi:10.1007/s10815-019-01499-6

Sahlin, E., Gustavsson, P., Liedén, A., Papadogiannakis, N., Bjareborn, L., Pettersson, K., et al. (2014). Molecular and cytogenetic analysis in stillbirth: results from 481 consecutive cases. *Fetal diagn. Ther.* 36 (4), 326–332. doi:10.1159/000361017

Shamseldin, H. E., Swaid, A., and Alkuraya, F. S. (2013). Lifting the lid on unborn lethal Mendelian phenotypes through exome sequencing. *Genet. Med.* 15 (4), 307–309. doi:10.1038/gim.2012.130

Tolmie, J. L., Patrick, A., and Yates, J. R. (1987). A lethal multiple pterygium syndrome with apparent X-linked recessive inheritance. *Am. J. Med. Genet.* 27 (4), 913–919. doi:10.1002/ajmg.1320270418

Vogt, J., Harrison, B. J., Spearman, H., Cossins, J., Vermeer, S., ten Cate, L. N., et al. (2008). Mutation analysis of CHRNA1, CHRNB1, CHRND, and RAPSN genes in multiple pterygium syndrome/fetal akinesia patients. *Am. J. Hum. Genet.* 82 (1), 222–227. doi:10.1016/j.ajhg.2007.09.016

Zhang, X., Huang, Q., Yu, Z., and Wu, H. (2021). Copy number variation characterization and possible candidate genes in miscarriage and stillbirth by next-generation sequencing analysis. *J. Gene Med.* 23 (12), e3383. doi:10.1002/jgm.3383

Zhao, C., Chai, H., Zhou, Q., Wen, J., Reddy, U. M., Kastury, R., et al. (2021). Exome sequencing analysis on products of conception: a cohort study to evaluate clinical utility and genetic etiology for pregnancy loss. *Genet. Med.* 23 (3), 435–442. doi:10.1038/s41436-020-01008-6

frontiers | Frontiers in Genetics

TYPE Original Research
PUBLISHED 23 September 2022
DOI 10.3389/fgene.2022.844381

OPEN ACCESS

EDITED BY
Safarina G. Malik,
Mochtar Riady Institute for Nanotechnology, Indonesia

REVIEWED BY
Ari Winasti Satyagraha,
Eijkman Institute for Molecular Biology, Indonesia
Marcela Vela-Amieva,
Instituto Nacional de Pediatría, Mexico
Mahamadou Diakite,
Université des Sciences, des Techniques et des Technologies de Bamako, Mali

*CORRESPONDENCE
Yulin Zhou,
zhou_yulin@126.com
Qiwei Guo,
guoqiwei@xmu.edu.cn

†These authors have contributed equally to this work

SPECIALTY SECTION
This article was submitted to Genetics of Common and Rare Diseases, a section of the journal Frontiers in Genetics

RECEIVED 28 December 2021
ACCEPTED 08 September 2022
PUBLISHED 23 September 2022

CITATION
Xia Z, Wang X, Ye H, Gao C, Zhou X, Chen J, Ge Y, Li J, Zhou Y and Guo Q (2022), Evaluation of strategies for identification of infants with pathogenic glucose-6-phosphate dehydrogenase variants in China.
Front. Genet. 13:844381.
doi: 10.3389/fgene.2022.844381

Evaluation of strategies for identification of infants with pathogenic glucose-6-phosphate dehydrogenase variants in China

Zhongmin Xia[1†], Xudong Wang[1†], Huiming Ye[2†], Chunliu Gao[1†], Xiaoman Zhou[1], Jing Chen[3], Yunsheng Ge[1], Juan Li[2], Yulin Zhou[1*] and Qiwei Guo[1*]

[1]United Diagnostic and Research Center for Clinical Genetics, Women and Children's Hospital, School of Medicine and School of Public Health, Xiamen University, Xiamen, Fujian, China, [2]Department of Clinical Laboratory, Women and Children's Hospital, School of Medicine, Xiamen University, Xiamen, Fujian, China, [3]Department of Child Health, Women and Children's Hospital, School of Medicine, Xiamen University, Xiamen, Fujian, China

Glucose-6-phosphate dehydrogenase (G6PD) deficiency, which is caused by pathogenic variants of *G6PD* that result in decreased G6PD activity, is an X-linked inherited inborn error of metabolism that occurs worldwide. Individuals with G6PD deficiency and heterozygous females with normal G6PD activity (i.e., all individuals with pathogenic *G6PD* variants) are at risk of developing hemolytic anemia under increased oxidative challenge. However, this risk can be minimized by timely diagnosis. Currently, two assays are used to diagnose G6PD deficiency in China: evaluation of enzymatic activity and targeted genotyping. In terms of identification of all individuals with pathogenic *G6PD* variants, the performance and cost of different diagnostic strategies (isolated or combined evaluation of G6PD activity and *G6PD* genotyping) can vary, and these factors should be comprehensively evaluated. In this study, we examined 555 infants (437 males and 118 females) who were positive for the newborn screening of G6PD deficiency. We first evaluated the diagnostic performances of enzymatic testing and targeted genotyping. Both assays attained 100% specificities and positive predictive values for both male and female infants. In contrast, the sensitivities and negative predictive values (NPVs) of the diagnostic tests were different for male and female infants. For male infants, the sensitivities were 99.8 and 98.3%, and the NPVs were 94.1% and 69.6%, for enzymatic testing and targeted genotyping, respectively. For female infants, the sensitivities were 62.5% and 97.9%, and the NPVs were 37.9% and 91.7%, for enzymatic testing and targeted genotyping, respectively. We also evaluated the cost of the five different diagnostic strategies. The combination of G6PD activity testing of all infants, followed by genotyping of female infants with normal G6PD activity, attained high diagnostic sensitivity (99.8%) at a low cost (8.60 USD per diagnosed case). In the future, simultaneous examination of G6PD activity and whole-exon or whole-gene *G6PD* sequencing could become a standard clinical practice. Our data provide references for clinical practice on the standardization of current and future interventions for G6PD deficiency in China.

KEYWORDS

G6PD deficiency, enzymatic activity, genotyping, cost analysis, diagnostic performance

Introduction

Glucose-6-phosphate dehydrogenase (G6PD), which is ubiquitously expressed in mammalian cells, functions as an oxidoreductase that catalyzes the oxidation of glucose-6-phosphate to 6-phosphogluconolactone while reducing nicotinamide adenine dinucleotide phosphate (NADP) to NADPH (Stanton 2012; Luzzatto, et al., 2020). NADPH is an electron donor that plays key roles in numerous biological processes, such as the biosynthesis of deoxyribonucleotides and fatty acids, metabolism of many drugs and xenobiotics, and defense against oxidative challenge (Stanton 2012; Luzzatto, et al., 2020). NADPH is an important antioxidant in red blood cells as it is involved in the enzymatic pathways that remove intracellular H_2O_2 (Stanton 2012; Luzzatto, et al., 2020). G6PD deficiency, caused by pathogenic variants of *G6PD* that result in decreased G6PD activity, is an X-linked inherited inborn error of metabolism that was the first identified red cell enzymopathy (Alving, et al., 1956). It is estimated that over 500 million people are affected by G6PD deficiency worldwide (Nkhoma, et al., 2009; Luzzatto, et al., 2020). However, the prevalence varies among different populations and is relatively high in Africa, Southern Europe, the Middle East, Southeast Asia, and the Mediterranean (Nkhoma, et al., 2009; Howes, et al., 2012). In China, the prevalence of G6PD deficiency varied in different provinces with regional and ethnic features and the integrated prevalence is approximately 0.767% (Liu, et al., 2020).

Although most individuals with G6PD deficiency are asymptomatic throughout their lifetime, they are at risk of developing acute, sometimes fatal, hemolytic anemia when oxidative challenge increases in red blood cells (Luzzatto, et al., 2020). Such scenarios can occur following the ingestion of fava beans, the intake of specific drugs (e.g., primaquine and rasburicase), and, in rare cases, infection (Luzzatto and Arese 2018; Luzzatto, et al., 2020; Onori, et al., 2021; Yang, et al., 2021). However, the risk of hemolytic anemia can be minimized by timely diagnosis of G6PD deficiency because the intake of these foods and drugs can then be avoided. In China, newborn screening (NBS) for G6PD deficiency, in which a fluorescent spot test is used to evaluate G6PD activity in a dried blood spot sample (Wang, et al., 2021), is the first-tier test for the timely diagnosis of G6PD deficiency. As illustrated in our previous study, infants with positive screening results, who are considered at high risk for G6PD deficiency, are recalled and subjected to further diagnostic testing to identify the G6PD-deficient infants (Wang, et al., 2021). In addition to G6PD-deficient infants, female infants with heterozygous pathogenic *G6PD* variants whose G6PD activity levels are normal should also be identified. These females are at risk of G6PD deficiency-associated complications, such as hemolysis when challenged by oxidizing agents (Shah, et al., 2012). In this sense, all infants with pathogenic *G6PD* variants should be diagnosed.

Several assays have been developed for the diagnosis of G6PD deficiency worldwide (Alam, et al., 2018; Ley, et al., 2022; Pal, et al., 2019; Roh, et al., 2016; von Fricken, et al., 2014; Zobrist, et al., 2021). Currently, two assays are approved by the domestic Food and Drug Administration for use in diagnosis of G6PD deficiency in China: evaluation of G6PD activity and targeted *G6PD* genotyping (Liu, et al., 2020; Luzzatto, et al., 2020). These two assays have been used in the national NBS program which delineated the profiles of G6PD deficiency in China (Liu, et al., 2020). Compared with G6PD activity testing, targeted genotyping has better sensitivity for diagnosing female heterozygotes (Xia, et al., 2016; Islam, et al., 2018). Previously, we reported the NBS program in Xiamen City and indicated a 1.39% prevalence of G6PD deficiency in this city (Wang, et al., 2021). Moreover, we noticed that in clinical practice of China, the diagnostic strategy (isolated or combined evaluation of G6PD activity and *G6PD* genotyping) varies and mainly depends on the opinions of physicians or the choice of guardians after genetic counseling. In terms of identification of all infants with pathogenic *G6PD* variants, the performance of different diagnostic strategies could differ and should be comprehensively evaluated, which is urgent considering the amount of affected babies in China. Moreover, in an era of globally contracting health care resources, the costs of diagnostic strategies are crucial concerns, especially in underdeveloped areas with a high prevalence of this genetic defect.

In this study, we aimed to evaluate the performances and costs of diagnostic strategies that are approved and frequently used in China for diagnosing individuals with pathogenic *G6PD* variants from infants with positive NBS results.

Materials and methods

Subjects

Based on NBS and diagnostic procedures in China (Wang, et al., 2021), infants with positive NBS results were recalled for diagnostic testing for G6PD deficiency. After obtaining informed consent from guardians, 555 infants (437 males and 118 females) with positive NBS results were recruited in 2020 in NBS center, Women and Children's Hospital of Xiamen University. These infants underwent diagnostic G6PD activity testing and targeted *G6PD* variant genotyping simultaneously. The ages of the infants at the time of sampling are shown in Table 1.

TABLE 1 Age of infants at the time of sampling for the diagnostic testing of G6PD deficiency.

Age (day)	Number of males	Number of females	Total number
1–30	240	49	289[a]
31–60	155	54	209
61–90	20	8	28
91–120	8	3	11
121–150	7	4	11
151–180	7	0	7
Total	437	118	555

[a]In Chinese tradition, people believe that keeping puerpera and neonates at home for approximately 1 month after labor would be good for their health. Although receiving the recall information before 2 weeks after labor, a number of families did not bring their neonates for diagnosis immediately if the neonates did not have visible clinical phenotypes. Therefore, only 289 of 555 neonates get the confirmatory test before 1 month of life.

Diagnostic testing of G6PD activity

G6PD activity was evaluated by determining the ratio of G6PD to 6-phosphogluconate dehydrogenase (6PGD) using the nitroblue tetrazolium G6PD/6PGD test kit (approved number: YZB/0829–2011, Micky Med, Guangzhou, Guangdong, China) according to the manufacturer's protocol. Briefly, 50 uL of EDTA-anticoagulated peripheral blood was used to evaluate the G6PD activity based on the quantification of the product of enzymatic reaction (i.e., NAPDH). In the meantime, 6PGD activity was evaluated as an internal control. A newborn with a G6PD/6PGD ratio <1.0 was considered G6PD-deficient, whereas a G6PD/6PGD ratio ≥1.0 was considered G6PD-normal (Chen, et al., 2018; Fu, et al., 2018; Liu, et al., 2020).

Diagnostic genotyping of target *G6PD* variants

Genomic DNA was extracted from 100 to 200 μl of EDTA-anticoagulated peripheral blood with the Super/HF16 plus DNA Extraction System (MagCore, Xiamen, China). After quantification with a Nanodrop 2000TM Spectrophotometer (Thermo Fisher Scientific, Wilmington, DE, United States), 10 ng of extracted DNA was analyzed using the MeltPro® *G6PD* genotyping kit (approved number: 20153400623, Zeesan Biotech, Xiamen, Fujian, China) to detect 12 common *G6PD* variants: c.95A > G (Gaohe), c.383T > C (Vanua Lava), c.392G > T (Quing Yan), c.487G > A (Mahidol), c.517T > C (Nankang), c.592C > T (Coimbra), c.871G > A (Viangchan), c.1004C > A (Fushan), c.1024C > T (Chinese-5), c.1360C > T (Maewo), c.1376G > T (Canton), and c.1388G > A (Kaiping). The reactions were performed on a SLAN-96 real-time PCR system (Hongshi, Shanghai, China). The PCR amplification and melting curve analyses have been described in detail in a previous report (Wang, et al., 2021).

Sanger sequencing of *G6PD* exons

Sanger sequencing was considered as the gold standard test to evaluate the performance of diagnostic tests. However, since the targeted genotyping demonstrated 100% concordance with Sanger sequencing for all targeted variants (Xia, et al., 2016), we only sequenced those samples which were negative for targeted genotyping instead of sequencing all samples. To perform Sanger sequencing of the *G6PD* coding exons (exons 2–13), genomic DNA (10 ng) was amplified with sequencing primers (Supplementary Table S1) on an ABI-Verity Thermal Cycler (Applied Biosystems, Foster City, CA, United States). The PCR conditions are described in detail in Supplementary Table S2. After amplification, the PCR products were analyzed by a commercial sequencing service (Sangon, Shanghai, China).

Cost analysis

The self-pay costs of these tests were calculated based on the median charges in three provinces with different levels of economic development (Fujian, Guangdong, and Jiangxi) (G6PD activity evaluation: $3; targeted genotyping: $50). The cost of diagnostic testing is denoted as the sum of the cost for diagnostic testing in a specific strategy branch, while the cost of testing per diagnosed case is denoted as the average cost for each diagnosed G6PD deficiency case in a specific strategy branch. The costs of all tests are expressed in United States dollars (USD), with a hypothetical exchange rate of 6.8 to the Chinese currency.

Ethics statement

Signed informed consent was obtained from the guardians of all study subjects. The study protocol was approved by the research ethics committees of the Women and Children's Hospital at the School of Medicine of Xiamen University.

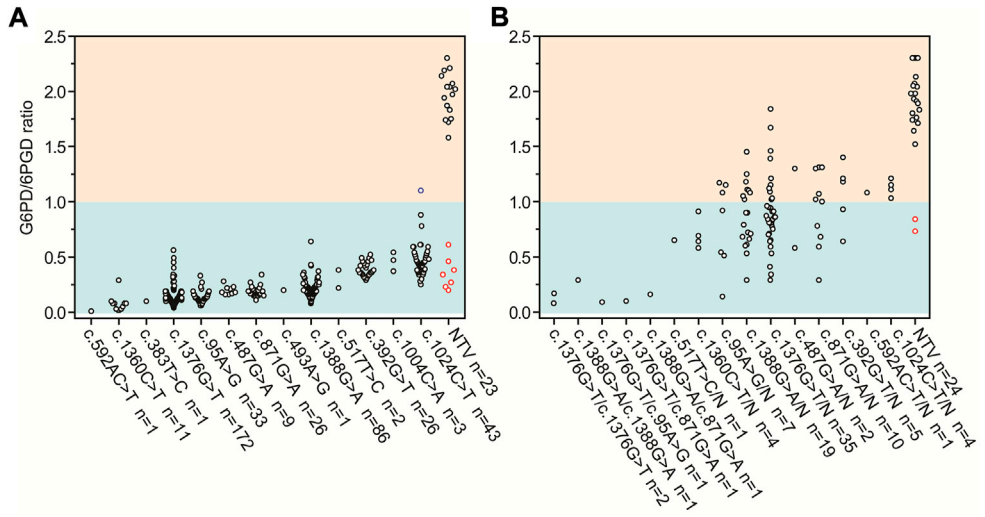

FIGURE 1
G6PD activities and targeted *G6PD* genotypes for **(A)** 437 male and **(B)** 118 female infants with positive newborn screening results. Red circles denote infants with G6PD activity deficiencies but negative for any of the target *G6PD* variants. Blue circle denotes the infant with the c.1024C > T variant and normal G6PD activity. G6PD, glucose-6-phosphate dehydrogenase; 6PGD, 6-phosphogluconate dehydrogenase; n, number; N, normal allele; NTV, negative for target variants.

TABLE 2 Sanger sequencing results of G6PD deficient cases who were negative for targeted genotyping.

Case number	Sex	Age	G6PD/6PGD	Variant
1	Male	1 m 8 d	0.61	c.98T > C
2	Male	1 m 4 d	0.34	c.202G > A (Asahi)
3	Male	19 d	0.27	c.305T > C
4	Male	1 m 9 d	0.23	c.305T > C
5	Male	29 d	0.20	c.305T > C
6	Male	1 m 11 d	0.46	c.739G > A
7	Male	2 m 16 d	0.38	c.835A > T (Chinese-1)
8	Female	1 m	0.84	Heterozygous c.305T > C
9	Female	26 d	0.73	Heterozygous c.563C > T (Mediterranean)

m, month; d, day.

Results

Diagnostic performances of enzymatic testing and targeted genotyping in male infants

The G6PD activity levels and *G6PD* variants of 437 tested male infants are shown in Figure 1A 420 infants were diagnosed with G6PD deficiency and 414 infants carried pathogenic variants based on the results of the G6PD activity test and targeted genotyping, respectively. Seven infants with G6PD activity deficiencies did not carry any of the target variants, and one infant with the c.1024C > T variant had normal G6PD activity (Figure 1A). 23 infants negative for targeted genotyping were examined using Sanger sequencing. The results showed that seven G6PD-defecient infants carried *G6PD* variants outside the detection regions of the MeltPro® *G6PD* genotyping kit (Figure 1A; Table 2), and the c.1024C > T variant was confirmed for the case with normal G6PD activity (Figure 1A). Because the c.1024C > T variant is a known pathogenic variant, this case was considered as a G6PD deficiency. Therefore, 421 out of 437 male infants carried pathogenic *G6PD* variants. The diagnostic

TABLE 3 Diagnostic performances of enzymatic testing and targeted genotyping.

	NBS-positive male infants		NBS-positive female infants	
	Enzymatic testing	Targeted genotyping	Enzymatic testing	Targeted genotyping
Sensitivity	99.8% (420/421)	98.3% (414/421)	62.5% (60/96)	97.9% (94/96)
Specificity	100% (16/16)	100% (16/16)	100% (22/22)	100% (22/22)
Positive predictive value	100% (420/420)	100% (414/414)	100% (60/60)	100% (94/94)
Negative predictive value	94.1% (16/17)	69.6% (16/23)	37.9% (22/58)	91.7% (22/24)

NBS, newborn screening.

performances of G6PD activity testing and targeted genotyping were listed in Table 3.

Diagnostic performances of enzymatic testing and targeted genotyping in female infants

The G6PD activity levels and *G6PD* variants of 118 female infants are shown in Figure 1B. 60 infants were diagnosed with G6PD deficiency and 94 infants carried pathogenic variants based on the results of the G6PD activity test and targeted genotyping, respectively. Two infants with G6PD activity deficiencies did not carry target variants, and 36 heterozygous infants with target variants had normal G6PD activity levels (Figure 1B). 24 infants negative for targeted genotyping were examined using Sanger sequencing. The results showed that two G6PD-deficient cases carry *G6PD* variants outside the detection range of the MeltPro® *G6PD* genotyping kit (Table 2). Therefore, 96 out of 118 female infants carried pathogenic *G6PD* variants. In terms of identification of these cases, the diagnostic performances of G6PD activity testing and targeted genotyping were listed in Table 3.

Comparison of different strategies for the diagnosis of G6PD deficiency

Based on the G6PD activities and genotypes of the 555 analyzed infants, a simplified decision-analytic model was developed to compare the cost of five diagnostic strategies for G6PD deficiency (Figure 2). In strategies 1 and 2, G6PD activity and target *G6PD* variants were independently evaluated, respectively. In strategy 3, all infants were evaluated for G6PD activity, and then female infants with normal G6PD activity levels were examined for target variants. In strategy 4, all infants were first evaluated for target variants, and then G6PD activity levels were examined in infants without target variants. In strategy 5, G6PD activity levels and target variants were simultaneously evaluated for all infants. The cost analysis of different strategies is listed in Table 4.

Discussion

G6PD deficiency is typically referred to as an X-linked recessive genetic trait. However, this is inaccurate because heterozygous females can also be affected (Luzzatto, et al., 2020). The ratio of normal to deficient red blood cells is highly variable among heterozygous females, and their phenotypic spectrum is wide, ranging from normal to G6PD deficiency, like that of hemizygous males (Figure 1B) (He et al., 2020; Wang et al., 2021). Moreover, even in an individual heterozygous female, G6PD activity may vary under different physiological or pathological conditions (Au et al., 2006). Therefore, heterozygous females, regardless of whether their G6PD activity levels are normal in a single assay, should be considered at risk of G6PD deficiency-associated complications, such as hemolysis when challenged by oxidizing agents. In this sense, heterozygous females require a definite diagnosis as much as hemizygous males (Shah et al., 2012).

To identify all infants with pathogenic *G6PD* variants, the enzymatic testing and targeted genotyping attained 100% specificities and positive predictive values for both male and female infants. In contrast, the sensitivities and negative predictive values (NPVs) of the diagnostic tests were different for male and female infants. For male infants, diagnostic sensitivity and NPV were higher for G6PD activity-based methods than for targeted genotyping (Table 3). Cases with G6PD activity deficiency but no target variants carried pathogenic variants outside the detection range (Table 2), confirming that all cases with deficient G6PD activity had genetic causes. In this sense, the diagnostic sensitivities and NPVs of the two methods would be equivalent if the detection range of genotyping was expanded. Notably, one infant with the c.1024C > T variant had normal G6PD activity according to the cut-off value of the detection kit. However, the G6PD activities of infants with the c.1024C > T variant were distinct from those of infants who did not carry variants (Figure 1A). Therefore, we attribute this discordance to the imperfect cut-off value, suggesting that further evaluation and optimization of the cut-

10.3389/fgene.2022.844381

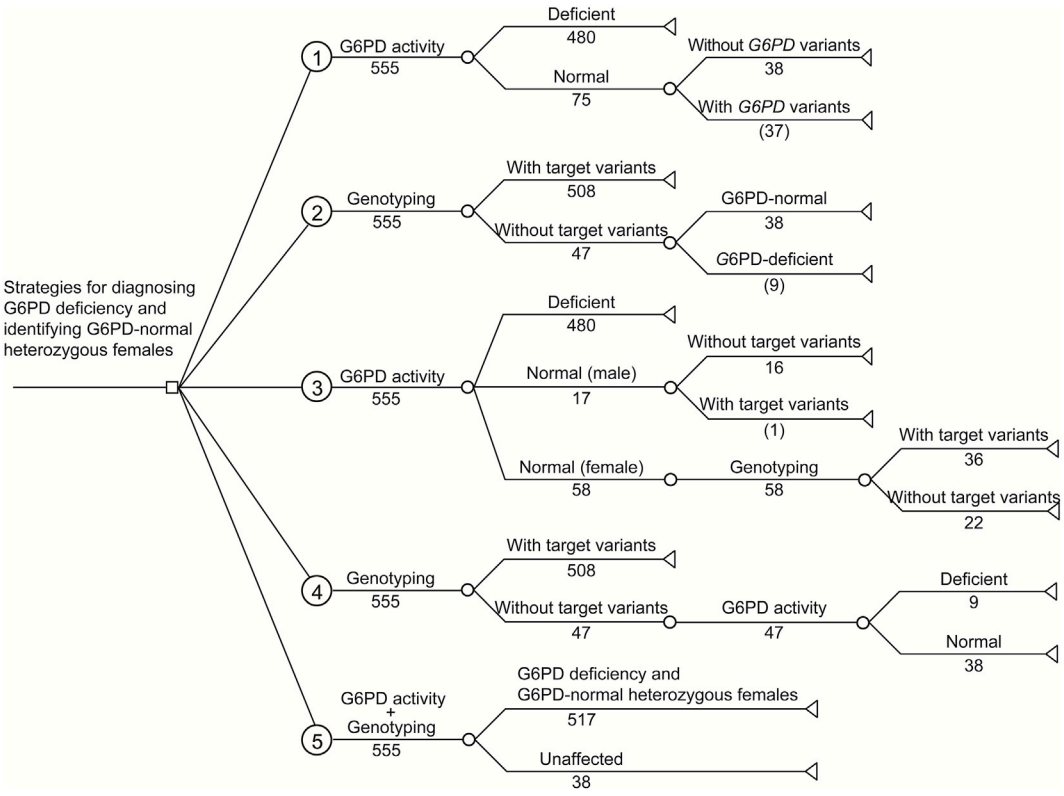

FIGURE 2
Decision-analytic model of five strategies for diagnosing G6PD deficiency and identifying G6PD-normal heterozygous females from infants with positive newborn screening results. Based on the experimental results, the numbers of cases are listed. Number in parenthesis indicates the number of infants with missing diagnosis or identification.

TABLE 4 Cost analysis of different strategies for the diagnosis of G6PD deficiency and female heterozygotes from infants with positive newborn screening results.

Strategy	Diagnosed/ undiagnosed cases	Diagnostic sensitivity (%)	Information of G6PD activity	Information of genotype	Genetic information		Cost of diagnostic testing	Cost of testing per diagnosed case
					Allele frequency	Genotype-phenotype correlation		
1	480/37	92.8	555	0			1,665	3.47
2	508/9	98.3	0	555	√		27,750	54.63
3	516/1	99.8	555	58			4,623	8.60
4	517/0	100	47	555	√		27,891	53.95
5	517/0	100	555	555	√	√	29,415	56.90

off value be considered by the kit manufacturer. We concluded that for the diagnosis of G6PD deficiency in male infants, evaluating G6PD activity had better performance than targeted genotyping. However, if the detection range of genotyping were to be expanded, these methods could have equivalent performance.

In contrast to what was observed for male infants, the diagnostic sensitivity and NPV were noticealy lower for the G6PD activity-based method than for targeted genotyping in female infants (Table 3). This is because a considerable portion of heterozygous females with normal G6PD activity was missed by the enzymatic testing. Therefore, for the diagnosis of all heterozygotes in female

infants, targeted genotyping outperformed G6PD activity testing. Moreover, similar to the findings in male infants, the diagnostic sensitivities of genotyping will increase with the expansion of detected genotypes, as two additional variants were found by Sanger sequencing (Table 2). It should, however, be noted that the G6PD activity test is still very useful for female heterozygotes because it is most predictive of the potential severity of hemolysis.

As shown in Table 4, independent testing of G6PD activity (strategy 1) was the most economical strategy in terms of the cost spent on a diagnosed case (3.47 USD), but had the lowest diagnostic sensitivity (92.8%). In comparison, due to the higher diagnostic sensitivity of genotyping for female infants, the use of genotyping, either independently (strategy 2) or combined with G6PD activity testing (strategies 3–5), noticeably increased the diagnostic sensitivity to 98.3%–100%. Moreover, genotyping enables us to study the genetic characteristics of G6PD deficiency in a specific population (Figure 1), such as allele frequency (strategies 2, 4, and 5) and genotype–phenotype correlations (strategy 5), which are valuable for our understanding of such genetic defects (Liu et al., 2020; Wang et al., 2021). However, in the current state, genotyping markedly increases the testing cost spent on a diagnosed case (Table 4). Therefore, the preferred diagnostic strategy depends on the objective and expectations. For example, for diagnosis only, strategy 3 is recommended. In this strategy, inexpensive testing of G6PD activity is used as a first-tier diagnostic method for all infants, and then genotyping is applied for female infants with normal G6PD activity to further identify heterozygous female infants. This strategy attained high diagnostic sensitivity (99.8%) but retained relatively low testing cost (8.60 USD per diagnosed case) compared to other strategies with comparable diagnostic sensitivities (strategies 4 and 5). Therefore, strategy 3 would be more favorable in underdeveloped regions where medical cost is a crucial concern. It should be noted that the methodology, accuracy, detection range, and the cost of enzymatic activity analysis and genotyping may vary in different countries and regions, suggesting re-evaluation of cost-effectiveness using this decision-analytical model on a case-by-case basis. Moreover, the cost of strategy 3 changes with the proportion of female infants, as more genotyping tests would be needed when the proportion of female infants increases. However, genotyping of *G6PD* is essential not only for diagnosis but also for epidemiological investigations and genotype-phenotype correlation studies, which are of great significance for genetic counseling, prognosis prediction, and the management of G6PD deficiency. Therefore, for the purpose of attaining comprehensive genetic information, simultaneous evaluation of G6PD activity and *G6PD* variants (strategy 5) is recommended despite the considerable cost of genotyping, as it is the only strategy to evaluate genotype-phenotype correlations (Table 4). Notably, with the development of detection methodologies, the detection range and cost of genotyping are continuously increasing and decreasing, respectively. For example, high-throughput sequencing, in which hundreds of genes, including *G6PD*, can be simultaneously and comprehensively examined, has very recently been used for expanded newborn screening (Luo, et al., 2020; Hao, et al., 2021). In this context, the cost for each target gene is limited. Therefore, it is reasonable to expect that simultaneous examination of G6PD activity and sequencing of the entire *G6PD* gene or exons will become the standard clinical practice for the diagnosis of G6PD deficiency in the near future.

In conclusion, we demonstrated the diagnostic performance of testing based on G6PD activity and targeted *G6PD* genotyping and evaluated the performance and cost of different strategies for the diagnosis of infants with pathogenic *G6PD* variants. Currently, testing all infants for G6PD activity, followed by genotyping of female infants with normal G6PD activity could attain high diagnostic sensitivity at a low cost. In the future, simultaneous examination of G6PD activity and sequencing of the entire *G6PD* gene or exons could become standard practice for the diagnosis of G6PD deficiency and those at risk of G6PD deficiency-associated complications. Our data provide references for the standardization of current and future interventions for G6PD deficiency.

Data availability statement

The original contributions presented in the study are included in the article/supplementary materials, further inquiries can be directed to the corresponding authors.

Ethics statement

The studies involving human participants were reviewed and approved by the Women and Children's Hospital at the School of Medicine of Xiamen University. Written informed consent to participate in this study was provided by the participants' legal guardian/next of kin.

Author contributions

ZX, XW, and XZ performed the *G6PD* genotyping tests. HY and JL performed the G6PD activity tests. ZX, XW, HY, CG, JC, and YG performed subject recruitment, sample collection, and data analysis. QG and YZ conceived and designed the study, QG drafted and revised the manuscript. All authors read and approved the final version of the manuscript.

Funding

This work was supported by the Young and Middle-aged Talent Cultivation Projects of Fujian Province (Grant No. 2019-

ZQNB-32), Medical Innovation Projects of Fujian Province (Grant No. 021CXB025), and Xiamen Science and Technology Major Project (Grant No. 3502Z20171006).

Acknowledgments

We thank all individuals and families for participating in this study.

Conflict of interest

The authors declare that the research was conducted in the absence of any commercial or financial relationships that could be construed as a potential conflict of interest.

Publisher's note

All claims expressed in this article are solely those of the authors and do not necessarily represent those of their affiliated organizations, or those of the publisher, the editors and the reviewers. Any product that may be evaluated in this article, or claim that may be made by its manufacturer, is not guaranteed or endorsed by the publisher.

Supplementary material

The Supplementary Material for this article can be found online at: https://www.frontiersin.org/articles/10.3389/fgene.2022.844381/full#supplementary-material

References

Alam, M. S., Kibria, M. G., Jahan, N., Price, R. N., and Ley, B. (2018). Spectrophotometry assays to determine G6PD activity from trinity biotech and pointe scientific G6PD show good correlation. *BMC Res. Notes* 11, 855. doi:10.1186/s13104-018-3964-7

Alving, A. S., Carson, P. E., Flanagan, C. L., and Ickes, C. E. (1956). Enzymatic deficiency in primaquine-sensitive erythrocytes. *Science* 124, 484–485. doi:10.1126/science.124.3220.484-a

Au, W. Y., Lam, V., Pang, A., Lee, W. M., Chan, J. L., Song, Y. Q., et al. (2006). Glucose-6-phosphate dehydrogenase deficiency in female octogenarians, nanogenarians, and centenarians. *J. Gerontol. A Biol. Sci. Med. Sci.* 61, 1086–1089. doi:10.1093/gerona/61.10.1086

Chen, Y., Xiu, W., Dong, Y., Wang, J., Zhao, H., Su, Y., et al. (2018). Mutation of glucose-6-phosphate dehydrogenase deficiency in Chinese Han children in eastern Fujian. *Med. Baltim.* 97, e11553. doi:10.1097/MD.0000000000011553

Fu, C., Luo, S., Li, Q., Xie, B., Yang, Q., Geng, G., et al. (2018). Newborn screening of glucose-6-phosphate dehydrogenase deficiency in Guangxi, China: Determination of optimal cutoff value to identify heterozygous female neonates. *Sci. Rep.* 8, 833. doi:10.1038/s41598-017-17667-6

Hao, C., Guo, R., Hu, X., Qi, Z., Guo, Q., Liu, X., et al. (2021). Newborn screening with targeted sequencing: A multicenter investigation and a pilot clinical study in China. *J. Genet. Genomics* 49 (1), 13–19. doi:10.1016/j.jgg.2021.08.008

He, Y., Zhang, Y., Chen, X., Wang, Q., Ling, L., and Xu, Y. (2020). Glucose-6-phosphate dehydrogenase deficiency in the Han Chinese population: Molecular characterization and genotype-phenotype association throughout an activity distribution. *Sci. Rep.* 10, 17106. doi:10.1038/s41598-020-74200-y

Howes, R. E., Piel, F. B., Patil, A. P., Nyangiri, O. A., Gething, P. W., Dewi, M., et al. (2012). G6PD deficiency prevalence and estimates of affected populations in malaria endemic countries: A geostatistical model-based map. *PLoS Med.* 9, e1001339. doi:10.1371/journal.pmed.1001339

Islam, M. T., Sarker, S. K., Talukder, S., Bhuyan, G. S., Rahat, A., Islam, N. N., et al. (2018). High resolution melting curve analysis enables rapid and reliable detection of G6PD variants in heterozygous females. *BMC Genet.* 19, 58. doi:10.1186/s12863-018-0664-1

Ley, B., Winasti Satyagraha, A., Kibria, M. G., Armstrong, J., Bancone, G., Bei, A. K., et al. (2022). Repeatability and reproducibility of a handheld quantitative G6PD diagnostic. *PLoS Negl. Trop. Dis.* 16, e0010174doi:10.1371/journal.pntd.0010174

Liu, Z., Yu, C., Li, Q., Cai, R., Qu, Y., Wang, W., et al. (2020). Chinese newborn screening for the incidence of G6PD deficiency and variant of G6PD gene from 2013 to 2017. *Hum. Mutat.* 41, 212–221. doi:10.1002/humu.23911

Luo, X., Sun, Y., Xu, F., Guo, J., Li, L., Lin, Z., et al. (2020). A pilot study of expanded newborn screening for 573 genes related to severe inherited disorders in China: Results from 1, 127 newborns. *Ann. Transl. Med.* 8, 1058. doi:10.21037/atm-20-1147

Luzzatto, L., Ally, M., and Notaro, R. (2020). Glucose-6-phosphate dehydrogenase deficiency. *Blood* 136, 1225–1240. doi:10.1182/blood.2019000944

Luzzatto, L., and Arese, P. (2018). Favism and glucose-6-phosphate dehydrogenase deficiency. *N. Engl. J. Med.* 378, 60–71. doi:10.1056/nejmra1708111

Nkhoma, E. T., Poole, C., Vannappagari, V., Hall, S. A., and Beutler, E. (2009). The global prevalence of glucose-6-phosphate dehydrogenase deficiency: A systematic review and meta-analysis. *Blood Cells Mol. Dis.* 42, 267–278. doi:10.1016/j.bcmd.2008.12.005

Onori, M. E., Ricciardi Tenore, C., Urbani, A., and Minucci, A. (2021). Glucose-6-phosphate dehydrogenase deficiency and hydroxychloroquine in the COVID-19 era: A mini review. *Mol. Biol. Rep.* 48, 2973–2978. doi:10.1007/s11033-021-06234-y

Pal, S., Bansil, P., Bancone, G., Hrutkay, S., Kahn, M., Gornsawun, G., et al. (2019). Evaluation of a novel quantitative test for glucose-6-phosphate dehydrogenase deficiency: Bringing quantitative testing for glucose-6-phosphate dehydrogenase deficiency closer to the patient. *Am. J. Trop. Med. Hyg.* 100, 213–221. doi:10.4269/ajtmh.18-0612

Roh, M. E., Oyet, C., Orikiriza, P., Wade, M., Mwanga-Amumpaire, J., Boum, Y., 2nd, et al. (2016). Screening for glucose-6-phosphate dehydrogenase deficiency using three detection methods: A cross-sectional survey in southwestern Uganda. *Am. J. Trop. Med. Hyg.* 95, 1094–1099. doi:10.4269/ajtmh.16-0552

Shah, S. S., Diakite, S. A., Traore, K., Diakite, M., Kwiatkowski, D. P., Rockett, K. A., et al. (2012). A novel cytofluorometric assay for the detection and quantification of glucose-6-phosphate dehydrogenase deficiency. *Sci. Rep.* 2, 299. doi:10.1038/srep00299

Stanton, R. C. (2012). Glucose-6-phosphate dehydrogenase, NADPH, and cell survival. *IUBMB Life* 64, 362–369. doi:10.1002/iub.1017

Von Fricken, M. E., Weppelmann, T. A., Eaton, W. T., Masse, R., Beau de Rochars, M. V., and Okech, B. A. (2014). Performance of the carestart glucose-6-phosphate dehydrogenase (G6PD) rapid diagnostic test in Gressier, Haiti. *Am. J. Trop. Med. Hyg.* 91, 77–80. doi:10.4269/ajtmh.14-0100

Wang, X., Xia, Z., He, Y., Zhou, X., Zhang, H., Gao, C., et al. (2021). Newborn screening for G6PD deficiency in Xiamen, China: Prevalence, variant spectrum, and genotype-phenotype correlations. *Front. Genet.* 12, 718503doi:10.3389/fgene.2021.718503

Xia, Z., Chen, P., Tang, N., Yan, T., Zhou, Y., Xiao, Q., et al. (2016). Rapid detection of G6PD mutations by multicolor melting curve analysis. *Mol. Genet. Metab.* 119, 168–173. doi:10.1016/j.ymgme.2016.07.006

Yang, H. C., Ma, T. H., Tjong, W. Y., Stern, A., and Chiu, D. T. (2021). G6PD deficiency, redox homeostasis, and viral infections: Implications for SARS-COV-2 (COVID-19). *Free Radic. Res.* 55, 364–374. doi:10.1080/10715762.2020.1866757

Zobrist, S., Brito, M., Garbin, E., Monteiro, W. M., Clementino Freitas, S., Macedo, M., et al. (2021). Evaluation of a point-of-care diagnostic to identify glucose-6-phosphate dehydrogenase deficiency in Brazil. *PLoS Negl. Trop. Dis.* 15, e0009649. doi:10.1371/journal.pntd.0009649

frontiers | Frontiers in Pediatrics

TYPE Clinical Trial
PUBLISHED 06 October 2022
DOI 10.3389/fped.2022.1001789

OPEN ACCESS

EDITED BY
Mingbang Wang,
South China Hospital of Shenzhen University, China

REVIEWED BY
Yang Liu,
Shenzhen University, China
Xueying Zhang,
Tongji University, China
Mohsen Norouzinia,
Shahid Beheshti University of Medical Sciences, Iran

*CORRESPONDENCE
Xiaowei Zhang
zhangivy726@163.com

†These authors have contributed equally to this work and share first authorship

SPECIALTY SECTION
This article was submitted to Genetics of Common and Rare Diseases, a section of the journal Frontiers in Pediatrics

RECEIVED 24 July 2022
ACCEPTED 29 August 2022
PUBLISHED 06 October 2022

CITATION
Huang C, Lyu J, Chu C, Ge L, Peng Y, Yang Z, Xiong S, Wu B, Chen X and Zhang X (2022) Dietary fiber and probiotics based on gut microbiota targeting for functional constipation in children with cerebral palsy. *Front. Pediatr.* 10:1001789. doi: 10.3389/fped.2022.1001789

Dietary fiber and probiotics based on gut microbiota targeting for functional constipation in children with cerebral palsy

Congfu Huang[1†], Jinli Lyu[2†], Chunuo Chu[3†], Lan Ge[4], Yuanping Peng[5], Zhenyu Yang[6], Shenghua Xiong[1], Bin Wu[1], Xiao Chen[1] and Xiaowei Zhang[2*]

[1]Department of Pediatrics, Longgang District Maternity and Child Healthcare Hospital, Shenzhen, China, [2]Department of Obstetrics and Gynecology, Peking University Shenzhen Hospital, Shenzhen, China, [3]Shenzhen Middle School, Shenzhen, China, [4]Department of Nutrition, BGI Nutrition Precision Co., Ltd., Shenzhen, China, [5]The Outpatient Department, Longgang District Social Welfare Center, Shenzhen, China, [6]Department of Microbial Research, WeHealthGene Institute, Joint Laboratory of Micro-Ecology and Children's Health, Shenzhen Children's Hospital, Shenzhen WeHealthGene Co., Ltd., Shenzhen, China

Gastrointestinal (GI) disorders are very common among children with cerebral palsy. Gut microbiota has been confirmed to maintain normal GI physiological function and further contributed to cerebral palsy through the gut-brain axis. Our study was to investigate the effect of dietary fiber combined with probiotics on functional constipated children with cerebral palsy. In total, 35 patient children were enrolled and divided into general diet group ($n = 14$) and liquid diet group ($n = 21$). All the participants received Compound Dietary Fiber (CDF) for 1 month and lactic acid-producing and butyric acid-producing probiotics for 6 months. After a 1-month intervention, the frequency of spontaneous and manual defecation, and Bristol score were all significantly improved ($P < 0.001$). The α-diversity of the gut microbiota was significantly increased after a 1-month intervention ($P < 0.05$), with a higher abundance of butyric acid-producing bacteria and a lower abundance of opportunistic pathogens ($P < 0.05$, FDR < 0.05). However, the impersistent effect of the 6-month intervention suggested the insufficient impact of intaking probiotics alone and the short duration of CDF intervention. Moreover, although the intervention had affected the constipation symptoms equally in cerebral palsy children with a general diet and liquid diet, the general diet group showed a greater and more durable change in gut microbiota and clinical phenotypes after intervention than the liquid diet group, which indicated that longer intervention time should be considered for liquid diet children. This study not only illustrated that supplementation of dietary fiber combined with probiotics can improve functional constipation in children with cerebral palsy, but also provides guidance for optimal intervention strategy for future studies, which will further benefit cerebral palsy children.

Clinical trial registration: http://www.chictr.org.cn/showproj.aspx?proj=46902, identifier: ChiCTR1900028257.

KEYWORDS

gut microbiota, dietary fiber, probiotics, cerebral palsy, functional constipation

Introduction

Gastrointestinal (GI) disorders are very common among children with cerebral palsy, among which the most common one is constipation. The incidence of constipation in children with cerebral palsy reaches 26–74%, which is much higher than it in healthy children (1–3). It is often accompanied by other symptoms, such as boating, vomiting, gastroesophageal refluxing, and GI bleeding (4). Recurrent constipation in children with cerebral palsy is a kind of functional constipation that is defined as the disorder of brain-gut axis interaction (5). Gut microbiota is crucial to maintain the normal physiological function of the GI tract. The imbalance of gut microbiota will result in GI diseases, including constipation, which may further contribute to the occurrence of cerebral palsy. Adjusting the dietary uptake has been confirmed to be an efficient way to improve GI function by modulating the gut microbiota.

Dietary fiber is a kind of carbohydrate that can be neither digested nor absorbed in the small intestine, and will be fermented by the bacteria in the GI tract (6). Dietary fiber provides a nutrient source for gut microbiota, maintaining the integrity of the intestinal barrier. It has been reported that dietary fiber deficiency can force gut microbiota to use host-secreted mucus glycoproteins as an alternative nutrient source, leading to erosion of the colonic mucus barrier with greater epithelial access and predisposition to colitis (7). In addition, it can stimulate the production of short-chain fatty acids (SCFAs) by modulating the gut microbiota, which will regulate the immune response of the host (8). Psyllium husk is one kind of dietary fiber, consisting of highly branched and gel-forming arabinoxylan, which can be utilized by many members of the gut microbiota as an energy source. Moreover, it is capable of retaining water in the small intestine, thereby increasing water flow into the ascending colon (9). It has been reported that psyllium husk was successfully used in the symptomatic therapy of constipation (10–12). It can improve the defecation frequency and the stool consistency of patients with chronic constipation (11). In addition, it has been listed as recommended dietary fiber for the treatment of chronic constipation by the World Gastroenterology Organization (WGO) and the American Gastroenterology Organization (13, 14). Recent studies have found that psyllium seed husk can be metabolized by gut microbiota and increase the abundance of butyric acid-producing bacteria (9). However, relevant clinical studies are limited to adult patients with chronic constipation, and there is no clinical trial on children with functional constipation.

Probiotics are live bacteria that contribute to human health after an adequate intake. They play crucial roles in maintaining the balance of the gut microbiota. Some probiotics are capable of producing butyric acid, which will maintain the integrity of the intestinal mucosal barrier by keeping the mitochondrial function of colon cells through the activation of the adenylate-activated protein kinase (AMPK) pathway (15). The damage to mitochondrial function may be related to functional dyspepsia and gastrointestinal motility disorder (16, 17). What is more, the decrease in the lactic acid-producing bacteria, such as *Lactobacillus,* might contribute to constipation, and the supplementation with *Lactobacillus* alleviates the symptoms of constipation (18, 19).

The aim of our study was to evaluate the efficacy of dietary fiber combined with probiotics on functional constipation in children with cerebral palsy. We compared the changes in gut microbiota before and after the intervention, especially the abundance of butyric acid- and lactic acid-producing bacterial genera.

Methods

Participant recruitment

A randomized controlled study was conducted. The study was approved by the Department of Pediatrics of Longgang District Maternity and Child Healthcare Hospital. Informed consent was obtained from all guardians of children (Ethical Approval Number: LGFYYXLLLQ-2020-002).

A total of 35 children with cerebral palsy were collected from Longgang District Social Welfare Center, all of whom experienced functional constipation and long-term bedridden and Gross Motor Function Classification System (GMFCS) level III or above. They were divided into two groups based on their daily dietary composition: 21 children with a liquid diet and 14 children with a general diet. In addition, 21 healthy children of the same age without constipation were selected as a reference group. The Nutrition Department of the Welfare Center prepared the daily diet of all the children under the supervision of a nutritionist. The liquid diet mainly consisted of milk, rice soup, and rice powder, while the general diet was primarily made up of cereals, potatoes, beans, fruits, vegetables, and a small amount of animal protein and fat. All of the participants met the diagnostic criteria for cerebral palsy, excluding those who had been diagnosed with metabolic diseases, complicated serious infections, and who had used antibiotics or probiotics within 2 weeks of intervention.

All the cerebral palsy children were administrated with Compound Dietary Fiber (CDF) powder and probiotics. CDF contained psyllium seed husk provided by BGI Precision Nutrition (Shenzhen) Technology Co., Ltd., China, which was packed as 20 g/bag. Two types of probiotic products were used in this study. One was Umeta® YiChang provided by BGI Precision Nutrition (Shenzhen) Technology Co., Ltd., China, which is administered with a dose of no $<1.8 \times 10^{10}$ CFU/sachet and consists of *Lactobacillus rhamnosus, Lactobacillus acidophilus, Lactobacillus paracasei, Lactobacillus plantarum, Bifidobacterium animalis subsp. lactis, sorbitol, fructose-oligosaccharides, and xylose*. The other one was

ChangLekang® (Shandong Sinovac Biopharma Co., Ltd., China), administered at a dose of 500 mg/day and includes *Clostridium butyricum* $\geq 1.0 \times 10^7$ CFU/g and *Bifidobacterium* $\geq 1.0 \times 10^6$ CFU/g.

Intervention

About 5 g of CDF powder was added on the 1st day for all cerebral palsy children. If no obvious GI symptoms occurred within 24 h after taking the powder, the dose should be increased by 5 g per day for those without spontaneous defecation, and the maximum daily dose should not exceed 20 g in the 1st week. In the 2nd week, the participants were given the optimal dose continuously for 1 month. At the same time, all cerebral palsy children were provided probiotics orally (1 bag/day) for 6 months. Stool samples were collected from all participants at three timepoints, including pre-intervention, 1 month, and 6 months after the intervention. The defecation frequency, stool consistency, frequency of enema used, and weight change were observed and recorded weekly, and water intake was recorded daily.

Clinical assessment

The frequency of spontaneous defecation and manual defecation and stool consistency were used to evaluate the changes in constipation conditions in children with cerebral palsy, and body weight reflected the physical development of the children. Spontaneous defecation refers to defecation without laxative use or manual assistance, indicating the real situation of the intestinal function of participants. Manual defecation refers to those who have no spontaneous defecation for more than 72 h. Stool consistency was determined according to the Bristol stool scale (20). Stools scored as 1 or 2 on the Bristol stool scale were defined as hard, those rated 6 or 7 were defined as loose, and those rated 3, 4, or 5 were defined as normal (21).

Sample collection

About 5 g of sample was collected from the central part of the feces and transferred to −80°C within 1 h after collection. Bacterial DNA was extracted from stool samples through PowerSoil® DNA Isolation Kit (MoBio, America), followed by the amplification of the 16s rRNA gene targeting the variable regions V3–V4. Sequencing was executed using the Illumina Miseq platform, which was performed by Novogene Co., Ltd., in China.

Data processing and statistical analysis

High-quality data obtained after filtration and FLASH (22) were used for sequence splicing. The spliced sequences were then clustered into OTUs via USEARCH. To obtain the taxonomy profile of all samples, the representative OTU sequences were annotated to the Greengenes database (V201305) by the RDP classifier. The abundances of the bacterial taxonomy were then calculated.

According to the composition and relative abundance of all samples at the genus level, R (v3.3.3) was applied to perform the principal coordinate analysis using the ade4 package. Wilcoxon's rank-sum test was applied for comparative analysis at different taxa before and after the intervention, and Benjamini–Hochberg method was used to adjust the differences. Then the bacteria with *P*-values lower than 0.05 and FDR lower than 0.05 were regarded as significantly different ones. At the same time, the gut microbiota of the intervention (cerebral palsy children) group was compared with that of the healthy group. Spearman's Rho was performed to investigate the correlation between bacterial genera and defecation properties.

Results

Participant characteristics and data output

A total of 35 participants were recruited for this study, all of whom completed a 1-month intervention. Twenty-eight patients completed the 6-month intervention, including 19 in the liquid diet group and 9 in the general diet group. All seven patients (two in the liquid diet group and five in the general diet group) who lost during the follow-up were hospitalized for aggravation of the pre-existing disease, and there was no gut microbiota sequencing data of 6-month intervention for these seven patients (Figure 1). No adverse event related to any treatment was observed in this study.

The average age of the 35 children with cerebral palsy was 13.48 ± 3.40 years. The average weekly spontaneous defecation was 2.17 ± 0.57 times, and the Bristol stool score was 1.68 ± 0.47. All the children received 1–3 times manual defecation per week (1.77 ± 0.55 times per week). There were no significant differences between the two groups in baseline characteristics, including age, epilepsy, weekly defecation frequency, stool consistency, and manual defecation frequency ($P > 0.05$). Significant differences in body weight and daily water intake were observed between the two groups. The body weight of the general diet group was higher than that in the liquid diet group ($P < 0.01$) and daily water intake was less than that in the liquid diet group ($P < 0.01$) (Table 1).

A total of 105 stool samples were collected from 28 patients in two different diet groups at three timepoints, and 21 samples

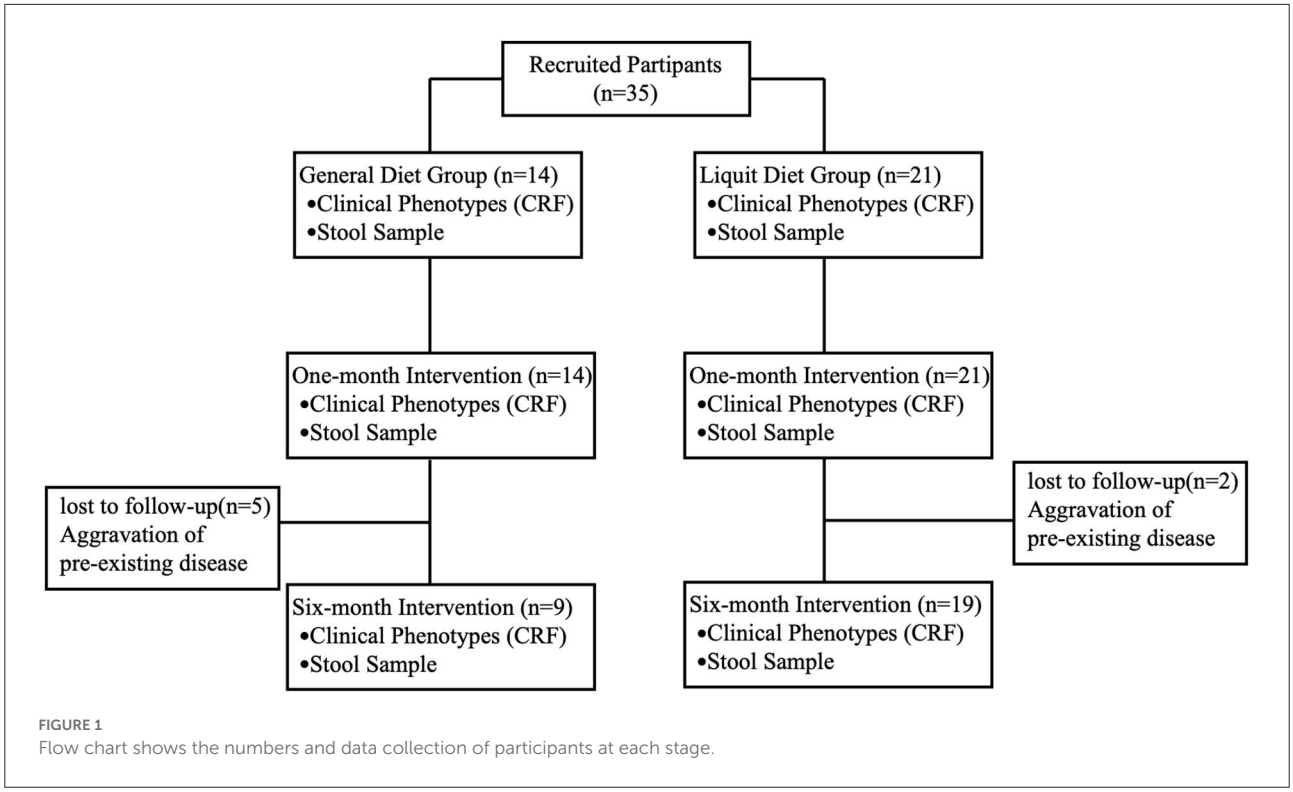

FIGURE 1
Flow chart shows the numbers and data collection of participants at each stage.

TABLE 1 Demographic and clinical characteristics of enrolled children at baseline.

Clinical phenotypes	All participants ($n = 35$)	Liquit diet group ($n = 21$)	General diet group ($n = 14$)	*P*-value between groups
Sex	19/16	9/10	4/5	0.3497
Age	13.48 ± 3.40	12.88 ± 3.09	14.38 ± 3.55	0.2242
Weight	15.75 ± 5.11	13.39 ± 3.22	19.29 ± 5.21	0.001614
Spontaneous defecation (times/week)	2.17 ± 0.57	2.29 ± 0.55	2.00 ± 0.53	0.1482
Bristol score	1.68 ± 0.47	1.71 ± 0.46	1.64 ± 0.50	0.4177
Manual defecation (times/week)	1.77 ± 0.55	1.86 ± 0.56	1.64 ± 0.48	0.2494
Water intake (mL/day)	1085.71 ± 429.87	1242.85 ± 400.71	850 ± 369.51	0.00574

from healthy children were also collected. After 16S rRNA sequencing, 33002.29 ± 1843.772 tags were obtained. The total number of OTUs in the cerebral palsy group was significantly higher than that in the healthy group ($P < 0.001$). A total of 19 phyla and 285 genera were generated from all stool samples by RDP database alignment. The number of genera in patients was significantly higher than in the healthy group ($P < 0.001$).

CDF combined with probiotics improves the constipation symptoms

After the 6-month intervention, the spontaneous defecation frequency of all the children in the cerebral palsy group increased significantly from 2.17 to 3.61 times per week ($P < 0.0001$), while manual defecation decreased from 1.77 to 0.28 times per week. The Bristol score significantly increased from 1.68 ± 0.47 to 3.71 ± 0.60 ($P < 0.0001$). The times of spontaneous defecation and Bristol score increased after 1-month intervention and then showed a decreasing trend at 6-month intervention. The times of manual defecation continued to increase from 1-month to 6-month intervention. Compared with pre-intervention, the times of spontaneous and manual defecation, and Bristol score were all significantly improved at 1-month intervention (Table 2), suggesting that CDF combined with probiotics significantly improved constipation symptoms in children with cerebral palsy.

The effect of dietary structure on constipation was also investigated. No significant differences were observed

10.3389/fped.2022.1001789

TABLE 2 Defecation and weight in two groups at pre-, 1-month, and 6-month intervention.

Clinical phenotypes	Pre-intervention	1-month's intervention	6-month's intervention	*P* for trend
Spontaneous defecation	2.17 ± 0.57	3.91 ± 0.85	3.61 ± 0.68	5.29E-14
General diet group	2.00 ± 0.55	3.71 ± 0.83	3.44 ± 0.73	1.21E-05
Liquid diet group	2.29 ± 0.56	4.05 ± 0.86	3.68 ± 0.82	7.71E-09
Bristol score	1.68 ± 0.47	3.80 ± 0.72	3.71 ± 0.60	1.29E-26
General diet group	1.64 ± 0.50	3.50 ± 0.52	3.89 ± 0.33	7.23E-10
Liquid diet group	1.71 ± 0.46	4.00 ± 0.77	3.63 ± 0.68	1.09E-17
Manual defecation	1.77 ± 0.55	0.25 ± 0.56	0.28 ± 0.60	1.62E-16
General diet group	1.64 ± 0.50	0.36 ± 0.50	0.11 ± 0.33	1.13E-06
Liquid diet group	1.86 ± 0.57	0.19 ± 0.60	0.37 ± 0.68	5.93E-11
Weight	15.75 ± 5.11	16.30 ± 5.16	17.51 ± 5.65	0.556
General diet group	19.29 ± 5.40	20.04 ± 5.15	23.17 ± 4.43	0.627
Liquid diet group	13.39 ± 3.30	13.81 ± 3.41	14.83 ± 3.96	0.556

in spontaneous defecation frequency, manual defecation frequency, and stool consistency between the liquid diet group and the general diet group ($P > 0.05$). The times of spontaneous defecations in both groups continued to increase from 1-month to 6-month intervention (compared with pre-intervention, liquid diet group P (for trend) <0.0001 and general diet group P (for trend) <0.001), while the times of manual defecation was significantly declined (compared with pre-intervention, liquid diet group P (for trend) <0.0001 and general diet group P (for trend) <0.0001). The results demonstrated that the treatment of CDF combined with probiotics had affected constipation symptoms equally in cerebral palsy patients with a general diet and liquid diet.

CDF combined with probiotics changed the structure of gut microbiota

The α-diversity was calculated based on OTUs and is represented by the Shannon index (Figure 2A). There were significant differences among four groups (including patient groups of three timepoints and healthy groups). The α-diversity in the patient groups of three timepoints was significantly higher than in the healthy group. In the patient groups, the α-diversity was significantly increased after 1-month and 6-month intervention periods ($P = 0.0025$ and $P = 0.047$, respectively). While no significant difference was observed between 1-month and 6-month intervention periods ($P = 0.430$). PCA was applied to investigate the correlation and difference between patient groups and healthy groups (Figure 2B). Stool samples of the healthy group were clustered independently and separated from the samples obtained from patients, suggesting that there were significant differences in gut microbiota structure between children with cerebral palsy and healthy children. Samples from 1-month and 6-month interventions were overlapped as well as dissociative, and both were highly co-gathered with samples from pre-intervention, which means that changes in the microbial structure could not deviate from their original state.

The composition of microbiota at the genus level was analyzed in all samples (Figure 3). The top 20 bacterial genera selected from the healthy group were presented. The dominant genera were *Bifidobacterium* and *Prevotella* in patient groups, while *Bacteroides* and *Faecalibacterium* dominated in the healthy group. There were various trends in relative abundances of genera before and after the intervention. *Prevotella*, *Collinsella*, *Sutterella*, and *Megamonas* consistently declined after the intervention. As for *Bacteroides, Faecalibacterium,* and *Lachnospiracea incertae sedis*, although they went upward at the 1-month visit, they all suffered from a downward trend at the 6-month visit. In contrast, there were opposite trends, falling to the lowest points and then rising again, such as *Bifidobacterium*, *Oscillibacter,* and *Parabacteroides*.

Gut microbiota was influenced by diet structure

Considering that diet is a crucial factor that shaped gut microbiota, the gut microbiota was also analyzed based on two diet groups: the liquid diet group and the general diet group. The PCA showed significant differences between the two groups (Figure 4A). There were statistical differences between general diet group and liquid diet group in the following genera: *Bifidobacterium* (8.82 vs. 20.68%, $P = 0.0344$, FDR $= 0.03789$), *Clostridium* IV (5.71 vs. 2.21%, $P = 0.0304$, FDR $= 0.3789$), *Fusobacterium* (3.27 vs. 0.23%, $P = 0.0304$, FDR $= 0.3789$), and *Collinsella* (0.89 vs. 4.34%, $P = 0.0027$, FDR $= 0.3789$). Gut microbiota in the general diet group was dominated by

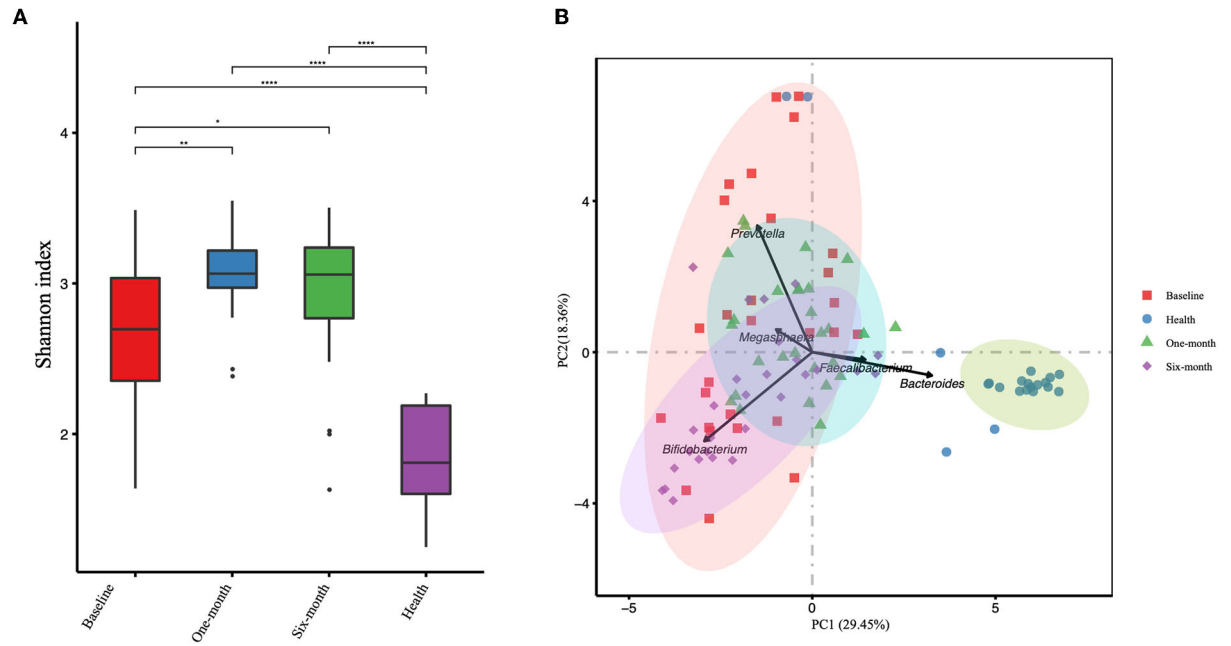

FIGURE 2
The gut microbial α-diversity analyzed by Shannon index **(A)** and the principal component analysis (PCA) **(B)** of the patient group and healthy group are presented. Three timepoints of the patient group are presented, including baseline, 1-month, and 6-month intervention. *P-value <0.05, **P-value <0.01, ****P-value <0.0001.

Prevotella, while that in the liquid diet group was dominated by *Bifidobacterium* (Figure 4B, Supplementary Table 1).

The number of bacterial genera gradually increased from 1 month to 6 months after the intervention in the two groups (Figure 5A). The α-diversity in the general diet group was higher than that in the liquid diet group at all three timepoints of intervention. The α-diversity in the general diet group kept increasing, while that in the liquid diet group increased first and then decreased, but was still higher than the baseline value at the end of the intervention period. The Bray–Curtis distance between the general diet and liquid diet groups gradually narrowed during the 6-month intervention (Figure 5B). It suggested that there was a sustained response in gut microbiota in the general diet group, while inadequate response was presented in the liquid diet group. Therefore, longer intervention time should be considered in future studies.

The top 20 abundant genera were selected to investigate the changes in the microbiota structure in two groups. In the general diet group, most genera responded significantly after 1-month intervention and responded weakly at 6-month intervention. In the liquid diet group, the abundance of most genera increased or decreased after 1-month intervention, and then reversed changes were observed after 6 months of intervention. For example, *Bifidobacterium* decreased at 1-month intervention and then increased at 6-month intervention, whereas *Prevotella* and *Bacteroides* elevated at 1-month intervention and then decreased at 6-month intervention. A few genera showed an increasing or a decreasing trend. The changes in relative abundance showed four patterns in the two groups: rise first and then decline again (*Bacteroides*, *Lachnospiracea incertae sedis*, *Faecalibacterium*, *Clostridium XlVa*, *Blautia*, *Escherichia/Shigella*, *Klebsiella*, *Akkermansia,* and *Streptococcus* in the general diet group; *Prevotella*, *Bacteroides*, *Faecalibacterium*, *Lachnospiracea incerta sedis*, *Clostridium XlVa*, *Akkermansia,* and *Blautia* in the liquid diet group), decline first and then rise (*Prevotella*, *Bifidobacterium*, *Clostridium IV*, *Oscillibacter*, *Fusobacterium*, *Megasphaera*, *Alloprevotella,* and *Collinsella* in the general diet group; *Bifidobacterium,* *Collinsella*, *Parabacteroides*, *Megasphaera*, *Alloprevotella*, *Megamonas*, *Sutterella*, *Gemmiger,* and *Alistipes* in the liquid diet group), sustained increase (*Parabacteroides* in general diet group; *Oscillibacter*, *Clostridium IV*, and *Catenibacterium* in liquid diet group), and sustained decrease (*Sutterella* in the general diet group; *Phascolarctobacterium* in the liquid diet group).

Probiotic supplements elevated the abundance of *Lactobacillus* and *Clostridium*

In order to evaluate the survival ability of the supplied probiotic, including *Bifidobacterium*, *Lactobacillus,* and

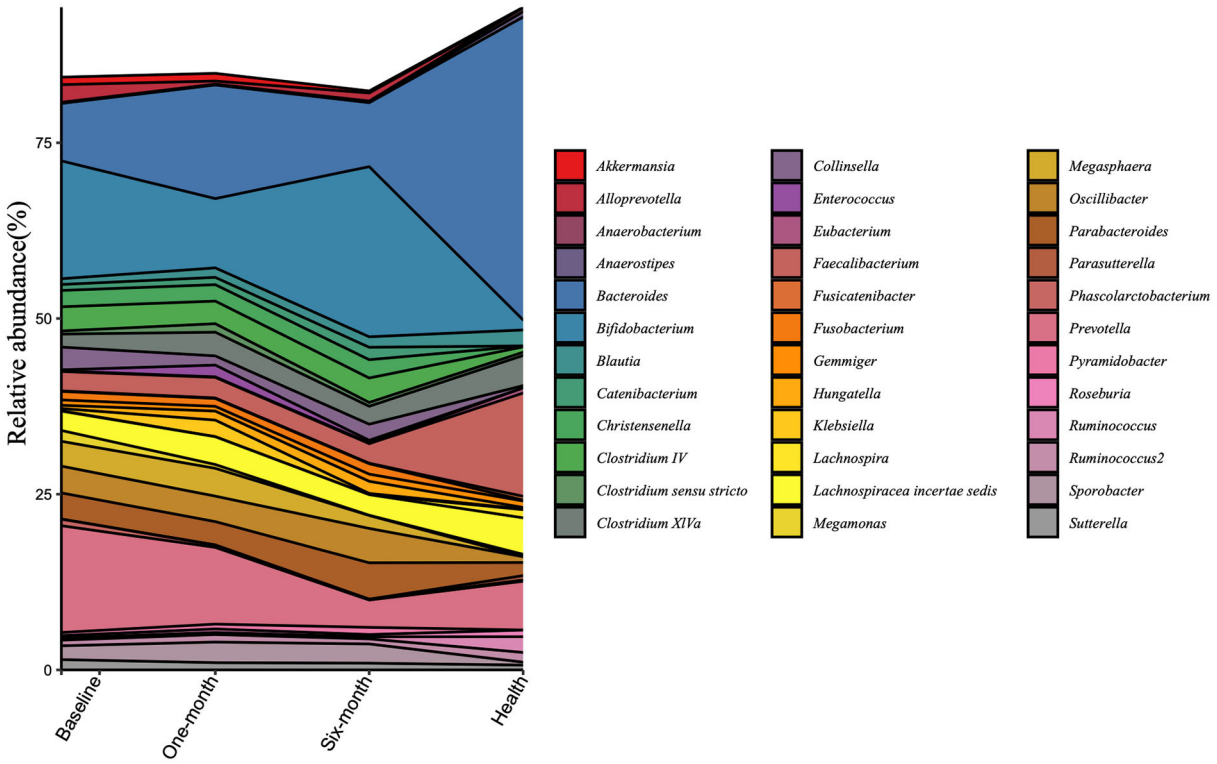

FIGURE 3
Changes in the gut microbiota at the genus level are calculated in the patient group and the healthy group at three timepoints. All the top 20 genera of each group were included.

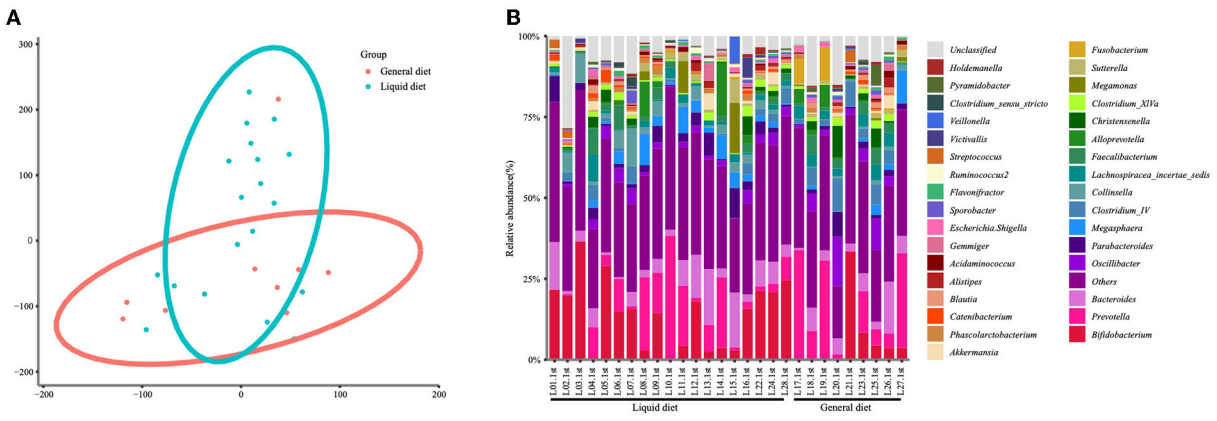

FIGURE 4
Changes in gut microbiota at the genus level in the children of the general diet group and liquid diet group. The clustering diagram of the two groups **(A)** and the stacked bars of the top 30 abundant genera of each participant are shown **(B)**.

Clostridium butyricum, in the GI tract after oral administration, their abundance changes in the two groups of children after intervention were investigated.

Lactobacillus and *Clostridium* consistently increased both in general diet and liquid groups during the 6-month intervention, suggesting that the supplemented probiotics may colonize in the gut. However, *Bifidobacterium* decreased at the 1-month visit and then increased at the 6-month visit, but no statistical differences were observed between the general diet and liquid diet groups (Supplementary Table 4). This finding indicated that the exogenous *Bifidobacterium* showed less ability to colonize

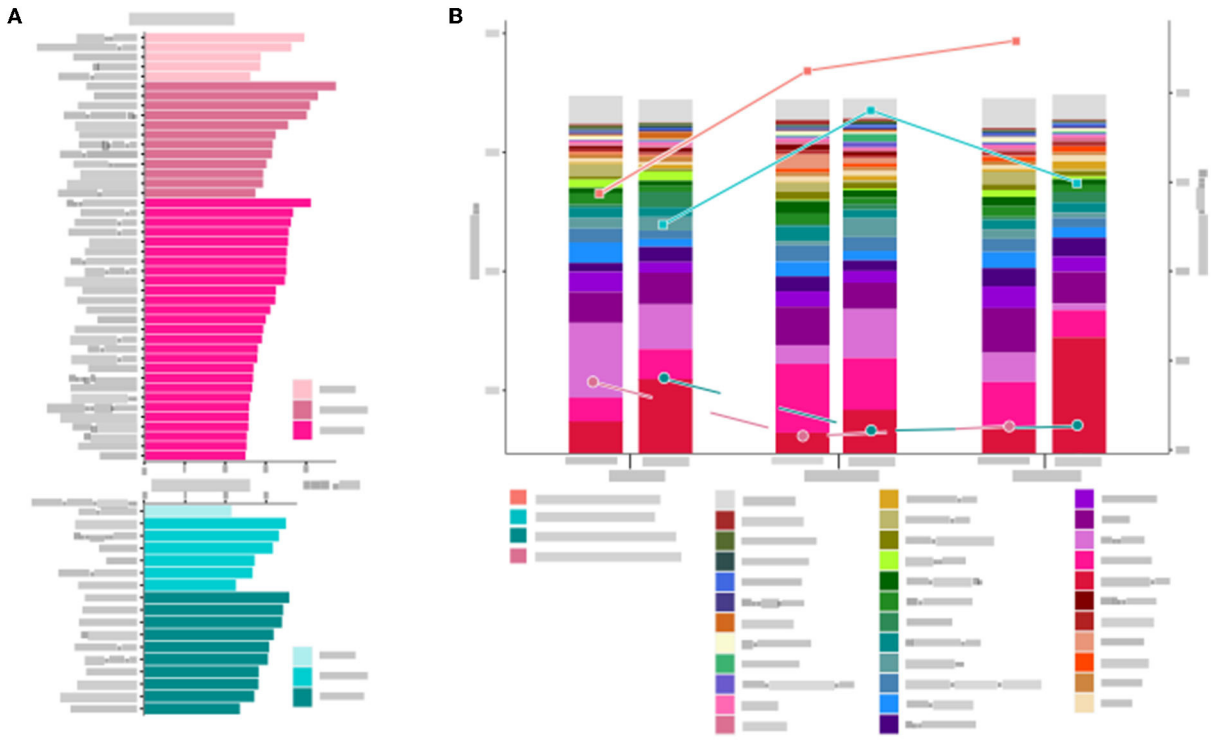

FIGURE 5
Microbial structure and diversity of the gut microbiota in the general diet group and liquid diet group at three timepoints are analyzed. **(A)** Changes in genera at three timepoints. **(B)** The stacked bars show microbial composition at the genus level, and the trend of α- and β- diversity at three timepoints are presented by Shannon index and Brat–Curtis distance, respectively.

the gut than *Lactobacillus* and *Clostridium* in children with constipation.

Clinical phenotypes were correlated with gut microbiota

The correlation analysis was applied to investigate the relationship between gut microbiota and clinical phenotypes, such as body weight, defecation, stool shape, and the need for an enema. In the general diet group, there was a negative correlation between body weight and abundance of *Sutterella,* while positively correlated with *Clostridium IV* at baseline (Figure 6). After the 1-month intervention, manual defecation was positively related to *Oscillibacter* and *Christensenella*, and fecal shape was positively correlated with *Clostridium IV* and *Christensenella*, while the defecation smoothness was negatively correlated with *Clostridium IV*. Therefore, defecation smoothness was positively correlated with *Bifidobacterium* after the 6-month intervention. While in the liquid diet group, the fecal shape was negatively related to *Sutterella* after the 1-month intervention and negatively correlated with *Faecalibacterium* and *Catenibacterium* after the 6-month intervention.

Discussion

Accurate supplementation of dietary fiber or probiotics based on gut microbiota characteristics can effectively improve functional constipation in children with cerebral palsy. In this study, supplementation with dietary fiber and probiotics resulted in a significant improvement in defecation frequency and water content of feces after a 1-month intervention, especially in the liquid diet group. This may be related to the raised abundance of *Lactobacillus* and butyrate-producing genera, which optimized the gut microbiota in children and therefore promoted colonic propulsive peristalsis. However, after short-term dietary fiber and long-term oral probiotics intervention, there were still two patients in the liquid diet group who experienced recurrent constipation and obviously required manual defecation, and the abundance of *Prevotella*, *Oscillibacter*, *Bacteroides,* and *Bifidobacterium* in their gut microbiota also rebounded, suggesting that the intervention time of dietary fiber is too short and supplement of probiotic alone fails to achieve the expected effect. Moreover, the loss of the live bacteria in the probiotic product may lead to lower bacterial colonization in the gut and further influence the outcome of the trial. Therefore, further research on the bacterial stability in the probiotic product is required.

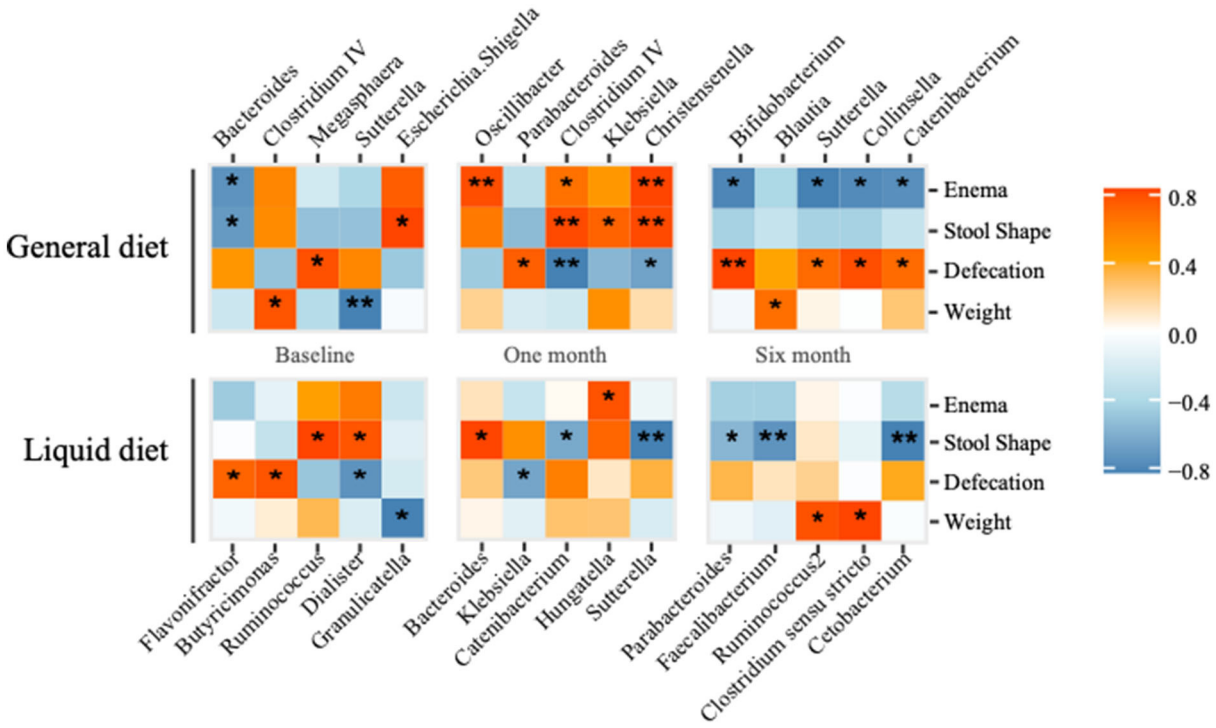

FIGURE 6
Correlation analysis between gut microbiota (top five abundant genera) and clinical phonotypes in general diet and liquid diet groups are calculated. *P-value <0.05, **P-value <0.01.

Moreover, insufficient course of dietary fiber and too little dietary carbohydrate intake may also be responsible for the higher recurrent rate in the liquid diet group.

There were significant differences in the abundance of bacterial genera between the liquid diet group and the general diet group at baseline, including *Fusobacterium*, *Alloprevotella*, *Bifidobacterium*, *Lachnospiracea incertae,* and *Collinsella*, which were similar to our previous study (23). Varied abundance of *Fusobacterium* and *Alloprevotella,* which could cause oral diseases such as periodontitis (24, 25) and intestinal inflammation (26, 27), was observed in the two groups of children. Consumption of milk powder was responsible for the high abundance of *Bifidobacterium* in the liquid diet group (28). Compared with the general diet group, we can see a higher abundance of opportunistic pathogen *Collinsella* and lower butyrate-producing genus *Lachnospiracea incertae* in the liquid diet group, which can induce severe intestinal inflammation (19, 29). The results reflect that the imbalance in the gut microbiota of children in the liquid group leads to more severe GI dysfunction, which is consistent with the incidence of constipation in the liquid group in this study and our previous study (30).

Significant changes in the gut microbiota between pre- and post-interventions were discovered in two groups. Particularly, after 1-month intervention, the abundance of butyrate-producing bacteria like *Bacteroides*, *Lachnospiracea incertae sedis*, *Faecalibacterium,* and *Clostridium XlVa* experienced a pronounced increase, while that of opportunistic pathogens like *Alloprevotella*, *Megasphaera,* and *Collinsella* declined. However, an opposite pattern occurred after the 6-month intervention. The abundance of butyrate-producing genera decreased, while the abundance of opportunistic pathogens rebounded. It was found that both groups showed an increasing trend in α-diversity after the 1-month intervention. Although this trend was more obvious in the liquid diet group, the trend reversed after the 6-month intervention, which may be related to the significant increase in the abundance of *Bifidobacterium* due to the intake of milk powder. In contrast, no significant changes were observed in *Bifidobacterium* in the general diet group before and after the intervention. The Bray–Curtis distance decreased after the intervention, indicating that the intervention could reduce the differences in the gut microbiota between the two groups, which was significantly correlated with the improvement in clinical constipation and was also in line with our expected goal. However, current sequencing technology can only explain the composition of the microbiota. Direct evidence of microbial metabolites and functions associated with the gut microbiome and their role in the progression of constipation in cerebral palsy children still needs further studies (31).

The correlation analysis between clinical phenotypes and gut microbiota in children with cerebral palsy showed that the changes in the abundance of some bacteria in two groups (liquid diet and general diet group) correlated

with constipation symptoms, the times of defecation, and the enema demand. In this study, defecation, stool shape, and enema were significantly correlated with *Sutterella*, *Oscillibacter*, *Clostridium IV*, *Christensenella*, *Bifidobacterium*, *Faecalibacterium,* and *Catenibacterium*. It was reported that *Sutterella* can cause digestive disorders (15), and *Oscillibacter* is associated with ulcerative colitis (32). In contrast, *Clostridium IV*, *Bifidobacterium*, and *Faecalibacterium* are beneficial bacteria in the human gut, which can protect the integrity of intestinal mucosa through metabolites such as short-chain fatty acids (33, 34). Based on correlation analysis, supplementation of butyrate-producing bacteria can reduce intestinal inflammation and relieve GI dysfunction in children with cerebral palsy.

In the current study, we also found that the intervention of diary fiber and probiotics increased the abundance of beneficial bacteria in the gut microbiota, such as *Lactobacillus* and *Bifidobacterium*. However, the abundance of *Bifidobacterium* decreased before increasing. *Bifidobacterium* is the dominant genus in the gut microbiota of infants, and its abundance will decrease along with the maturity of gut microbiota. The abundance of *Bifidobacterium* significantly decreased and that of butyrate-producing bacteria increased after the intake of dietary fiber combined with probiotics, indicating that this intervention method may be beneficial to the maturity of children's gut microbiota. Moreover, in the subsequent probiotic intervention, the abundance of *Bifidobacterium* rose again, indicating that the effect of probiotic intervention alone may be insufficient when compared to combined intervention. Further randomized controlled studies are still needed to prove the independent effect of each product.

The purpose of this study was to solve practical clinical problems. The lack of a control group and relatively small sample size may not reflect the accurate outcomes in the real world. Due to the lack of the previous exploration of intervention dose and course of treatment, the children received probiotics for 6 months but CDF for only 1 month, resulting in recurrent constipation cases in the liquid diet group, which should be improved in the future study. We speculated that if the intervention time of dietary fiber and probiotics is prolonged, constipation in children would show long-term remission, which would further promote the absorption and metabolism of nutrients, improve immunity, and further contribute to the recovery of brain function.

Conclusion

Based on the characteristics of gut microbiota in children with cerebral palsy, different diet structures influence the composition of gut microbiota. Long-term consumption of a liquid diet causes an imbalance in the gut microbiota and thus leads to GI dysfunction in children with cerebral palsy. The supplement of CDF and probiotics can effectively improve this situation, which significantly increased the abundance of protective bacteria and lowered the abundance of symbiotic pathogens. Simultaneously, supplementation of CDF combined with probiotics can improve functional constipation in children with cerebral palsy.

Data availability statement

The data presented in the study are deposited in the NCBI SRA database repository, accession number PRJNA881289.

Ethics statement

The studies involving human participants were reviewed and approved by Department of Pediatrics of Longgang District Maternity and Child Healthcare Hospital. Written informed consent to participate in this study was provided by the participants' legal guardian/next of kin. This study was approved by the Ethics Committee of Longgang District Maternity and Child Healthcare Hospital of Shenzhen city with the registration number of LGFYYXLL-024.

Author contributions

CH and CC conceived the project. CH recruited the participants and performed the sampling. CC assisted the sample collection, responsible for the sample transportation and preservation, as well as the basic information collection, and organized the discussion. LG was responsible for the process of project and participants' follow-up. JL, YP, and ZY performed data analysis. SX, BW, and XC contributed to patients recruiting and information collection. CH, JL, CC, and XZ accomplished the manuscript, among which CH and JL drafted the manuscript. XZ revised the manuscript and responsible for the whole project. All authors contributed to the article and approved the submitted version.

Funding

This work has been strongly supported by Longgang District Science and Technology Innovation Bureau (LGKCYLWS2020104) and National Natural Science Foundation of China (82201793).

Conflict of interest

Author LG was employed by the company BGI Nutrition Precision Co., Ltd. Author ZY was employed by the company Shenzhen WeHealthGene Co., Ltd.

The remaining authors declare that the research was conducted in the absence of any commercial or financial

relationships that could be construed as a potential conflict of interest.

Publisher's note

All claims expressed in this article are solely those of the authors and do not necessarily represent those of their affiliated organizations, or those of the publisher, the editors and the reviewers. Any product that may be evaluated in this article, or claim that may be made by its manufacturer, is not guaranteed or endorsed by the publisher.

Supplementary material

The Supplementary Material for this article can be found online at: https://www.frontiersin.org/articles/10.3389/fped.2022.1001789/full#supplementary-material

References

1. Araújo LA, Silva LR, Mendes FA. Digestive tract neural control and gastrointestinal disorders in cerebral palsy. *J Pediatr.* (2012) 88:455–64. doi: 10.2223/jped.2241

2. Trivić I, Hojsak I. Evaluation and treatment of malnutrition and associated gastrointestinal complications in children with cerebral palsy. *Pediatr Gastroenterol Hepatol Nutr.* (2019) 22:122–31. doi: 10.5223/pghn.222.122

3. Veugelers R, Benninga MA, Calis EA, Willemsen SP, Evenhuis H, Tibboel D, et al. Prevalence and clinical presentation of constipation in children with severe generalized cerebral palsy. *Dev Med Child Neurol.* (2010) 52:e216–21. doi: 10.1111/j.1469-8749.2010.03701.x

4. Quitadamo P, Thapar N, Staiano A, Borrelli O. Gastrointestinal and nutritional problems in neurologically impaired children. *Eur J Paediatr Neurol.* (2016) 20:810–5. doi: 10.1016/j.ejpn.05019

5. Hyams JS, Lorenzo CD, Saps M, Shulman RJ, Tilburg MV. Functional disorders: children and adolescents. *Gastroenterology.* (2016) 150:1456–68.

6. Cantu-Jungles TM, Hamaker BR. New view on dietary fiber selection for predictable shifts in gut microbiota. *mBio.* (2020) 11:19. doi: 10.1128/mBio.02179-19

7. Desai MS, Seekatz AM, Koropatkin NM, Kamada N, Hickey CA. Wolter, M, et al. A dietary fiber-deprived gut microbiota degrades the colonic mucus barrier and enhances pathogen susceptibility. *Cell.* (2016) 167:1339–53.e1321. doi: 10.1016/j.cell.10043

8. Bosch G, Verbrugghe A, Hesta M, Holst JJ, van der Poel AF, Janssens GP, et al. The effects of dietary fibre type on satiety-related hormones and voluntary food intake in dogs. *Br J Nutr.* (2009) 102:318–25. doi: 10.1017/s000711450814 9194

9. Jalanka J, Major G, Murray K, Singh G, Nowak A, Kurtz C, Spiller R. The effect of psyllium husk on intestinal microbiota in constipated patients and healthy controls. *Int J Mol Sci.* (2019) 20:433. doi: 10.3390/ijms2002 0433

10. Ashraf W, Park F, Lof J, Quigley EM. Effects of psyllium therapy on stool characteristics, colon transit and anorectal function in chronic idiopathic constipation. *Aliment Pharmacol Ther.* (1995) 9:639–47. doi: 10.1111/j.1365-1995tb00433.x

11. Erdogan A, Rao SS, Thiruvaiyaru D, Lee YY, Coss Adame E, Valestin J, et al. Randomised clinical trial: mixed soluble/insoluble fibre vs. psyllium for chronic constipation. *Aliment Pharmacol Ther.* (2016) 44:35–44. doi: 10.1111/apt. 13647

12. Yang J, Wang HP, Zhou L, Xu CF. Effect of dietary fiber on constipation: a meta analysis. *World J Gastroenterol.* (2012) 18:7378–83. doi: 10.3748/wjg.v18.i48.7378

13. Bharucha AE, Pemberton JH, Locke GR III. American Gastroenterological Association technical review on constipation *Gastroenterology.* (2012) 144:218–38. doi: 10.1053/j.gastro.10028

14. Lindberg G, Hamid SS, Malfertheiner P, Thomsen OO, Fernandez LB, Garisch J, et al. World gastroenterology organisation global guideline: constipation–a global perspective. *J Clin Gastroenterol.* (2011) 45:483–7. doi: 10.1097/MCG.0b013e31820fb914

15. Zhang JQ, Zhang LY, Wang X, Xie JY, Wang FY, Tang XD, et al. Effects of mitochondrial dysfunction on gastrointestinal dysmotility in functional dyspepsia. *China J Trad Chin Med Pharm.* (2019) 34:3637–3639.

16. Li DD, Jawale CV, Zhou C, Lin L, Trevejo-Nunez GJ, Rahman S, et al. Fungal sensing enhances neutrophil metabolic fitness by regulating antifungal Glut1 activity. *Cell Host Microbe.* (2022) 30:530–44. doi: 10.1016/j.chom.2022.02.017

17. Subramanian S, Huq S, Yatsunenko T, Haque R, Mahfuz M, Alam M, et al. Persistent gut microbiota immaturity in malnourished Bangladeshi children. *Nature.* (2014) 510:417–21. doi: 10.1038/nature13421

18. Chen J, Ryu E, Hathcock M, Ballman K, Chia N, Olson JE, et al. Impact of demographics on human gut microbial diversity in a US Midwest population. *PeerJ.* (2016) 4:e1514. doi: 10.7717/peerj.1514

19. Chen J, Wright K, Davis JM, Jeraldo P, Marietta EV, Murray J, et al. An expansion of rare lineage intestinal microbes characterizes rheumatoid arthritis. *Gen Med.* (2016) 8:43. doi: 10.1186/s13073-016-0299-7

20. Lewis SJ, Heaton KW. Stool form scale as a useful guide to intestinal transit time. *Scand J Gastroenterol.* (1997) 32:920–4. doi: 10.3109/00365529709011203

21. Tian H, Ding C, Gong J, Ge X, McFarland LV, Gu L, et al. Treatment of slow transit constipation with fecal microbiota transplantation: a pilot study. *J Clin Gastroenterol.* (2016) 50:865–70. doi: 10.1097/mcg.0000000000000472

22. Magoč T, Salzberg SL. FLASH: fast length adjustment of short reads to improve genome assemblies. *Bioinformatics.* (2011) 27:2957–63. doi: 10.1093/bioinformatics/btr507

23. Huang C, Li X, Wu L, Wu G, Wang P, Peng Y, et al. The effect of different dietary structure on gastrointestinal dysfunction in children with cerebral palsy and epilepsy based on gut microbiota. *Brain Dev.* (2021) 43:192–9. doi: 10.1016/j.braindev.2020.09.013

24. Ganly I, Yang L, Giese RA, Hao Y, Nossa CW, Morris LG, et al. Periodontal pathogens are a risk factor of oral cavity squamous cell carcinoma, independent of tobacco and alcohol and human papillomavirus. *Int J Cancer.* (2019) 45:775–84. doi: 10.1002/ijc.32152

25. Song B, Ren B, Cheng L. Research progress on the relationship between *Fusobacterium nucleatum* and periodontitis. *J Prevent Treat Stomatol Dis.* (2021) 29:557–61. doi: 10.12016/j.issn.2096-202108.009

26. Liu L, Liang L, Liang H, Wang M, Lu B, Xue M, et al. Fusobacterium nucleatum aggravates the progression of colitis by regulating M1 macrophage polarization via AKT2 pathway. *Front Immunol.* (2019) 10:1324. doi: 10.3389/fimmu.2019.01324

27. Wang CS, Li WB, Wang HY, Ma YM, Zhao XH, Yang H, et al. VSL#3 can prevent ulcerative colitis-associated carcinogenesis in mice. *World J Gastroenterol.* (2018) 24:4254–62. doi: 10.3748/wjg.v24.i37.4254

28. Ch A, Xl A, Lw A, Gfw A, Pw A, Yp B, et al. The effect of different dietary structure on gastrointestinal dysfunction in children with cerebral palsy and epilepsy based on gut microbiota. *Brain Develop.* (2021) 43:192–9.

29. Meehan CJ, Beiko RG. A phylogenomic view of ecological specialization in the lachnospiraceae, a family of digestive tract-associated bacteria. *Gen Biol Evolut.* (2014) 3:703–13. doi: 10.1093/gbe/evu050

30. Zhang A, Huang C, Li X, Peng Y, Wang L. *The Effect of Different Dietary Structure on Gastrointestinal Dysfunction in Children With Cerebral Palsy and Epilepsy Based on Intestinal Flora.* (2020).

31. Rezasoltani S, Ahmadi Bashirzadeh D, Nazemalhosseini Mojarad E, Asadzadeh Aghdaei H, Norouzinia M, Shahrokh S, et al. Signature of gut microbiome by conventional and advanced analysis techniques: advantages and disadvantages. *Middle East J Dig Dis.* (2020) 12:5–11. doi: 10.15171/mejdd.2020.157

32. Makki K, Deehan EC, Walter J, Bckhed F. The impact of dietary fiber on gut microbiota in host health and disease. *Cell Host Microb.* (2018) 23:705–15. doi: 10.1016/j.chom.2018.05.012

33. Martín R, Miquel S, Benevides L, Bridonneau C, Robert V, Hudault S. Functional characterization of novel faecalibacterium prausnitzii strains isolated from healthy volunteers: a step forward in the use of F. *prausnitzii as a Next-Generation. Probio Front Microbiol.* (2017) 8:226. doi: 10.3389/fmicb.2017.01226

34. van Zanten GC, Knudsen A, Röytiö H, Forssten S, Lawther M, Blennow A, et al. The effect of selected synbiotics on microbial composition and short-chain fatty acid production in a model system of the human colon. *PLoS ONE.* (2012) 7:e47212. doi: 10.1371/journal.pone.0047212

frontiers | Frontiers in Pediatrics

TYPE Original Research
PUBLISHED 14 November 2022
DOI 10.3389/fped.2022.999596

OPEN ACCESS

EDITED BY
Mingbang Wang,
South China Hospital of Shenzhen University, China

REVIEWED BY
Bixia Zheng,
Nanjing Children's Hospital, China
Wenjuan Qiu,
Shanghai Jiao Tong University, China

*CORRESPONDENCE
Jian-She Wang
jshwang@shmu.edu.cn

SPECIALTY SECTION
This article was submitted to Genetics of Common and Rare Diseases, a section of the journal Frontiers in Pediatrics

RECEIVED 21 July 2022
ACCEPTED 26 October 2022
PUBLISHED 14 November 2022

CITATION
Du J, Dou L-M, Jin Y-H, Wen Q-F, Lin Y-F and Wang J-S (2022) Glycogen storage disease type Ia misdiagnosed as multiple acyl-coenzyme A dehydrogenase deficiency by mass spectrometry.
Front. Pediatr. 10:999596.
doi: 10.3389/fped.2022.999596

Glycogen storage disease type Ia misdiagnosed as multiple acyl-coenzyme A dehydrogenase deficiency by mass spectrometry

Juan Du[1], Li-Min Dou[2], Yong-Hong Jin[1], Qing-Fen Wen[1], Ya-Fen Lin[1] and Jian-She Wang[2]*

[1]Department of Pediatrics, Jinshan Hospital of Fudan University, Shanghai, China, [2]The Center for Pediatric Liver Diseases, Children's Hospital of Fudan University, Shanghai, China

Objective: To report a case of glycogen storage disease (GSD) type Ia misdiagnosed as multiple acyl-coenzyme a dehydrogenase deficiency (MADD) by mass spectrometry.

Methods: A 7 months old boy was admitted to our hospital for elevated transaminase levels lasting more than 1 month. His blood biochemistry showed hypoglycemia, metabolic acidosis, hyperlipidemia, elevated lactate and uric acid, elevated alanine amino transferase (ALT), aspartate amino transaminase (AST) and gamma-glutamyl transferase (GGT). Mass spectrometry analysis of blood and urine showed elevated blood acylcarnitines and dicarboxylic aciduria, indicating multiple acyl-coenzyme A dehydrogenase deficiency. Sanger sequencing of all exons of glucose-6-phosphatase (G6Pase) and electronic transfer flavoprotein dehydrogenase (ETFDH) was performed for the patient and his parents.

Results: Coding and flanking sequences of the G6Pase gene detected two heterozygous single base substitutions in the boy. One variant was in exon 1 (c.209G > A), Which was also detected in the father. Another was in exon 5 (c.648G > T), which was detected in the mother. Coding and flanking sequences of the ETFDH gene revealed no pathogenic/likely pathogenic variants in the boy.

Conclusion: GSD Ia can manifest elevated blood acyl carnitines and dicarboxylic aciduria which were the typical clinical manifestations of MADD. So the patient with clinical manifestations similar to MADD is in need of differential diagnosis for GSD Ia. Genetic testing is helpful to confirming the diagnosis of inherited metabolic diseases.

KEYWORDS

glycogen storage disease type Ia, glucose-6-Phosphatase, multiple acyl- coenzyme a dehydrogenase deficiency, mass spectrometry, gene variant

Introduction

Glycogen storage disease (GSD) type Ia (OMIM#232200) is a glycogen metabolism disorder due to a gene defect in glucose-6-phosphatase (G6Pase). This disease is autosomal recessive with typical clinical features of hypoglycemia, an enlarged liver, growth retardation and a tendency to bleed, accompanied by hyperlipidemia,

hyperuricemia, and hyperlactatemia. Long-term complications of this disease can include gout, hepatocellular adenoma, platelet dysfunction, renal insufficiency, osteoporosis and others (1). Multiple acyl-coenzyme A dehydrogenase deficiency (MADD) (OMIM#231680) is a fatty acid oxidation metabolic disorder caused by a gene defect in mitochondrial electron transport flavoprotein (ETF) or electronic transfer flavoprotein-ubiquinone oxidoreductase [ETF-QO, also known as electronic transfer flavoprotein dehydrogenase (ETFDH)]. MADD is an autosomal recessive disease with multiple clinical features, predominantly intermittent myasthenia; however, other symptoms such as drowsiness, vomiting, hypoglycemia, metabolic acidosis, and enlarged liver during acute attacks may also be present. GSD Ia shares similar clinical manifestations with MADD, such as hypoglycemia, enlarged liver, elevated liver transaminase, and metabolic acidosis. GSD Ia is rarely reported with abnormal carnitine and/or abnormal urine organic acid levels. A child patient was admitted to the pediatric department of Jinshan Hospital Fudan University in July 2012 with suspicious MADD as diagnosed by mass spectrometry and was eventually diagnosed with GSD Ia by genetic studies. The case is reported below.

Materials and methods

The boy (7 months old) was admitted to our hospital for elevated transaminase levels lasting more than 1 month. One month previously, he was admitted to a local hospital due to bronchopneumonia. During the stay, elevated transaminases were occasionally revealed by laboratory tests. He was referred to us for persistently elevated transaminases during multiple follow-ups and the reappearance of cough and fever two days previously. The child was G1P1 and was born at full-term with a birth weight of 2,290 g. He was once hospitalized for "neonatal hypoglycemia and hyperbilirubinemia" in another hospital with detailed information unavailable. The patient received mixed feeding after his discharge. He drank milk more frequently and appeared easy hungry than the common infant. The child was given solid food supplementation from 4 months and rice supplementation from 7 months, which he liked. The child could raise his head in the third month of age but still could not climb or sit alone at presentation. Both parents of the child were healthy and were in a non-consanguineous marriage with no history of genetic disease.

Physical examination at admission showed a body temperature of 37.4°C, a heart rate of 120 beats/min, a breath count of 35 times/min, and a body weight of 8.75 kg. The child had a round, fleshy face and a loud cry. No jaundice was present in the skin and sclera, and no bleeding or rash was apparent. There was no systemic superficial lymph node enlargement. The bregma was soft and sized 1.0 cm × 1.0 cm. The lip and mouth were not pale and did not exhibit cyanosis, but the throat was congested, and his breath sounds in the lungs were slightly rough with no rattles. The heart rate was regular, and the heart sound was strong with a mild murmur. Significant abdominal distension was observed, and the epigastric veins were obvious. His enlarged liver reached the umbilical level and felt hard, while his enlarged spleen was 3 cm below the costal margin. Limb activity was fair. The simian line was not seen in both hands. The child patient had obvious palmar erythema but no spider angioma. The neurological examination was negative.

Laboratory testing at admission showed low plasma glucose (2.0 mmol/L, reference 3.0–5.9 mmol/L), metabolic acidosis (pH 7.22, PCO_2 4.39 KPa, PO_2 10.6 KPa, HCO_3^- 13.0 mmol/L, BE −13.6 mmol/L), elevated lactate (8.7 mmol/L, reference 0.5–1.6 mmol/L), alanine amino transferase (ALT) (161 U/L, reference 10–60 U/L), aspartate amino transaminase (AST) (377 U/L, reference 8–40 U/L), gamma-glutamyl transferase (GGT) (206 U/L, reference 11–50 U/L), serum uric acid (467 μmol/L, reference 208–428 μmol/L), and triglycerides (6.82 mmol/L, reference 0–1.7 mmol/L), and positive results for both blood and urine ketones. Whole blood cell count, plasma total bile acid, total cholesterol, coagulation, urea and creatinine, thyroid function test, creatine kinase (CK)–MB, and blood ammonia were unremarkable. Blood tandem mass spectrometry showed elevation of a variety of acyl carnitines (**Table 1**), indicating multiple acyl-coenzyme A dehydrogenase deficiency or secondary liver damage. Urine gas chromatography mass spectrometry showed elevated levels of dicarboxylic acids and 3-hydroxyl dicarboxylic acids (**Supplementary Table S2**). Chest radiography showed that the texture of two lungs was increased, thickened and obscure. The intestines were in the left middle and lower abdomen with a visible twist and grinding-like appearance and tubular inflation. Ultrasonic B mode images showed that the morphologies of the liver and spleen were enlarged, and the liver was 60 mm below the ribs. No intrahepatic bile duct expansion, hepatic venous system, or common bile duct expansion was observed, and the two kidneys were normal in shape and size. The echocardiography results were normal.

Results

Molecular genetics

Because the changes in blood carnitine and urinary organic acid spectra suggested MADD, whereas the clinical and routine biochemical changes indicated GSD Ia, Sanger sequencing (primers showed in **Supplementary Table S1**) on coding and flanking sequences of G6Pase and ETFDH

10.3389/fped.2022.999596

TABLE 1 Results of blood tandem mass spectrometry.

Test index	Results (μmol/L)	Prompting	Reference Value (μmol/L)
alanine	344.60	↑	60.00–300.00
glutamic acid	211.64	↑	45.00–200.00
ornithine	10.26	↓	15.00–80.00
acetyl-L-carnitine	72.81	↑	6.00–30.00
3-hydroxy butyryl carnitine	0.77	↑	0.02–0.35
caproyl carnitine	0.33	↑	0.01–0.15
caprylyl carnitine	0.44	↑	0.01–0.30
octene acyl carnitine	0.65	↑	0.03–0.50
suberoyl carnitine	0.06	↑	0.00–0.06
lauroyl carnitine	0.29	↑	0.02–0.20
nutmeg acryloxyethyl carnitine	0.36	↑	0.01–0.30
palmitoyl carnitine	2.33	↑	0.30–2.00
palm enoyl carnitine	0.28	↑	0.02–0.20
18-carbonyl carnitine	1.54	↑	0.20–1.20
18-carbon enoyl carnitine	2.52	↑	0.30–1.80
18-carbon di enoyl carnitine	0.71	↑	0.05–0.60
3-hydroxyl-18-carbonyl carnitine	0.04	↑	0.00–0.03

from periphery blood sample was ordered for the patient and his parents. The variants nomenclature follows the Human Genome Variation Society guidelines (www.hgvs.org/mutnomen) and refers to the G6Pase gene coding sequence (transcript: NM_000151.4). Coding and flanking sequences of the G6Pase gene detected two variants: one nonsense variant c.209G > A (p.Trp70Ter) was paternally inherited and another synonymous variant c.648G > T (p.Leu216Leu) was maternally inherited (**Figure 1**). c.209G > A was classified as pathogenic variant according to ACMG guideline for a very low frequency in gnomAD (1/140,200, PM2_ Supporting), predicting to form a stop code that causes premature termination of the transcript (PVS1), and segregated with a phenotype or disease in multiple affected family members and multiple families (PP1_ Strong) (2–4). c.648G > T was classified as pathogenic variant according to ACMG guideline for a very low frequency in gnomAD (11/121,406, PM2_ Supporting), a pathogenic variant detected in trans (PM3), segregated with a phenotype or disease in multiple affected family members and multiple families (PP1_ Strong) (2, 5) and altered splicing by producing an aberrant transcript that eliminated 91 nucleotides deletion in exon 5 resulting in a premature termination (PS3) (5). Sequencing all exon and flanking sequences of the ETFDH gene revealed no variants in the proband.

Management

Based on the clinical manifestations, biochemical changes and blood and urine mass spectrometry results, we suspected that the child had GSD Ia or MADD; therefore, oral uncooked cornstarch and high-dose vitamin B2 were administered with other symptomatic and/or supporting management. During hospitalization, the child experienced secondary rotavirus enteritis and acute otitis media with episode hypoglycemia and transaminase fluctuations. After 20 days, the child was discharged with a stable body temperature, no cough, stable blood glucose levels, corrected metabolic acidosis, negative blood and urine ketones and normal blood lactate and uric acid levels. A number of biochemical parameters were significantly improved (ALT 87 U/L, AST 155 U/L, GGT 178 U/L, triglycerides 3.14 mmol/L).

After discharge, the patient continued to receive oral uncooked cornstarch while gradually stopping vitamin B2 supplementation. The reexamination results of blood tandem mass spectra and urine gas mass spectra (**Supplementary Table S2**) were normal. At the age of 12 months, the patient's weight was 11 kg, and he was in good general condition without growth retardation. The blood biochemical indices were as follows: blood glucose 5.7 mmol/L, ALT 84 U/L, AST 82 U/L, GGT 66 U/L; serum uric acid 243 μmol/L, triglycerides 5.0 mmol/L, total cholesterol 3.1 mmol/L. Ultrasonic B mode images showed an enlarged liver morphology, regular capsule, fine and enhanced liver echo with nonuniform distribution, the liver 34 mm below the costal margin, and a slightly large spleen. When the child was 29 months old, his weight was 15.3 kg, and his body length was 92.6 cm. The child was followed up to 33 months of age, and the blood biochemical indices returned to normal as follows: blood glucose 3.79 mmol/L, ALT 22 U/L, AST 27 U/L, GGT 22 U/L; serum uric acid 370 μmol/L, triglycerides 2.42 mmol/L, total cholesterol 4.57 mmol/L. Ultrasonic B mode images showed an enlarged liver morphology, smooth surface, uniform echo, clear blood vessels, and normal sized gallbladder, pancreas, spleen and kidney.

Discussion

GSD Ia shares some clinical manifestations with MADD such as liver enlargement, hypoglycemia and acidosis. But these two diseases should be managed differently and carries a different prognosis. The treatment of GSD Ia mainly consists of oral uncooked cornstarch to prevent the occurrence of hypoglycemia (6). The main treatment for

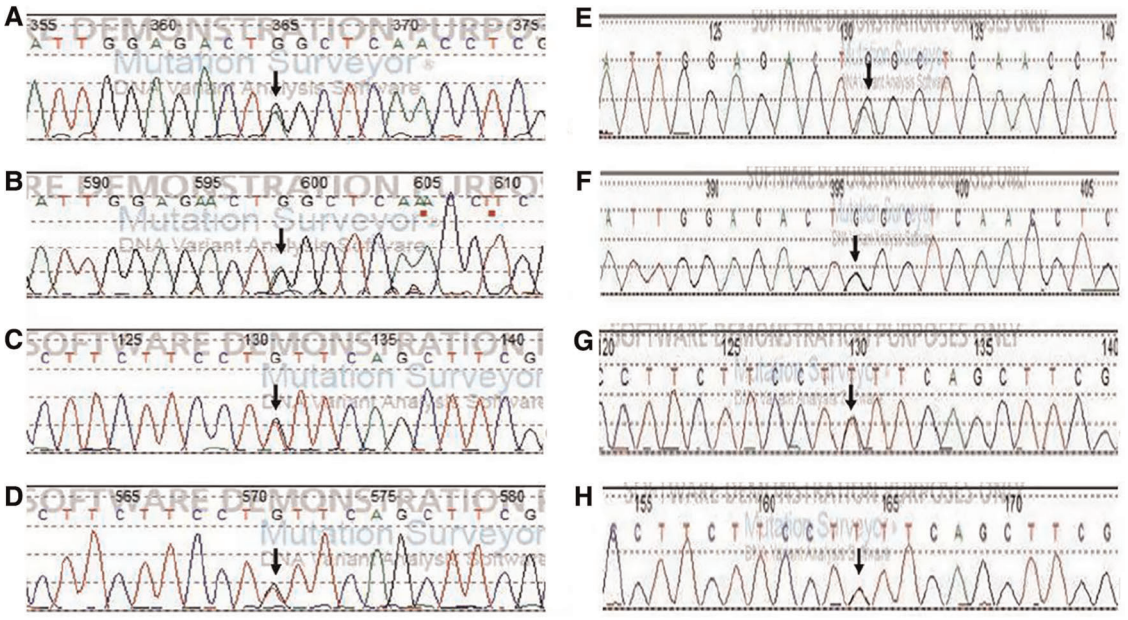

FIGURE 1
Sequencing results of the G6PC in the patient and his parents. Note: The mutation sites are indicated by arrows. (A) c.209G > A in exon1 by forward sequencing in the patient. (B) c.209G > A in exon1 by reverse sequencing in the patient. (C) c.648G > T in exon 5 by the forward sequencing in the patient. (D) c.648G > T in exon 5 by reverse sequencing in the patient. (E,F) c.209G > A in exon 1 from his father (by forward and reverse sequencing). (G,H) c.648G > /T in exon 5 from his mother (by forward and reverse sequencing).

MADD consists of a low fat, low protein diet with supplementation of riboflavin and carnitine, which can significantly improve the symptoms and biochemical indexes, and the prognosis is good if the diagnosis is timely and early preventive treatment is given (7–10). Therefore, the differential diagnosis of GSD Ia from MADD is very important.

The child patient we reported was suspected to have MADD due to changes in mass spectra; however, he was eventually genetically diagnosed as having GSD Ia. MADD is a relatively common congenital metabolic disorder of fatty acid oxidative metabolism. It has been reported that approximately 62% of patients with fatty acid oxidation metabolism disorders in China suffered from MADD (11), and ETFDH defects are the most common form of this disease (12, 13). According to the clinical manifestation, MADD can be divided into three types, as follows: type I: newborn with congenital anomalies (such as polycystic kidney, cardiomyopathy, and facial deformity); type II: newborn without congenital anomalies; and type III: late-onset type or light type.

The clinical manifestations of MADD in children include myasthenia, enlarged liver, paroxysmal hypoglycemia, hypertrophic cardiomyopathy and rash during onset of the disease, while laboratory biochemical tests may show increased AST, ALT, CK, CK-MB and lactate dehydrogenase (LDH) levels and metabolic acidosis. Increased CK and CK-MB can be seen in MADD when cardiac muscle and skeletal muscle are involved. Mass spectrometry was characteristic changes in MADD. Increased levels of short-chain, middle-chain and long-chain acyl carnitines by blood tandem mass spectrometry and possible dicarboxylic aciduria of ethyl malonic acid, glutaric acid, adipic acid and pimelic acid by urine gas chromatography mass spectrometry may be observed (14).

In recent years, with the extensive development of mass spectrometry, blood tandem mass spectrometry and urine gas chromatography mass spectrometry play an important role in the screening and diagnosis of inherited metabolic diseases (15). However, different genetic metabolic diseases may share similar metabolite fluctuations, and the diseases may be misdiagnosed if mass spectrometry is only relied on for diagnosis. Therefore, the confirmation of a MADD diagnosis requires further genetic evidence. Riboflavin-reactive MADD can typically be cured, especially for patients with the ETFDH variant, thus highlighting the important role of genetic testing in these patients (16).

Based on the combined results of clinical manifestations, blood tandem mass spectrometry and urine gas chromatography mass spectrometry of the patient, MADD was a diagnosis that needed more investigation. So we treated the patient with oral vitamin B2 at the beginning. However, the normal serum CK level and no pathogenic/likely pathogenic variants in exons of ETFDH in this patient did not support the diagnosis of MADD. More importantly, the abnormal results of the blood tandem mass spectrometry and

urine gas chromatography mass spectrometry normalized quickly after the hypoglycemia was corrected in the child, even after the discontinuation of vitamin B2 administration, which make the diagnosis of MADD very unlikely. Up to now, no signs of MADD developed.

The main clinical manifestations of GSD Ia are liver enlargement, fasting hypoglycemia, short stature, obesity, etc. Blood biochemical examination showed elevated blood lipids, metabolic acidosis, hyperlactatic acidemia, elevated uric acid. GSD Ia does not involve the heart and muscle, so CK and CK-MB are mostly normal. In reviewing the history of the child patient who showed a significant enlarged liver, elevated transaminases, hypoglycemia, lactic acidosis, hyperlipidemia, and hyperuricemia, it was found that these symptoms were all typical clinical manifestations of GSD. However, because the mass spectra of the child showed increased blood acyl carnitines and dicarboxylic aciduria, which are not reported in GSD cases, make the diagnosis process more complicated. We tested the G6Pase gene of the patient and his parents and found compound heterozygous single-base variants in the G6Pase gene in the patient. c.209G > A was derived from the father, leading to amino acid 70 being changed from tryptophan to the termination codon (p.Trp70Ter). Furthermore, c.648G > T (p.Leu216Leu) from the mother, was reported as the most common pathogenic variant in Chinese GSD Ia patients (17). The child was finally diagnosed with GSD Ia. Thus, for patients with increased blood acylcarnitines and dicarboxylic aciduria as evidenced by mass spectrometry, the possibility of GSD should also be considered during differential diagnosis.

The abnormal mass spectrum change in this child was the main reason for the misdiagnosis. No similar report has been published to our best knowledge. Why did the results of mass spectrometry in this patient show similar changes to MADD? The exact mechanism is unknown. However, the following speculations can be made. G6Pase is a key enzyme for glycogenolysis and glucose production, which plays an important role in maintaining normal blood glucose levels. When there is a congenital defect in G6Pase, glycogen cannot break down into glucose, leading to hypoglycemia. Hypoglycemia causes fat mobilization, which produces large amounts of fatty acids, Oxidative metabolism of fatty acids requires multiple acyl-coenzyme A dehydrogenase. When fatty acids are produced too much, these enzymes may be relatively inadequate. In addition, stress may affect the activity of these enzymes, such as fever, fatigue, hunger, etc.. In this case, the child patient was born with hypoglycemia, indicating that he was in serious condition. After fat mobilization, a large amount of fatty acids were produced. When levels are relatively insufficient and intermediate metabolites are increased, increased blood carnitine levels and dicarboxylic aciduria result, with even more energy needed during infection. Because mass spectrometry is not routinely ordered in patients with suspected GSD Ia, we don't know whether these metabolic changes occur in other GSD Ia patients with severe hypoglycemia.

In summary, GSD Ia can mimic the abnormal mass spectrum results as well as the typical clinical manifestations of MADD. Blood tandem mass spectrometry and urine gas chromatography mass spectrometry play an important role in the diagnosis of inherited metabolic diseases; however, these diseases may be misdiagnosed if simply relying on mass spectrometry. Therefore, genetic testing is currently very important for confirming the diagnosis of inherited metabolic diseases. One limitation of this paper is that the G6Pase genes and ETFDH genes were not completely sequenced. One reason is that the c.209G > A or c.648G > T variant that cause MADD are very rare and another is that the rapid and persistent normalization of blood acyl carnitine and urinal organic acid profiles without specific administration is very unlikely.

Data availability statement

The datasets presented in this study can be found in online repositories. The names of the repository/repositories and accession number(s) can be found in the article/ **Supplementary Material**.

Ethics statement

The studies involving human participants were reviewed and approved by Medical ethics committe, Jinshan Hospital of Fudan University. Written informed consent to participate in this study was provided by the participants' legal guardian/ next of kin. Written informed consent was obtained from the individual(s), and minor(s)' legal guardian/next of kin, for the publication of any potentially identifiable images or data included in this article.

Author contributions

All authors have contributed to and agreed on the content of the manuscript, and the respective roles of each author. All authors contributed to the article and approved the submitted version.

Acknowledgments

We sincerely thank the patient's parents for their close cooperation.

Conflict of interest

The authors declare that the research was conducted in the absence of any commercial or financial relationships that could be construed as a potential conflict of interest.

Publisher's note

All claims expressed in this article are solely those of the authors and do not necessarily represent those of their affiliated organizations, or those of the publisher, the editors and the reviewers. Any product that may be evaluated in this article, or claim that may be made by its manufacturer, is not guaranteed or endorsed by the publisher.

Supplementary material

The Supplementary Material for this article can be found online at: https://www.frontiersin.org/articles/10.3389/fped.2022.999596/full#supplementary-material.

References

1. Chen M, Burehell A. Glycogen storage diseases. In: CR Scfiver, editors. *The metabolic and molecular bases of inherited disease*. New York: Mcgraw-Hill Press (1995). p. 935–65.

2. Abdul Wahab SA, Yakob Y, Mohd Khalid MKN, Ali N, Leong HY, Ngu LH. Molecular, biochemical, and clinical characterization of thirteen patients with glycogen storage disease 1a in Malaysia. *Genet Res (Camb).* (2022) 2022:5870092. doi: 10.1155/2022/5870092

3. Miltenberger-Miltenyi G, Szonyi L, Balogh L, Utermann G, Janecke AR. Mutation spectrum of type I glycogen storage disease in Hungary. *J Inherit Metab Dis*. (2005) 28(6):939–44. doi: 10.1007/s10545-005-0186-7

4. Trioche P, Francoual J, Chalas J, Capel L, Bernard O, Labrune P. Identification of three novel mutations (Q54P, W70X and T108I) in the glucose-6-phosphatase gene of patients with glycogen storage disease type Ia. *Hum Mutat*. (1999) 14(1):91. doi: 10.1002/(SICI)1098-1004(1999)14:1<91::AID-HUMU21>3.0.CO;2-B

5. Kajihara S, Matsuhashi S, Yamamoto K, Kido K, Tsuji K, Tanae A, et al. Exon redefinition by a point mutation within exon 5 of the glucose-6-phosphatase gene is the major cause of glycogen storage disease type 1a in Japan. *Am J Hum Genet*. (1995) 57(3):549–55. PMID: 7668282; PMCID: PMC1801279

6. Wen B, Dai T, Li W, Zhao Y, Liu S, Zhang C, et al. Riboflavin-responsive lipid-storage myopathy caused by ETFDH gene mutations. *J Neurol Neurosurg Psychiatry*. (2010) 81:231–6. doi: 10.1136/jnnp.2009.176404

7. Xi J, Wen B, Lin J, Zhu W, Luo S, Zhao C, et al. Clinical features and ETFDH mutation spectrum in a cohort of 90 Chinese patients with late-onset multiple acyl-CoA dehydrogenase deficiency. *J Inherit Metab Dis*. (2014) 37:399–404. doi: 10.1007/s10545-013-9671-6

8. Zhang RN, Qiu WJ, Ye J, Han LS, Zhang HW, Qiu R, et al. Clinical and biochemical characteristics in children and adults with multiple aeyl-CoA dehydrogenase deficiency. *J Clin Pediatr*. (2012) 30:446–9. doi: 10.1038/ejhg.2010.171

9. American College of Medical Genetics Newborn Screening Expert Group. Newborn screening: toward a uniform screening panel and system-executive summary. *Pediatrics*. (2006) 117:S296–S307. doi: 10.1542/peds.2005-2633I

10. Er TK, Liang WC, Chang JG, Jong YJ. High resolution melting analysis facilitates mutation screening of ETFDH gene: applications in riboflavin-responsive multiple acyl-CoA dehydrogenase deficiency. *Clin Chim Acta*. (2010) 411:690–9. doi: 10.1016/j.cca.2010.01.033

11. Qiu WJ, Gu XF, Ye J, Han LS, Zhang YF, Liu XQ, et al. Gene mutation and clinical study in the patients with glycogen storage disease type Ia. *Clin J Endocrinol Metab*. (2004) 20:502–5.

12. Shah KK, O'Dell SD. Effect of dietary interventions in the maintenance of normoglycaemia in glycogen storage disease type 1a: a systematic review and meta-analysis. *J Hum Nutr Diet*. (2013) 26:329–39. doi: 10.1111/jhn.12030

13. Xin ZY, Qiu WJ. Progresses of diagnosis and therapy in multiple acyl-CoA dehydrogenase defidency. *Int J Pediatr*. (2010) 37:518–20.

14. Pollard LM, Williams NR, Espinoza L, Wood TC, Spector EB, Schroer RJ, et al. Diagnosis, treatment, and long-term outcomes of late-onset (type III) multiple acyl-CoA dehydrogenase deficiency. *J Child Neurol*. (2010) 25:954–60. doi: 10.1177/0883073809351984

15. Ishii K, Komaki H, Ohkuma A, Nishino I, Nonaka I, Sasaki M. Central nervous system and muscle involvement in an adolescent patient with riboflavin-responsive multiple acyl-CoA dehydrogenase deficiency. *Brain Dev*. (2010) 32:669–72. doi: 10.1016/j.braindev.2009.08.008

16. Izumi R, Suzuki N, Nagata M, Hasegawa T, Abe Y, Saito Y, et al. A case of late onset riboflavin-responsive multiple acyl-CoA dehydrogenase deficiency manifesting as recurrent rhabdomyolysis and acute renal failure. *Intern Med*. (2011) 50:2663–8. doi: 10.2169/internalmedicine.50.5172

17. Han F, Han LS, Ye J, Qiu WJ, Zhang HW, Gao XL, et al. A disease spectrum analysis of 564 cases of inherited metabolic diseases tested by gas chromatography-mass spectrometry. *Clin J Endocrinol Metab*. (2013) 29:693–5.

frontiers | Frontiers in Genetics

TYPE Case Report
PUBLISHED 07 December 2022
DOI 10.3389/fgene.2022.1015021

OPEN ACCESS

EDITED BY
Maria Elisabetta Baldassarre,
University of Bari Aldo Moro, Italy

REVIEWED BY
Hua Chen,
Beijing Institute of Genomics (CAS), China
Jie Zheng,
Shanghai Tech University, China

*CORRESPONDENCE
Yikun Zhou,
yikunzhou22@sina.com
Yun Zheng,
zhengyun5488@gmail.com

†These authors have contributed equally to this work

SPECIALTY SECTION
This article was submitted to Genetics of Common and Rare Diseases, a section of the journal Frontiers in Genetics

RECEIVED 09 August 2022
ACCEPTED 16 November 2022
PUBLISHED 07 December 2022

CITATION
Zhou Y, Liu J, Wu S, Li W and Zheng Y (2022), Case report: A heterozygous mutation in *ZNF462* leads to growth hormone deficiency.
Front. Genet. 13:1015021.
doi: 10.3389/fgene.2022.1015021

Case report: A heterozygous mutation in *ZNF462* leads to growth hormone deficiency

Yikun Zhou[1*†], Jianmei Liu[1†], Shuai Wu[2†], Wanran Li[2] and Yun Zheng[1,2,3*]

[1]Department of Endocrinology and Metabolism, The First People's Hospital of Yunnan Province, The Affiliated Hospital of Kunming University of Science and Technology, Kunming, China, [2]State Key Laboratory of Primate Biomedical Research, Institute of Primate Translational Medicine, Kunming University of Science and Technology, Kunming, China, [3]College of Horticulture and Landscape, Yunnan Agricultural University, Kunming, China

Weiss–Kruszka syndrome (WSKA) is a rare disease most often caused by mutations in the *ZNF462* gene. To screen for hereditary diseases, exons from the patient's genome were sequenced. Genomic PCR experiments followed by Sanger sequencing were used to confirm the mutated genomic regions in the patient and his parents. We report a new mutation site, a heterozygous mutation (NM_021224.6:c.6311dup) in *ZNF462* in a male patient of 8 years old. The mutation in the *ZNF462* gene caused WSKA. This patient is the first case with WSKA characterized by attention-deficit hyperactivity disorder and complete growth hormone deficiency without pituitary lesions. Our results suggest that the heterozygous mutation in *ZNF462* is the direct cause of WSKA in this patient. Mutations in other genes interacting with *ZNF462* result in similar symptoms of WSKA. Furthermore, *ZNF462* and its interacting proteins ASXL2 and VPS13B may form a protein complex that is important for normal development but awaits more studies to reveal its detailed functions.

KEYWORDS

growth hormone deficiency (GHD), *ZNF462*, Weiss–Kruszka syndrome (WSKA), mutation, case report

1 Introduction

Weiss–Kruszka syndrome (WSKA) is usually characterized by mild overall developmental delays and common craniofacial abnormalities, according to the OMIM database (Amberger et al., 2019). It is a rare genetic disorder, usually associated with *ZNF462* gene dysfunction, with reported autosomal dominant inheritance (Kruszka, 1993).

The *ZNF462* gene is located on chromosome 9p31.2 and encodes the protein ZNF462, which belongs to the C2H2 zinc finger protein family (C2H2-ZNF) (Al-Naama et al., 2020). The function of ZNF462 is unclear, but studies have shown that it plays a key role in early embryonic development and neuronal differentiation (Laurent et al., 2009; Massé et al., 2011). ZNF462 is expressed in a graded pattern

in the mouse cerebral cortex, with the strongest expression in the marginal zone, cortical plate, and subventricular zone of the cortical layer (Chang et al., 2007). Homozygous *ZNF462* knockout (*ZNF462*$^{-/-}$) has been shown to be fatal in mice, while heterozygous (*ZNF462*$^{+/-}$) mice showed anxiety-like stunting behavior, low brain weight, and over-self-grooming; anxiety symptoms and over-self-grooming behavior were alleviated after imipramine treatment (Wang et al., 2017).

At present, 30 cases of WSKA associated with *ZNF462* gene mutations have been reported. Among them, 28 studies did not investigate other genes but only the effect of *ZNF462* mutation on WSKA disease. One study investigated the chromosomal rearrangement of *ASXL2* and *KIAA1803* in WSKA patients (Ramocki et al., 2003), and the other study reported that disrupted *KLF12* and *ZNF462* incurred similar WSKA symptoms (Cosemans et al., 2018). Our study reports a new mutation of *ZNF462* that differs from those previously reported. We also discuss the effects of genes cooperating with *ZNF462* on disease.

2 Case description

2.1 Symptoms and physical and routine examination

A boy aged 8 years and 6 months came to the Affiliated Hospital at Kunming University of Science and Technology (the First People's Hospital of Yunnan Province) for evaluation of growth retardation. His parents are non-consanguineous. The proband was born *via* spontaneous vaginal delivery at 40 weeks, with birth length 50.0 cm (27.3rd) and weight 2.8 kg (5.3rd). He has no brothers or sisters. The heights of his father and mother are 167.0 cm and 157.0 cm, respectively.

At the first visit, the height of the proband was 126.5 cm (14.0th), weight 34.1 kg, and BMI 21.3 kg/m^2 (obese). He had a metopic ridge, arched eyebrows, bilateral ptosis, epicanthal folds, down-slanting palpebral fissures, a short upturned nose with a bulbous tip, and a marked cupid bow (Supplementary Figure S1). The ears were low-set, but his hearing was normal. There was no significant difference between the patient and his peers in speech or motor development, and no feeding difficulties or snoring problems. The proband has no other congenital abnormalities except cryptorchidism. There is no history of ptosis, dwarfism, or intellectual disability in other family members.

Upon the proband's routine inspection, his liver, kidneys, electrolytes, blood fat, and thyroid were normal. Testing revealed a FSH of 1.45 mIU/ml (3.5–12.5 mIU/ml), LH < 0.100 pmol/L (1.24–8.62 pmol/L), E2 42.35 pmol/L (20–75 pmol/L), Prog 0.452 nmol/L, PRL 10.68 ng/ml, and T < 0.087 pmol/L. Serum 25 hydroxyvitamin D was 15.07 ng/ml (>30 ng/ml), and PTH was 49.1 pg/ml (14–72 pg/ml). The serum IGF-1 and IGFBP-3 levels were 174 ng/ml (64.00–358.00 ng/ml) and 4.09 ng/ml (1.6–6.5 ng/ml), respectively. A growth hormone excitation test with levodopa combined with arginine was conducted, and it produced a peak of 1.35 ng/ml, indicating complete growth hormone deficiency (GHD).

His bone age was 1.6 years older than his chronological age. According to his bone age and other elements, his final height should be 156.8 cm (<3rd percentile of the normal heights of peers in the same area). Cranial magnetic resonance imaging (MRI) showed demyelinating changes in both parietal lobes, but the structures of the corpus callosum and pituitary gland were intact. Sleep monitoring indicated obstructive sleep apnea (OSA). Bone mineral density (BMD) was normal (Z:1.4). Fundus examination and echocardiography were normal.

The patient was evaluated by Wechsler intelligence assessment and Chinese children cognitive system. The comprehensive score of cognitive ability was 78 points that was lower than the average of his peers, and his cognitive level was located at the lowest 7.0% level of his peers. The results of the patient's comprehensive attention test showed that the patient had attention deficit hyperactivity disorder (ADHD).

2.2 Materials and methods

2.2.1 Sample information and sequencing profiles obtained

Peripheral blood samples from the patient were collected at the First People's Hospital of Yunnan Province. Whole-exon sequencing was performed by Beijing Golden Gene Technology Co., Ltd. The obtained exon sequencing has been stored in the NCBI SRA database under the accession number SRR18969535.

2.2.2 Analysis of the exon sequencing profile to identify genomic mutations

FastQC (Andrews, 2010) was used to check the sequencing quality of the obtained whole-exon sequencing data, and clean reads were obtained by fastp (Chen et al., 2018). BWA (v0.7.5a-r405) (Richard & Heng, 2009) was used to align the clean reads of the sequencing file to human genome sequences (hg38) downloaded from the UCSC Genome Browser (Kent et al., 2002). The resulting SAM file was converted to a BAM file using SAMtools (Li et al., 2009). Next, the BAM file was sorted with SAMtools and used to identify mutations with GATK (v4.2.1.0) (McKenna et al., 2010). Briefly, the MarkDuplicates program was used to remove PCR duplicates; BaseRecalibrator and ApplyBQSR were used to recalibrate the base quality score; and then, Mutect2 was used to identify mutations in exons and to produce a VCF file of the identified mutations. Then, ANNOVAR (v20200607) (Wang

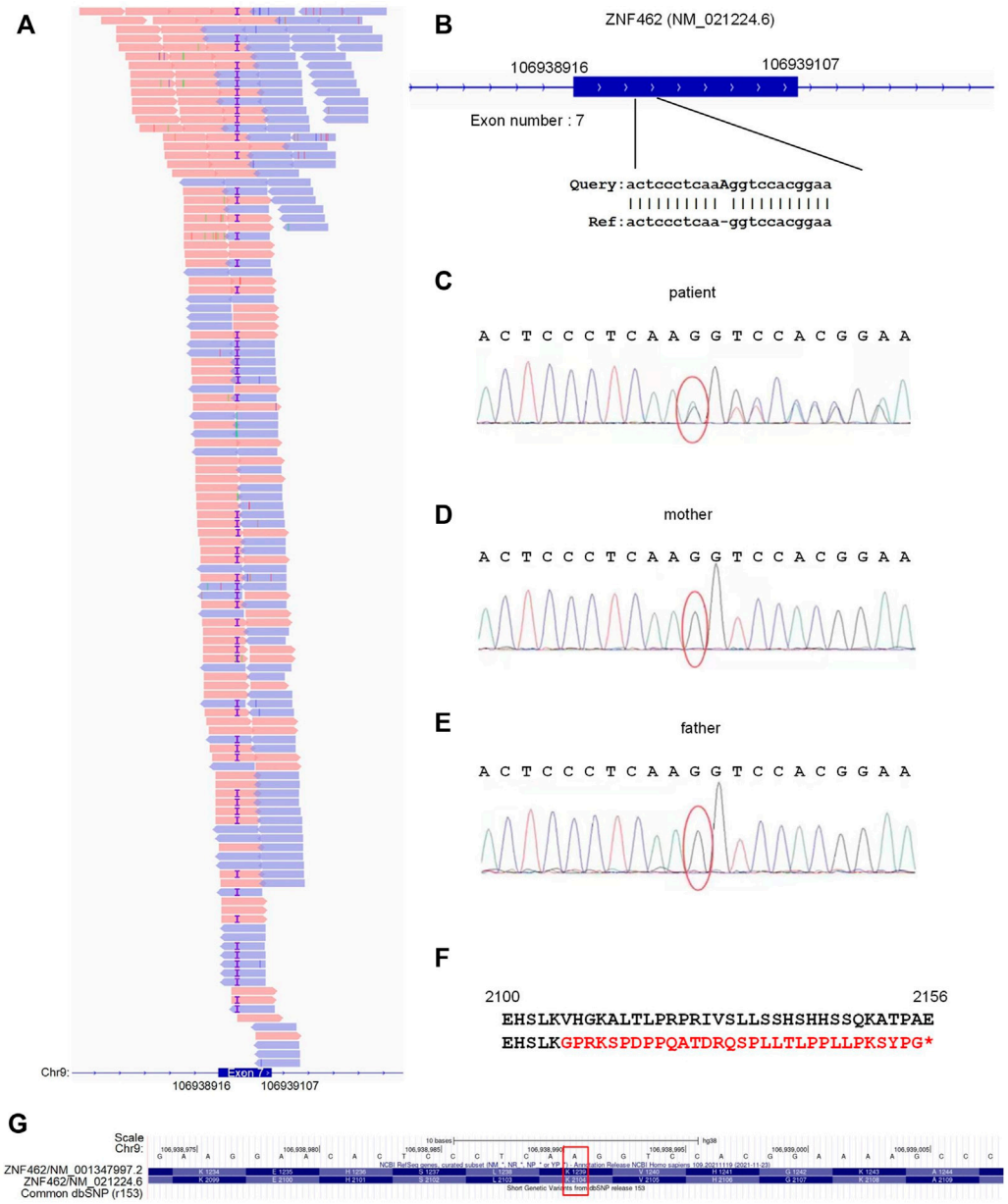

FIGURE 1
Identified mutation locus of *ZNF462* in the patient. **(A)** Locus of the adenosine insertion in *ZNF462* and the exome sequencing reads at the locus. The reads marked with purple "I"s are those with the adenosine insertions. **(B)** Insertion of adenosine occurs in the seventh exon of *ZNF462* (NM_021224.6). **(C–E)** Sanger sequencing results of the patient and his parents. Red ovals indicate the insertion site of adenosine. **(F)** Amino acid sequences of *ZNF462* without (up) and with the adenosine insertion (down). In the mutated *ZNF462* amino acid sequence, the adenosine insertion causes a variation from Val to Gly and different subsequent amino acids, and introduces premature translation terminations. **(G)** When compared with the dbSNP (r153) in the UCSC Genome Browser, the identified insertion site of adenosine was not a known SNP, as indicated by the red rectangle.

et al., 2010) was used to annotate the VCF file to obtain the gene mutations.

2.2.3 Verification of the new mutation in *ZNF462*

Whole-blood samples from the patient and his parents were collected. Then, the DNA samples were extracted and sequenced by Sanger sequencing. The obtained sequences were aligned to the human genomic sequence (hg38) with BLASTN (Altschul et al., 1990). A heterozygous insertion of adenosine was found in the seventh exon of the *ZNF462* gene by manual examination with IGV (Thorvaldsdottir et al., 2013). The protein–protein interaction network of

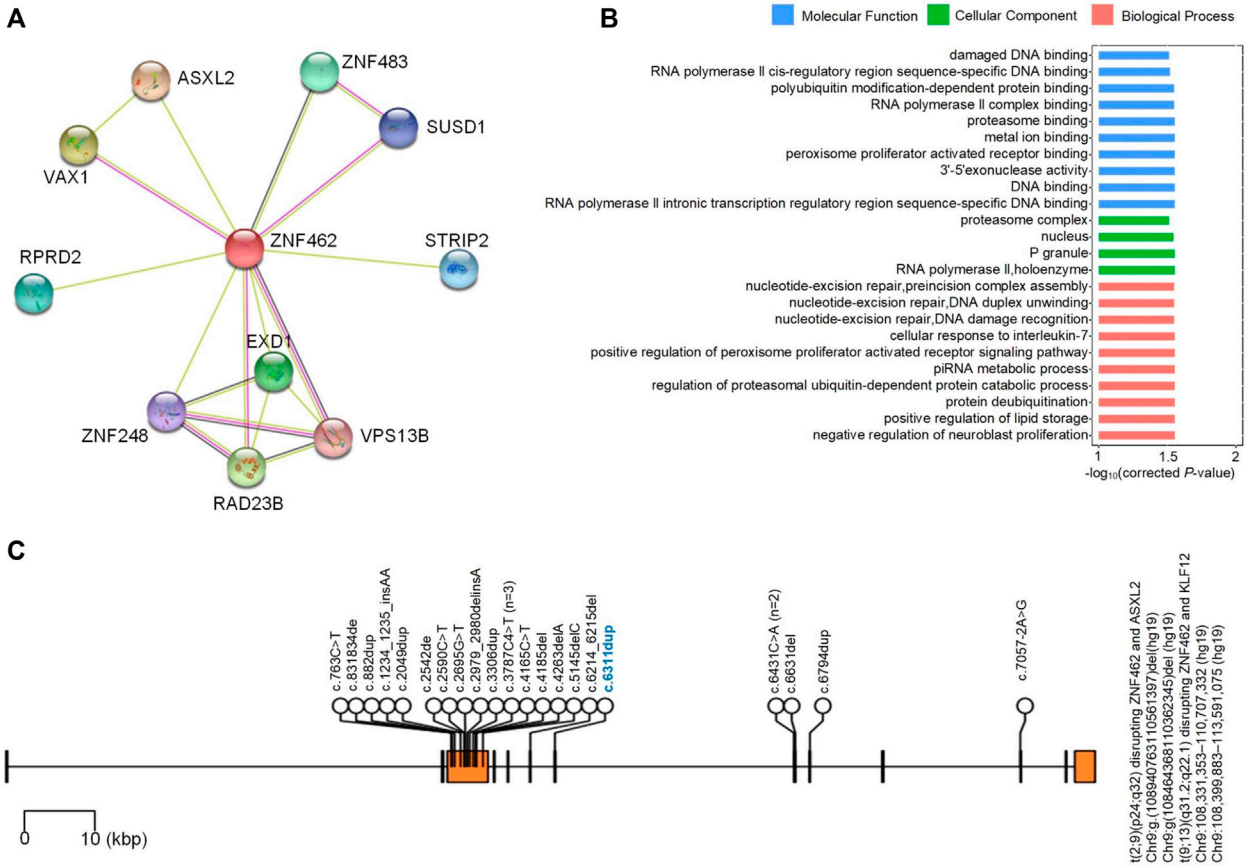

D

gene	ZNF462	VPS13B	ASXL2
disease	Weiss-Kruszka Syndrome	Cohen syndrome	Shashi-Pena syndrome
symptom	ptosis, developmental delay, autistic features, abnormalities of the corpus callosum, hearing loss, feeding difficulties , arched eyebrows, craniofacial deformities, congenital heart defects.	truncal obesity, hypotonia developmental delay, microcephaly, retinal dystrophy, mental deficiency, leukopenia, craniofacial and limb anomalies, developmental regression, down-slanting pupils, high myopia.	ptosis, macrocephaly or scaphocephaly, neonatal feeding difficulties, developmental delay, hypotonia, prominent eyes, arched eyebrows, minor ear abnormalities, intellectual disabilities, minor congenital heart disease.

FIGURE 2
Proteins interacting with ZNF462 and mutations in ZNF462. **(A)** Proteins interacting with ZNF462. STRING (v 11.5) was used to prepare the figure. **(B)** Enriched GO terms for genes in **(A)**. Only top GO terms were shown, and details are provided in Materials and Methods. **(C)** Reported mutations in *ZMF462* that are related to WSKA. The blue mutation is the one newly identified in this study. See Supplementary Table S1 for details. **(D)** Diseases and symptoms caused by genetic mutations in *ZNF462*, *VPS13B*, and *ASXL2*. Common symptoms of at least two diseases are shown in blue.

ZNF462 was studied using STRING (v11.5) (Szklarczyk et al., 2021).

The reported mutations in *ZNF462* were manually retrieved from the literature. Then, 30 reported mutations in *ZNF462* and the new mutation in *ZNF462* identified in this study were visualized with trackViewer (v1.6.1) (Ou & Zhu, 2019).

2.2.4 GO term analysis for ZNF462 and its interacting proteins

Gene Ontology (GO) enrichment analysis of ZNF462 and its interacting proteins was performed with KOBAS (v3.0) (Bu et al., 2021). The obtained GO terms were grouped into three major categories: molecular function, cellular component, and biological

TABLE 1 Timeline with relevant data from the episode of care.

Time	Examination	Treatment	Diagnosis
2021.07 (8 years and 6 months)	Height: 126.5 cm; weight: 34.1 kg	Whole-exon sequencing	GHD, dwarfism, and bilateral cryptorchidism
	Peak of the growth hormone excitation test: 1.4 ng/ml		
	Bone age: 10 years and 1 month (method:TW3-RUS)		
	MRI: the pituitary gland and corpus callosum were normal		
	B ultrasound: bilateral cryptorchidism		
	IGF-1:17 4 .0 ng/ml (64.0–358.0 ng/ml)		
2021.08	Height: 126.5 cm; weight: 34.1 kg	Injection of rhGH 3.4 U/d	WSKA, GHD, dwarfism, and bilateral cryptorchidism
	Mutation in *ZNF462* (NM_021224.6:c.6311dup)	Cryptorchidism surgery	
2021.12	Height: 129.0 cm; weight: 40.2 kg	Injection of rhGH 3.0 U/d	
	IGF: 540.5 ng/ml (64.0–358.0 ng/ml)		
2022.01 (9 years)	Height: 130.0 cm; weight: 39.6 kg	Injection of rhGH 3.0 U/d	
	Glucose tolerance, liver and kidney function, and blood lipids were normal		
	IGF: 480.5 ng/ml (73.0–385.0 ng/ml)		
2022.02 (9 years and 1 month)	Height: 131.0 cm; weight: 39.6 kg	Injection of rhGH 2.5 U/d	WSKA, GHD, dwarfism, intellectual disability, and ADHD
	Bone age: 11 years and 1 month (method Rus-CHN)		
	Composite score intelligence quotient: 78		
	Comprehensive attention test: ADHD		
	IGF: 462.16 ng/ml (73.0–385.0 ng/ml)		
2022.04	Height 133.0 cm; weight: 40 kg	Withdrawal of rhGH	
	IGF: 460.22 ng/ml (73.0–385.0 ng/ml)		
2022.07 (9 years and 6 months)	Height 134.0 cm; weight: 40 kg	Injection of rhGH 4.5 U/d	
	Bone age: 11 years and 10 months		
	Serum sex hormone levels were normal		
	IGF: 171.95 ng/ml (73.0–385.0 ng/ml)		
Now	—	Injection of rhGH 4.5 U/d	

Remarks: The three bone age tests were all different from the same instrument; IGF-1, reference range: 8 years old (64.0–358.0 ng/ml); 9 years old (73.0–385.0 ng/ml).

process. The top 10 GO terms with the smallest multiple test-corrected *p*-values in these three categories were chosen for visualization.

2.3 Results

2.3.1 Characterizing the genomic mutations of the patient

To obtain a molecular diagnosis, exon sequencing was performed for the patient. Figure 1A shows the high-throughput sequencing reads for the seventh exon of the patient's *ZNF462* gene, where 54% of these sequences carried the A insertion (or duplication), suggesting a heterozygous mutation at the A insertion site in the patient. Using GATK to analyze the exon sequencing data revealed an insertion of adenosine at the seventh exon of the *ZNF462* gene [NM_021224.6: c.6311dup; p. (Val2105GlyfsTer32)] (Figure 1B). Then, we sequenced the same genomic regions in the patient and his parents with Sanger sequencing (Figures 1C–E). In the Sanger sequencing results for the patient, there were continuous secondary peaks from the insertion site of adenosine (red oval in Figure 1C), suggesting two different sequences for the heterozygous insertion site of adenosine. However, as shown in Figures 1D,E, the Sanger sequencing of the mother and father clearly indicated no mutations. As shown in Figure 1F, due to a code shift introduced by the additional adenosine, valine (Val) at the 2105th amino acid was transformed into glycine (Gly); the subsequent 32 amino acids were encoded incorrectly and terminated prematurely. Therefore, the heterozygous A insertion may lead to a half-loss of functional ZNF462 protein in the patient. The mutation (NM_021224.6:c.6311dup) was not a reported SNP after being compared to dbSNP (v153) Figure 1G.

2.3.2 The protein–protein interaction network of ZNF462

We next examined the interacting proteins of ZNF462 with STRING (v11.5) (Talisetti et al., 2003), as shown in Figure 2A. To

TABLE 2 Common clinical manifestations and frequency of WSKA patients.

Item	Number	Frequency
Inheritance	—	—
De novo	23	74%
Paternally/maternally inherited	5	16%
Unknown	3	10%
ACC	7	23%
Metopic ridging/cranio synostosis	14	45%
Developmental delay	24	77%
Speech	13	42%
Motor	12	39%
Intellectual disability	5	16%
ASD	8	26%
Hypotonia	15	48%
Ptosis	27	87%
Down-slanting palpebral fissures	18	58%
Arched eyebrows	16	52%
Epicanthal folds	13	42%
Short upturned nose with bulbous tip	14	45%
Exaggerated cupid bow/wide philtrum	18	58%
Feeding issues	12	39%
Congenital heart disease	7	23%
Limb anomalies	6	19%
Ears	16	52%
Other	—	—
GHD	2	7%
Microrchidia/cryptorchid	3	10%
Attention disorder	3	10%
OSA	3	10%

Abbreviations: ACC: corpus callosum dysgenesis; ASD: autism spectrum disorder; GHD: growth hormone deficiency; OSA: obstructive sleep apnea.

determine the function of the ZNF462 protein and its interacting proteins, GO enrichment analysis was used with KOBAS. The top GO terms for these genes are "polyubiquitin modification-dependent protein binding," "RNA polymerase II complex binding," "proteasome binding," "metal ion-binding," "peroxisome proliferator-activated receptor binding," "3′-5′ exonuclease activity," "DNA binding," and "RNA polymerase II intronic transcription regulatory region sequence-specific DNA binding," as shown in Figure 2B.

We also manually retrieved the previously reported *ZNF462* mutations related to WSKA, then visualized them with the mutation newly identified in this study (Figure 2C). Most reported mutations are located in the third exon of *ZNF462* (details in Supplementary Table S1). The new mutation identified in this study is located in the seventh exon of the *ZNF462* gene.

Among the proteins interacting with ZNF462, the *ASXL2* gene encodes a member of the epigenetic regulator family that binds various histone modification enzymes and participates in the assembly of transcription factors at specific genomic sites (Lai & Wang, 2013). Recent studies have found that pathogenic mutations in the *ASXL2* gene could lead to Shashi–Pena syndrome, which is characterized by facial abnormalities and developmental delays (Shashi et al., 2016) (Figure 2D). *ASXL2*-deficient mice showed weight loss, enlarged hearts, and skeletal abnormalities (Baskind et al., 2009). Chromosome translocation t (2; 9) leads to a fused transcript of *ASXL2* and *KIAA1803*, resulting in a complex phenotype of the corpus callosum, ocular colobomas, and periventricular ectopic dysplasia (Ramocki et al., 2003). Weiss et al. (2017) have suggested that *ZNF462* and *ASXL2* might work together in the WSAK phenotype.

VPS13B is another protein interacting with ZNF462 (Figure 2A). Mutations in the *VPS13B* gene have been associated with Cohen's syndrome, a rare autosomal recessive syndrome associated with a variety of clinical manifestations including growth retardation, hypotonia, joint hyperactivity, microcephaly, intellectual impairment, and craniofacial and limb abnormalities (Cohen et al., 1973) (Figure 2D). The VPS13 protein family is involved in vesicular transportation and membrane events (Kolehmainen et al., 2004). To date, more than 150 VPS13B mutations have been reported in more than 200 patients with Cohen syndrome (Momtazmanesh et al., 2020).

VAX1 interacts with both ZNF462 and ASXL2 (Figure 2A). Heterozygous deletion of *Vax1* leads to infertility in mice and irregular estrous cycles in female mice (Hoffmann et al., 2014).

These results suggest that mutations in other genes interacting with *ZNF462* (Figure 2A) may result in symptoms similar to WSKA (Figure 2D). We hypothesize that ZNF462 and its interacting proteins may form a protein complex that is important for normal development and which awaits more studies to reveal its detailed functions.

3 Diagnosis and treatment

In summary, the patient was diagnosed with WSKA syndrome, GHD, dwarfism, intellectual disability, and ADHD. The proband had bilateral cryptorchidism and underwent surgery 3 months later. To promote his height growth, the proband received 3.4U/day (0.1 U/kg/day) subcutaneous injections of recombinant human growth hormone (rhGH). However, the IGF of this patient significantly increased and exceeded the normal range after normal and even lower usage of rhGH (Table 1). Considering the side effects of high IGF-1 levels, the patient discontinued rhGH treatment, and the IGF-1 dropped to the normal range. Finally, the patient had grown 6.5 cm in 7 months during the rhGH injections. After stopping the rhGH injections, the

patient only grew 1 cm in 3 months. The patient was therefore given rhGH again, and his ADHD improved after using tomoxetine.

4 Discussion

The patient showed growth retardation associated with GHD, but his level of IGF-1 and advanced bone age were inconsistent with the clinical symptoms of GHD. We speculate that the patient was IGF-1-insensitive and that a mutation in his *ZNF462* gene caused WSKA, a rare genetic disease often accompanied by growth retardation, craniofacial malformation, and/or corpus callosum dysplasia (González-Tarancón et al., 2020).

Since the first case of WSKA was reported in 2003 (Talisetti et al., 2003), only 30 patients have been reported. According to Table 2, most of them (74%) have some type of developmental delay, with speech delay being the most common, accounting for 42%, and motor delay being the second, noticed in 39% of patients. Almost half of patients have hypotonia, which is a contributor to motor delay. A few of them (16%) have intellectual disabilities. It cannot be ignored that 39% of patients have feeding problems.

We found that common craniofacial features include ptosis (87%), down-slanted palpebral fissures (58%), exaggerated cupid bow/wide philtrum (58%), arched eyebrows (52%), ear malformation/hearing loss (52%), short upturned nose with bulbous tip (45%), metopic ridging/craniosynostosis (45%), and epicanthal folds (42%). Corpus callosum dysgenesis is the most frequent manifestation of craniocerebral dysplasia, which is also considered to be a typical manifestation of WSKA but occurs in only 23% of patients.

Twenty-six percent of patients have autism spectrum disorder (ASD), which is consistent with the idea that ZNF462 disorder is an independent risk factor for autism (Krumm et al., 2015). However, this patient shows ADHD, which may be related to the demyelination of white matter in the parietal lobe (Silk et al., 2009). However, patients 5, 8, and 28 also have attention disorder. Furthermore, ASD, attention deficit, and ADHD have high rates of co-occurrence (Ohta et al., 2020). Therefore, the patient's ADHD might be caused by his *ZNF462* genetic mutation.

Seventy-four percent of WSKA patients have developmental delay, but only 12 patients had their height described. The patient identified in this study has WSKA with GHD, which is similar to the patient reported by Park et al. (2021). However, Park reported a patient with low bone age, empty sella syndrome, adenohypophysis dysfunction, and delayed puberty, while our patient's pituitary structure is intact (Park et al., 2021). It may be that the *ZNF462* mutation is responsible for the lack of growth hormone in WSKA patients, rather than the structural and functional dysfunction of the pituitary gland.

The patient identified in this study has a mutation at 9p31.2 on the *ZNF462* gene and shows GHD and short stature. Meanwhile, he presented with ptosis, arched eyebrows, down-slanting palpebral fissures, a short upturned nose with a bulbous tip, a marked cupid bow, and ADHD. This is the first report of a *ZNF462* gene mutation in patients with GHD but no pituitary lesions. It also provides new insights into endocrine symptoms related to dwarfism. When patients present with GHD and these craniofacial features, we should suspect WSKA.

Data availability statement

The data presented in the study are deposited in the NCBI SRA repository, accession number SRR18969535.

Ethics statement

The studies involving human participants were reviewed and approved by the Ethics Committee of the First People's Hospital of Yunnan Province. Written informed consent to participate in this study was provided by the participant's legal guardian/next of kin. Written informed consent was obtained from the individual(s) and minor(s)' legal guardian/next of kin for the publication of any potentially identifiable images or data included in this article.

Author contributions

YiZ and YuZ: conceived and designed this study; YiZ: clinical diagnosis, examinations of the patient, and collection of the clinical samples; JL and SW: writing of the original draft, analyzing sequencing data, and preparing figures; YiZ, YuZ, SW, and WL: writing and revision.

Funding

This work was supported by the Yunnan Provincial Department of Science and Technology and Kunming Medical University Joint Foundation for Applied Basic Research (No. 202001AY070001-119) and Yunnan Clinical Medical Center Open Project (No. 2019LCZXKF-NM07) to YiZ, as well as a grant from the National Natural Science Foundation of China (No. 31460295) and an Open Research Fund (No. SKLGE-2107) from the State Key Laboratory of Genetic Engineering, Fudan University, China to YuZ.

Conflict of interest

The authors declare that the research was conducted in the absence of any commercial or financial relationships that could be construed as a potential conflict of interest.

Publisher's note

All claims expressed in this article are solely those of the authors and do not necessarily represent those of their affiliated organizations, or those of the publisher, the editors, and the reviewers. Any product that may be evaluated in this article, or claim that may be made by its manufacturer, is not guaranteed or endorsed by the publisher.

Supplementary material

The Supplementary Material for this article can be found online at: https://www.frontiersin.org/articles/10.3389/fgene.2022.1015021/full#supplementary-material

References

Al-Naama, N., Mackeh, R., and Kino, T. (2020). C_2H_2-Type zinc finger proteins in brain development, neurodevelopmental, and other neuropsychiatric disorders: Systematic literature-based analysis. *Front. Neurol.* 11, 32. doi:10.3389/fneur.2020.00032

Altschul, S. F., Gish, W., Miller, W., Myers, E. W., and Lipman, D. J. (1990). Basic local alignment search tool. *J. Mol. Biol.* 215 (3), 403–410. doi:10.1016/S0022-2836(05)80360-2

Amberger, J. S., Bocchini, C. A., Scott, A. F., and Hamosh, A. (2019). OMIM.org: Leveraging knowledge across phenotype-gene relationships. *Nucleic Acids Res.* 47 (D1), D1038–D1043. doi:10.1093/nar/gky1151

Andrews, S. (2010). FastQC: A quality control tool for high throughput sequence data. version 0.11.9. Available at: https://www.bioinformatics.babraham.ac.uk/projects/fastqc/

Baskind, H. A., Na, L., Ma, Q., Patel, M. P., Geenen, D. L., and Wang, Q. T. (2009). Functional conservation of Asxl2, a murine homolog for the Drosophila enhancer of trithorax and polycomb group gene Asx. *PLoS One* 4 (3), e4750. doi:10.1371/journal.pone.0004750

Bu, D. C., Luo, H. T., Huo, P. P., Wang, Z. H., Zhang, S., and He, Z. H. (2021). KOBAS-I: Intelligent prioritization and exploratory visualization of biological functions for gene enrichment analysis. *Nucleic Acids Res.* 49 (W1), W317–W325. doi:10.1093/nar/gkab447

Chang, Y. S., Stoykova, A., Chowdhury, K., and Gruss, P. (2007). Graded expression of Zfp462 in the embryonic mouse cerebral cortex. *Gene Expr. Patterns* 7 (4), 405–412. doi:10.1016/j.modgep.2006.11.009

Chen, S., Zhou, Y., Chen, Y., and Gu, J. (2018). fastp: an ultra-fast all-in-one FASTQ preprocessor. *Bioinformatics* 34 (17), i884–i890. doi:10.1093/bioinformatics/bty560

Cohen, M. M. J., Hall, B. D., Smith, D. W., Graham, C. B., and Lampert, K. J. (1973). A new syndrome with hypotonia, obesity, mental deficiency, and facial, oral, ocular, and limb anomalies. *J. Pediatr.* 83, 280–284. doi:10.1016/s0022-3476(73)80493-7

Cosemans, N., Vandenhove, L., Maljaars, J., Van Esch, H., Devriendt, K., and Baldwin, A. (2018). ZNF462 and KLF12 are disrupted by a de novo translocation in a patient with syndromic intellectual disability and autism spectrum disorder. *Eur. J. Med. Genet.* 61, 376–383. doi:10.1016/j.ejmg.2018.02.002

González-Tarancón, R., Salvador-Rupérez, E., Miramar Gallart, M. D., Barroso, E., Díez García-Prieto, I., and Pérez Delgado, R. (2020). A novel mutation in the ZNF462 gene c.3306dup; p.(Gln1103Thrfs*10) is associated to Weiss–Kruszka syndrome. A case report. *Acta Clin. belg.* 77 (1), 118–121. doi:10.1080/17843286.2020.1780391

Hoffmann, H. M., Tamrazian, A., Xie, H., Perez-Millan, M. I., Kauffman, A. S., and Mellon, P. L. (2014). Heterozygous deletion of ventral anterior homeobox (vax1) causes subfertility in mice. *Endocrinology* 155, 4043–4053. doi:10.1210/en.2014-1277

Kent, W. J., Sugnet, C. W., Furey, T. S., Roskin, K. M., Pringle, T. H., and Zahler, A. M. (2002). The human genome browser at UCSC. *Genome Res.* 12, 996–1006. doi:10.1101/gr.229102

Kolehmainen, J., Wilkinson, R., Lehesjoki, A. E., Chandler, K., Kivitie-Kallio, S., and Clayton-Smith, J. (2004). Delineation of Cohen syndrome following a large-scale genotype-phenotype screen. *Am. J. Hum. Genet.* 75, 122–127. doi:10.1086/422197

Krumm, N., Turner, T. N., Baker, C., Vives, L., Mohajeri, K., and Witherspoon, K. (2015). Excess of rare, inherited truncating mutations in autism. *Nat. Genet.* 47, 582–588. doi:10.1038/ng.3303

Kruszka, P. (1993). *Weiss–Kruszka syndrome*. Seattle (WA): University of Washington. Seattle, WA, USA.

Lai, H. L., and Wang, Q. T. (2013). Additional sex combs-like 2 is required for polycomb repressive complex 2 binding at select targets. *PLOS ONE* 8 (9), e73983. doi:10.1371/journal.pone.0073983

Laurent, A., Masse, J., Omilli, F., Deschamps, S., Richard-Parpaillon, L., and Chartrain, I. (2009). ZFPIP/Zfp462 is maternally required for proper early *Xenopus laevis* development. *Dev. Biol.* 327, 169–176. doi:10.1016/j.ydbio.2008.12.005

Li, H., Handsaker, B., Wysoker, A., Fennell, T., Ruan, J., and Homer, N. (2009). The sequence alignment/map format and SAMtools. *Bioinformatics* 25, 2078–2079. doi:10.1093/bioinformatics/btp352

Massé, J., Piquet-Pellorce, C., Viet, J., Guerrier, D., Pellerin, I., and Deschamps, S. (2011). ZFPIP/Zfp462 is involved in P19 cell pluripotency and in their neuronal fate. *Exp. Cell Res.* 317, 1922–1934. doi:10.1016/j.yexcr.2011.04.015

Mckenna, A., Hanna, M., Banks, E., Sivachenko, A., Cibulskis, K., and Kernytsky, A. (2010). The genome analysis toolkit: A MapReduce framework for analyzing next-generation DNA sequencing data. *Genome Res.* 20, 1297–1303. doi:10.1101/gr.107524.110

Momtazmanesh, S., Rayzan, E., Shahkarami, S., Rohlfs, M., Klein, C., and Rezaei, N. (2020). A novel VPS13B mutation in cohen syndrome: A case report and review of literature. *BMC Med. Genet.* 21, 140. doi:10.1186/s12881-020-01075-1

Ohta, H., Aoki, Y. Y., Itahashi, T., Kanai, C., Fujino, J., and Nakamura, M. (2020). White matter alterations in autism spectrum disorder and attention-deficit/hyperactivity disorder in relation to sensory profile. *Mol. Autism* 11, 77. doi:10.1186/s13229-020-00379-6

Ou, J., and Zhu, L. J. (2019). trackViewer: a Bioconductor package for interactive and integrative visualization of multi-omics data. *Nat. Methods* 16 (6), 453–454. doi:10.1038/s41592-019-0430-y

Park, J., Ha, D. J., Seo, G. H., Maeng, S., Kang, S. M., and Kim, S. (2021). Empty sella syndrome associated with growth hormone deficiency: The first case report of Weiss–Kruszka syndrome. *J. Korean Med. Sci.* 36, e133. doi:10.3346/jkms.2021.36.e133

Ramocki, M. B., Dowling, J., Grinberg, I., Kimonis, V. E., Cardoso, C., and Gross, A. (2003). Reciprocal fusion transcripts of two novel Zn-finger genes in a female with absence of the corpus callosum, ocular colobomas and a balanced translocation between chromosomes 2p24 and 9q32. *Eur. J. Hum. Genet.* 11, 527–534. doi:10.1038/sj.ejhg.5200995

Richard, D., and Heng, D. (2009). Fast and accurate short read alignment with Burrows-Wheeler Transform. *Bioinformatics* 25, 1754–1760. doi:10.1093/bioinformatics/btp324

Shashi, V., Pena, L. D., Kim, K., Burton, B., Hempel, M., and Schoch, K. (2016). De novo truncating variants in ASXL2 are associated with a unique and recognizable clinical phenotype. *Am. J. Hum. Genet.* 99, 991–999. doi:10.1016/j.ajhg.2016.08.017

Silk, T. J., Vance, A., Rinehart, N., Bradshaw, J. L., and Cunnington, R. (2009). White-matter abnormalities in attention deficit hyperactivity disorder: A diffusion tensor imaging study. *Hum. Brain Mapp.* 30, 2757–2765. doi:10.1002/hbm.20703

Szklarczyk, D., Gable, A. L., Nastou, K. C., Lyon, D., Kirsch, R., and Pyysalo, S. (2021). The STRING database in 2021: Customizable protein-protein networks, and functional characterization of user-uploaded gene/measurement sets. *Nucleic Acids Res.* 49 (D1), D605–D612. doi:10.1093/nar/gkaa1074

Talisetti, A., Forrester, S. R., Gregory, D., Johnson, L., Schneider, M. C., and Kimonis, V. E. (2003). Temtamy-like syndrome associated with translocation of 2p24 and 9q32. *Clin. Dysmorphol.* 12, 175–177. doi:10.1097/01.mcd.0000072161.33788.56

Thorvaldsdottir, H., Robinson, J. T., and Mesirov, J. P. (2013). Integrative genomics viewer (IGV): High-performance genomics data visualization and exploration. *Brief. Bioinform.* 14, 178–192. doi:10.1093/bib/bbs017

Wang, B., Zheng, Y., Shi, H., Du, X., Zhang, Y., and Wei, B. (2017). Zfp462 deficiency causes anxiety-like behaviors with excessive self-grooming in mice. *Genes Brain Behav.* 16, 296–307. doi:10.1111/gbb.12339

Wang, K., Li, M., and Hakonarson, H. (2010). Annovar: Functional annotation of genetic variants from high-throughput sequencing data. *Nucleic Acids Res.* 38, e164. doi:10.1093/nar/gkq603

Weiss, K., Wigby, K., Fannemel, M., Henderson, L. B., Beck, N., and Ghali, N. (2017). Haploinsufficiency of ZNF462 is associated with craniofacial anomalies, corpus callosum dysgenesis, ptosis, and developmental delay. *Eur. J. Hum. Genet.* 25, 946–951. doi:10.1038/ejhg.2017.86

frontiers | Frontiers in Pediatrics

TYPE Original Research
PUBLISHED 09 December 2022
DOI 10.3389/fped.2022.1032659

OPEN ACCESS

EDITED BY
Maria Elisabetta Baldassarre,
University of Bari Aldo Moro, Italy

REVIEWED BY
Daw-Yang Hwang,
National Health Research Institutes, Taiwan
Shahid Mahmood Baig,
National Institute for Biotechnology and Genetic Engineering, Pakistan

*CORRESPONDENCE
Ruihuan Xu
xrh69@126.com
Zhangxing Wang
wzx776@163.com

†These authors have contributed equally to this work and share first authorship

SPECIALTY SECTION
This article was submitted to Genetics of Common and Rare Diseases, a section of the journal Frontiers in Pediatrics

RECEIVED 31 August 2022
ACCEPTED 21 November 2022
PUBLISHED 09 December 2022

CITATION
Liang J, Yu Z, Wang Z, Chen J, Liu Y, Yin Z and Xu R (2022) A frameshift mutation of *TMPRSS3* in a Chinese family with non-syndromic hearing loss.
Front. Pediatr. 10:1032659.
doi: 10.3389/fped.2022.1032659

A frameshift mutation of *TMPRSS3* in a Chinese family with non-syndromic hearing loss

Jingwen Liang[1†], Zhuoheng Yu[1†], Zhangxing Wang[2], Jianxia Chen[1], Yihuan Liu[3], Zhaoqing Yin[4*] and Ruihuan Xu[5*]

[1]Clinical Laboratory, Longgang Central Hospital of Shenzhen, Shenzhen, China, [2]Division of Neonatology, Longhua People's Hospital, Shenzhen, China, [3]Clinical Laboratory, Shenzhen Mental Health Center, Shenzhen, China, [4]Division of Pediatrics, The People's Hospital of Dehong Autonomous Prefecture, Dehong Hospital of Kunming Medical University, Mangshi, Yunnan, China, [5]Department of Clinical Laboratory, The Second Affiliated Hospital, School of Medicine, The Chinese University of Hong Kong, Shenzhen, P. R. China & Longgang District People's Hospital of Shenzhen, Shenzhen, China

Background: Deafness is the most common sensory defect in humans worldwide. Approximately 50% of cases are attributed to genetic factors, and about 70% are non-syndromic hearing loss (NSHL).
Objectives: To identify clinically relevant gene variants associated with NSHL in a Chinese family using trio-based whole-exome sequencing (WES).
Materials and methods: WES was performed on the 18-month-old female proband, and her parents. Gene variants specific to the family were identified by bioinformatics analysis and evaluated for their relevance to NSHL. We verified the novel variant in this family by the next-generation sequencing.In order to elucidate the frameshift mutation of *TMPRSS3* in a Chinese family, we used the Mass spectrometry to detect the gene from 1,010 healthy subjects.
Results: We identified a novel homozygous deletion (c.51delA) in exon 2 of the type II transmembrane serine protease 3 gene *TMPRSS3*, which resulted in a frameshift mutation just before the protein transmembrane domain (*p*.Q17fs). The deletion was present in the proband and her father, but not in her mother and the healthy controls. We also found mutations with potential relevance to hearing loss in *DCAF17*, which encodes a protein of unknown function (c. T555A: *p*.H185Q), and *ZNF276*, which encodes zinc finger protein 276 (c.1350−2A > G).
Conclusions and significance: We shown a novel frameshift mutation in *TMPRSS3* associated with autosomal recessive NSHL in a Han Chinese family.

KEYWORDS
TMPRSS3, homozygous, non-syndromic hearing loss, whole-exome sequencing, mutation

Introduction

Hearing loss is the most common sensory defect in humans worldwide. Genetic factors account for at least 50% of congenital hearing loss (1). About 80% of hereditary hearing impairment is due to autosomal recessive non-syndromic prelingual sensorineural hearing loss (2). Variants of the *TMRPSS3* gene have been associated with both familial and sporadic cases of autosomal recessive

non-syndromic hearing loss (NSHL; DFNB8/10) (3). *TMPRSS3*, which encodes a transmembrane serine protease, is composed of 13 exons, with exon 2 containing the start codon (4). Many mutations in *TMPRSS3* have been reported to have potential roles in NSHL, including an 8-bp deletion, an insertion of multiple beta-satellite repeat units, and a frameshift mutation (4).

In our research, we studied the frameshift mutation of *TMPRSS3* that has thrown new light on the cause of the autosomal recessive NSHL in a Chinese patient.

Materials and methods

The proband was an 18-month-old girl with NSHL. Her gestation period and birth weight (3.15 kg) were both normal, and she did not experience either asphyxia or hypoxia during delivery. Her postnatal development was normal, with head-raising at 3 months, sitting at 6 months, and walking at 14 months of age, with the exception of a small head circumference (44.5 cm) recorded at 18 months of age. General physical check-ups performed at standard times were normal. However, she was unable to speak and a hearing impairment was detected at 18 months of age. The child was diagnosed with profound sensorineural hearing loss at a local hospital. The parents have normal hearing and claim no family history of deafness or consanguinity.

To identify gene mutations that are candidates for the proband's deafness, we obtained peripheral blood samples (2 ml) from the proband, both parents, and 1,010 healthy subjects for DNA analysis. Genomic DNA was extracted using a Protease K DNA extraction kit (D3392), and the DNA was purified (OD260/280 = 1.8–2.0) and stored at −20°C until analysis.

We performed whole-exome sequencing (WES) on the proband, her parents, and detected the gene locus in a large cohort of healthy controls by mass spectrometry.Variants identified in the proband were detected using trio-based bioinformatics analysis and evaluated for their potential association with NSHL by comparison with a PubMed database search. Candidate variants were then validated by sequencing of the proband and her family (**Figure 1**).

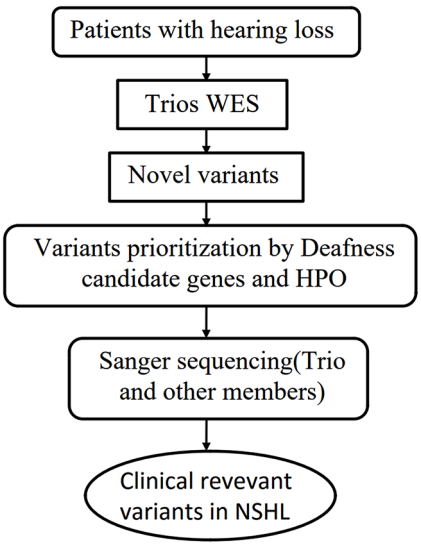

FIGURE 1
Flowchart to detect rare variants relevant to NSHL by WES. Abbrebiation: WES, Whole Exome Sequencing, HPO, Human Phenotype Ontology.

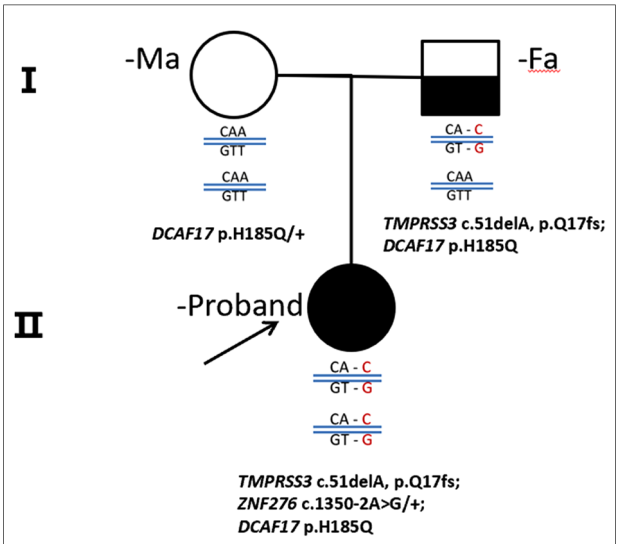

FIGURE 2
A pedigree drawings of the family with non-syndromic hearing imparemt. The proband's parent showed Normal hearing audiograms, while the affected gilrl, carried homozygous mutation, showed profound sensorineural hearing loss.

Results

We conducted whole exome sequencing (WES) on the proband affected by NSHL and her corresponding parents.A novel candidate loci of *TMPRSS3* was identified in this case. The variants of *TMPRSS3* that were subsequently confirmed by next-generation sequencing on the Chinese Family. Family pedigree is shown in **Figure 2**. The proband (II-1) and her parents (I-1, I-2) carried *DCAF17*: c. T555 > A (*p*.H185Q). The proband (II-1) and her father, but not her mother and the healthy contrlos, carried *TMPRSS3*: c.51delA (*p*.Q17fs), showed profound sensorineural hearing loss. *TMPRSS3*: c.51delA (rs780609668) is a frameshift variant located in exon 2 and is known to be associated with autosomal recessive NSHL.

Discussion

Mutations in a number of genes have been shown to cause severe non-syndromic deafness, including autosomal recessive NSHL (DFNB8/10), which is characterised by bilateral, severe to profound hearing loss. Such mutations have been identified in Palestinian, Tunisian, Korean, Indian, Spanish, and Greek populations (4, 8, 9, 16).

Our study found a frameshift mutation in *TMPRSS3* that causes autosomal recessive NSHL in a Chinese patient. The exon 2 deletion identified, c.51del, leads to a frameshift of glutamate at position 17 (*p*.Q17fs) in the protein. Confirmation of the putative disease-causing variant and analysis of *TMPRSS3* in all members of the Chinese family were performed by Sanger sequencing. The proband's father had a heterozygous *TMPRSS3* deletion, which leads to double tracing as shown in the left to the black line on **Figure 3**. **Figure 1** shown that the proband had the homozygous deletion. The explanation would be a novel TMPRSS3 *p*.Q17fs mutation that occurred in her mother. But the proband's mother did not carry this frameshift *TMPRSS3* *p*.Q17fs mutation. Maybe the proband's mother had a deletion that is spanning over the TMPRSS3 *p*.Q17fs exon (or several exons, which leads to no PCR amplification), which made the proband looked like to have the homozygous deletion. Not only that, the mutation of *TMPRSS3* was undetectable among 1,010 healthy subjects by Mass-spectrometric technique. These results indicate that the proband's deafness is likely to be caused by the homozygous *TMPRSS3*: c.51del mutation. The first mutation in a transmembrane protease associated with hearing loss was reported by Scott et al. in 2,001 (4). Since then, 24 mutations in *TMPRSS3* have been identified as potentially pathogenic for inheritable deafness (**Table 1**). Among these, 22 are missense mutations, one is a nonsense mutation, and one is a deletion. The *TMPRSS3* *p*.Q17fs in our study would be very rare that frameshift mutation occurs in both alleles. Our discovery therefore adds another example of NSHL caused by a deletion mutation.

We identified several other candidate deafness genes in the proband (**Table 2**). WES analyses showed that both parents were homozygous for *DCAF17*: c.T555 > A variant, and the proband was a carrier of the mutation. Mutations in *DCAF17* are associated with Woodhouse–Sakati syndrome, a rare disorder characterised by alopecia, hypogonadotropic hypogonadism, sensorineural hearing loss, diabetes mellitus, and extrapyramidal movement (12). Another study suggested

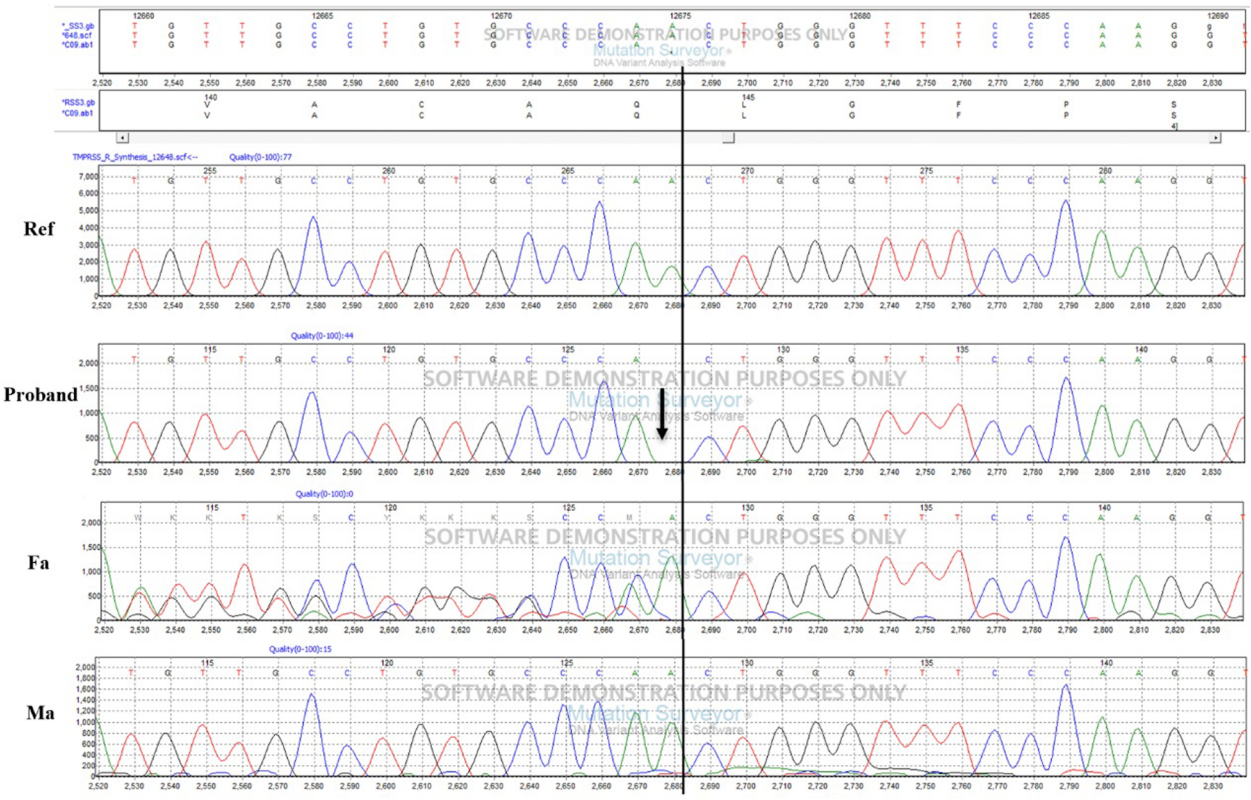

FIGURE 3
Validation of the frameshift mutation in *TMPRSS3* by sanger sequencing.

Table 1 Overview of the part of deafness-associated mutations in *TMPRSS3*.

Ethnicity	Amino Acid Change	Functional Domain	Type of Variant
China (this study)	Q17fs	Just before TM (11)	del
British (5)	Ala138Glu	SRCR	mis
Dutch (5)	Ala426Thr	TM	mis
Pakistan (6), Spanish (10)	Thr70fs	Truncation after TM	del
Tunisian (6)	Pro404Leu	Serine protease	mis
Korean (7), German (18)	Ala306Thr	TM	mis
Italian (8)	Thr340Arg	Serine protease	mis
Italian (8)	Pro431Ser	Serine protease	mis
Turkish (8)	Arg216Leu	TM	mis
Turkish (8)	Gln398X	Serine protease	mis
Tunisian (9)	Tpr251Cys	Serine protease	mis
Pakistani (16)	Cys407Arg	Serine protease	mis
Pakistani (16)	Cys194Phe	SRCR	mis
China Taiwan (17)	Arg80His	Serine protease	mis
China Taiwan (17)	Leu184Ser	Serine protease	mis
China Taiwan (17)	Ala418Val	LDLRA	mis
Greek (18)	Asp103Gly	LDLRA	mis
German (18)	Asp216Cys	Just before Serine protease	mis
Pakistani (19)	Cys425Arg	Serine protease	mis
Pakistani (19)	Glu104Lys	LDLRA	mis
Pakistani (19)	Glu104Stop	LDLRA	non
Pakistani (19)	Arg256Val	Serine protease	mis
Pakistani (19)	Arg109Trp	LDLRA	mis
UK Caucasian (20)	Ala90Thr	LDLRA	mis
Korean (21)	Thr248Met	Serine protease	mis

TM, transmembrane, SRCR, scavenger receptor cysteine-rich protein, LDLRA, low density lipoprotein receptor class A domains, del, deletion, mis, missense, Non, nonsynonymous.

that *DCAF17* may play as yet unexplored roles in tissue development and maintenance in adults (12). It is reported recently that *DCAF17* have played an important role in gametes growth and development (13). The development of embryonic chromosomes abnormalities is directly related to the quality of gametes.We identified a homozygous missense (c. T555>A: *p*.H185Q) in exon 6 of *DCAF17* in all members of the family (**Table 2**). *DCAF17*: c.555T > A has an allele frequency of 3% and is classified as a benign variant in the ClinVar database. Although, this variant does not associate with hearing loss. But, whether it was the homozygous missense matation in *DCAF17* that caused embryonic dysplasia resulting in deafness remained to be further studied.

In contrast, the affected girl was the only carrier of the mutation detected in *ZNF276* (c.1350–2A > G). The protein encoded by this gene is a 614-amino acid protein containing five C2H2-type zinc fingers and one zinc finger-associated domain. *ZNF276* mutations have been identified in breast cancer (14) and may also be involved in the progression of Fanconi anaemia (15).

In conclusion, we report a identification of a frameshift mutation in the *TMPRSS3* gene (c.51delA) resulting in a frameshift mutation in the protein (*p*.Q17fs) in the Han Chinese population. Our results thus provide a new example of autosomal recessive NSHL caused by a *TMPRSS3* mutation.

Data availability statement

The datasets presented in this study can be found in online repositories. The names of the repository/repositories and accession number(s) can be found in the article/ Supplementary Material.

Ethics statement

Written informed consent was obtained from the individual(s), and minor(s)' legal guardian/next of kin, for the publication of any potentially identifiable images or data included in this article.

Author contributions

JL, ZY: These authors contributed equally to this work and should be considered co-first authorship. RX, ZY: These authors contributed equally to this work and should be considered co-corresponding authorship. ZW, JC, YL: These authors contributed equally to this work and should be considered co-senior authorship. All authors contributed to the article and approved the submitted version.

TABLE 2 Candidate genes identified in the proband with NSHL.

Gene Symbol	Transcript	Exon	Nucleotide Change	Amino Acid Change	Position	Mode
TMPRSS3	NM_032404	Eexon2	c.51delA	*p*.Q17fs	Chr21-43,808,526	Hom
DCAF17	NM_001164821	Eexon6	c.T555 > A	*p*.H185Q	Chr2-172,309,651	Hom
ZNF276	NM_152287	–	c.1350-2A > G	–	Chr16-89,804,382	Het

Funding

The research was funded by Special fund for National Natural Science Foundation of China (Program No. 81960290), Economic and Technological development of Longgang District, Shenzhen (Program No. LGKCYLWS2019000334 and Program No. LGKCYLWS2019000335) and High Level Project of Medicine in Longhua, ShenZhen (Program No. HLPM2019 07020103). None of this organizations influencede the study design, the collection, analysis, and management of data, the writing of the report, or the decision to submit to the manuscript for publication.

Acknowledgments

We thank the Chinese family for their participation and cooperation we identified a homozygous deletion. This research was partially supported by National Natural Science Foundation of China (No.81960290), District Special Fund for Economic and Technological Development in Longgang, Shenzhen (No.LGKCYLWS20190003334, No.LGKCYLWS20190003335), and High Level Project of Medicine in Longhua, ShenZhen (No.HLPM201907020103).

Conflict of interest

The authors declare that the research was conducted in the absence of any commercial or financial relationships that could be construed as a potential conflict of interest.

Publisher's note

All claims expressed in this article are solely those of the authors and do not necessarily represent those of their affiliated organizations, or those of the publisher, the editors and the reviewers. Any product that may be evaluated in this article, or claim that may be made by its manufacturer, is not guaranteed or endorsed by the publisher.

References

1. Morton CC, Nance WE. Newborn hearing screening-a silent revolution. *N Engl J Med*. (2006) 354(20):2151–64. doi: 10.1056/NEJMra050700

2. Petit C, Levilliers J, Hardelin JP. Molecular genetics of hearing loss. *Annu Rev Genet*. (2001) 35(35):589–646. doi: 10.1146/annurev.genet.35.102401.091224

3. Bonné-Tamir B, DeStefano AL, Briggs CE, Adair R, Franklyn B, Weiss S, et al. Linkage of congenital recessive deafness (gene DFNB10) to chromosome 21q22.3. *Am J Hum Genet*. (1996) 58(6):1254–9. doi: 10.1063/1.370701

4. Scott HS, Kudoh J, Wattenhofer M, Shibuya K, Berry K, Chrast AR, et al. Insertion of beta-satellite repeats identifies a transmembrane protease causing both congenital and childhood onset autosomal recessive deafness. *Nat Genet*. (2001) 27(1):59–63. doi: 10.1038/83768

5. Sarrias MR, Grønlund J, Padilla O, Madsen J, Holmskov U, Lozano F. The scavenger receptor cysteine-rich (SRCR) domain: an ancient and highly conserved protein module of the innate immune system. *Crit Rev Immunol*. (2004) 24(1):1–37. doi: 10.1615/CritRevImmunol.v24.i1.10

6. Ahmed ZM, Li XC, Powell SD, Riazuddin S, Young TL, Ramzan K, et al. Characterization of a new full length *TMPRSS3* isoform and identification of mutant alleles responsible for nonsyndromic recessive deafness in Newfoundland and Pakistan. *BMC Med Genet*. (2004) 5(1):24. doi: 10.1186/1471-2350-5-24

7. Weegerink NJD, Margit S, Jaap O, Huygen PLM, Storm TM, Granneman S, et al. Genotype-phenotype correlation in DFNB8/10 families with TMPRSS3 mutations. *J Assoc Res Otolar*. (2011) 12(6):753–66. doi: 10.1007/s10162-011-0282-3

8. Wattenhofer M, Sahin-Calapoglu N, Andreasen D, Kalay E, Caylan R, Braillard B, et al. A novel *TMPRSS3* missense mutation in a DFNB8/10 family prevents proteolytic activation of the protein. *Hum Genet*. (2005) 117 (6):528–35. doi: 10.1007/s00439-005-1332-x

9. Masmoudi S, Antonarakis SE, Schwede T, Ghorbel AM, Gratri M, Pappasavas MP, et al. Novel missense mutations of *TMPRSS3* in two consanguineous Tunisian families with nonsyndromic autosomal recessive deafness. *Hum Mutat*. (2001) 18 (2):101–8. doi: 10.1002/humu.1159

10. Wattenhofer M, Di IM, Rabionet R, Dougherty L, Pampanos A, Schwede T, et al. Mutations in the *TMPRSS3* gene are a rare cause of childhood nonsyndromic deafness in Caucasian patients. *J Mol Med-jmm*. (2002) 80(2):124–31. doi: 10.1007/s00109-001-0310-6

11. Chung J, Park SM, Chang SO, Chung T, Lee KY, Kim AR, et al. A novel mutation of *TMPRSS3* related to milder auditory phenotype in Korean postlingual deafness:a possible future implication for a personalized auditory rehabilitation. *J Mol Med*. (2014) 92(6):651–63. doi: 10.1007/s00109-014-1128-3

12. Sheridan MB, Wohler E, Batista DAS, Applegate C, Hoover-Fong J. The use of high-density SNP array to map homozygosity in consanguineous families to efficiently identify candidate genes:application to woodhouse-sakati syndrome. *Case Rep Genet*. (2015) 2:169482. doi: 10.1155/2015/169482

13. Xu BL, Liu XQ, Wang L. Advances in functions of *DCAF* family proteins. *Life Sci Res*. (2020) 24(1):75–80. doi: 10.16605/j.cnki.1007-7847.2020.01.011

14. AJ Brenner,CM Aldaz. The genetics of sporadic breast cancer. *Prog Clin Biol Res*. (1997) 396:63–82.

15. Nakamura A, Matsuura S, Tauchi H, Ohashi H, Hasegawa T, Honda K, et al. Four novel mutations of the fanconi anemia group A gene (FAA) in Japanese patients. *J Hum Genet*. (1999) 44(1):48–51. doi: 10.1007/s100380050106

16. Benyoseft T, Wattenhofer M, Riazuddin S, Ahmed ZM, Scott HS, Kudon J, et al. Novel mutations of *TMPRSS3* in four DFNB8/B10 families segregating congenital autosomal recessive deafness. *J Med Genet*. (2001) 38(6):396–400. doi: 10.1136/jmg.38.6.396

17. Wong SH, Yen YC, Li SY, Yang YY. Novel mutations in the *TMPRSS3* gene may contribute to Taiwanese patients with nonsyndromic hearing loss. *Int J Mol Sci*. (2020) 21(7):2382. doi: 10.3390/ijms21072382

18. Elbracht M, Senderek J, Eggermann T, Thürmer C, Park J, Maetin W, et al. Autosomal recessive postlingual hearing loss (DFNB8): compound heterozygosity for two novel TMPRSS3 mutations in German siblings. *J Med Genet*. (2007) 44:e81.

19. Guipponi M, Toh MY, Tan J, Park D, Hanson K, Ballana E, et al. An integrated genetic and functional analysis of the role of type II transmembrane serine proteases (TMPRSSs) in hearing loss. *Hum Mutat*. (2008) 29(1):130–41.

20. Lee J, Baek JI, Choi JY, Kim UK, Lee SH, Lee KY, et al. Genetic analysis of TMPRSS3 gene in the Korean population with autosomal recessive nonsyndromic hearing loss. *Gene*. (2013) 532(2):276–80.

21. Martinez VG, Moestrup SK, Holmskov U, Mollenhauer J, Lozano F. The conserved scavenger receptor cysteine-rich superfamily in therapy and diagnosis. *Pharmacol Rev*. (2011) 63(4):967–1000.

frontiers | Frontiers in Genetics

TYPE Original Research
PUBLISHED 28 February 2023
DOI 10.3389/fgene.2023.1083779

OPEN ACCESS

EDITED BY
Maria Elisabetta Baldassarre,
University of Bari Aldo Moro, Italy

REVIEWED BY
Weizhen Ji,
Yale University, United States
Asami Oguro-Ando,
University of Exeter, United Kingdom

*CORRESPONDENCE
Xiu Xu,
xuxiu@fudan.edu.cn
Qiong Xu,
xuqiong@fudan.edu.cn

†These authors have contributed equally to this work and share first authorship

SPECIALTY SECTION
This article was submitted to Genetics of Common and Rare Diseases, a section of the journal Frontiers in Genetics

RECEIVED 29 October 2022
ACCEPTED 05 January 2023
PUBLISHED 28 February 2023

CITATION
Hu C, Wang Y, Li C, Mei L, Zhou B, Li D, Li H, Xu Q and Xu X (2023), Targeted sequencing and clinical strategies in children with autism spectrum disorder: A cohort study.
Front. Genet. 14:1083779.
doi: 10.3389/fgene.2023.1083779

Targeted sequencing and clinical strategies in children with autism spectrum disorder: A cohort study

Chunchun Hu[1†], Yi Wang[1†], Chunyang Li[2], Lianni Mei[1], Bingrui Zhou[1], Dongyun Li[1], Huiping Li[1], Qiong Xu[1*] and Xiu Xu[1*]

[1]Department of Child Health Care, Children's Hospital of Fudan University, Shanghai, China, [2]Department of Child Health Care, Xi'an Children's Hospital, Xi'an, China

Objectives: Autism spectrum disorder (ASD) is a neurodevelopmental disorder with genetic and clinical heterogeneity. Owing to the advancement of sequencing technologies, an increasing number of ASD-related genes have been reported. We designed a targeted sequencing panel (TSP) for ASD based on next-generation sequencing (NGS) to provide clinical strategies for genetic testing of ASD and its subgroups.

Methods: TSP comprised 568 ASD-related genes and analyzed both single nucleotide variations (SNVs) and copy number variations (CNVs). The Autism Diagnostic Observation Schedule (ADOS) and the Griffiths Mental Development Scales (GMDS) were performed with the consent of ASD parents. Additional medical information of the selected cases was recorded.

Results: A total of 160 ASD children were enrolled in the cohort (male to female ratio 3.6:1). The total detection yield was 51.3% for TSP (82/160), among which SNVs and CNVs accounted for 45.6% (73/160) and 8.1% (13/160), respectively, with 4 children having both SNVs and CNV variants (2.5%). The detection rate of disease-associated variants in females (71.4%) was significantly higher than that in males (45.6%, p = 0.007). Pathogenic and likely pathogenic variants were detected in 16.9% (27/160) of the cases. *SHANK3, KMT2A,* and *DLGAP2* were the most frequent variants among these patients. Eleven children had *de novo* SNVs, 2 of whom had *de novo ASXL3* variants with mild global developmental delay (DD) and minor dysmorphic facial features besides autistic symptoms. Seventy-one children completed both ADOS and GMDS, of whom 51 had DD/intellectual disability (ID). In this subgroup of ASD children with DD/ID, we found that children with genetic abnormalities had lower language competence than those without positive genetic findings (p = 0.028). There was no correlation between the severity of ASD and positive genetic findings.

Conclusion: Our study revealed the potential of TSP, with lower cost and more efficient genetic diagnosis. We recommended that ASD children with DD or ID, especially those with lower language competence, undergo genetic testing. More precise clinical phenotypes may help in the decision-making of patients with genetic testing.

KEYWORDS

targeted sequencing, NGS, autism spectrum disorder, gene, ASXL3

Introduction

Autism spectrum disorder (ASD) is a highly heterogeneous neurodevelopmental disorder characterized by social deficits and restricted, repetitive patterns of behavior and interests (Lord et al., 2020). The ASD occurrence in the United States is estimated to be approximately 1 in 44, with an overall male-to-female prevalence ratio of 3.4:12). As one of the most heritable medical conditions, ASD is associated with over a thousand risk genes (He et al., 2013), of which more than 100 genes and genomic regions meet rigorous statistical thresholds for the correlation with ASD phenotype (Satterstrom et al., 2020). Models of genetic risk for ASD tend to favor complex inheritance; nevertheless, rare inherited and *de novo* variants contribute to a substantial risk of individuals with ASD (Iossifov et al., 2014; Sanders et al., 2015). According to recently published large case–control studies (Satterstrom et al., 2020; Fu et al., 2022; Zhou et al., 2022), the genetic contribution to ASD continues to increase. Children with a diagnosis of ASD are recommended for etiological assessments. Chromosomal microarray analysis (CMA), detecting large duplications or deletions, was used as first-tier genetic testing for children with ASD, multiple congenital anomalies (MCA) and developmental delay (DD)/intellectual disability (ID) (Miller et al., 2010), in addition to fragile X analysis and *MECP2* testing. Many physician organizations recommend next-generation sequencing (NGS) testing when CMA-based evaluation has no positive identifications. In recent years, with the remarkable maturity of technical aspects of NGS variant discovery, it has been reported that rare genetic variants can be found in up to 30% of the ASD population (Vorstman et al., 2017).

ASD is always accompanied by cooccurring conditions, such as DD/ID, language disorders, motor difficulties, attention deficit hyperactivity disorder (ADHD), and epilepsy. It is generally acknowledged that established ASD risk variants are associated with these comorbidities (Vorstman et al., 2017). Approximately 50% of children diagnosed with ASD will have ID (Shaw et al., 2021). The presence of ID and dysmorphic features are considered to account for a higher detection rate of genetic susceptibility factors contributing to ASD etiology (Tammimies et al., 2015; Husson et al., 2020). Likewise, finding genetic abnormalities may facilitate a better understanding of the pathophysiology of ASD, lead to early detection of cooccurring conditions and develop preventative guidance for children and families.

Here, we report the detection yields of the designed targeted sequencing panel (TSP) containing 568 ASD-related genes. ASD children were divided into subgroups according to clinical assessments, hoping to find the value of guidance for genetic testing and facilitate effective intervention based on pathological pathways inferred from the genetic information.

Materials and methods

Patients

The study included 160 patients who were diagnosed with ASD in the Department of Child Healthcare, Children's Hospital of Fudan University, from June 2017 to March 2019 for genetic testing. The inclusion criteria for the cases were as follows: children met the criteria of ASD diagnosed by experienced pediatricians according to the Diagnostic and Statistical Manual of Mental Disorders, fifth edition (DSM-V) (American Psychiatric Association, 2013). Patients were also recommended to complete the Autism Diagnostic Observation Schedule, second edition (ADOS-2) (Lord C et al., 2012). The results of the ADOS included two subdomains: social affect (SA) and restricted and repetitive behavior (RRB). The total raw score was converted into the ADOS calibrated severity score, from 1 (none) to 10 (severe). The Griffiths Mental Development Scales (GMDS) (Griffiths, 1984; Huntley, 1996) were also performed with the consent of ASD parents. The raw scores of the 5 subscales (Locomotor (Lm), Personal and Social (P/S), Hearing and Speech (H/Sp), Eye and Hand (E/Hd), and Performance (Pf)) of the GMDS were transformed into developmental quotients (DQ). A DQ lower than 70 was considered delayed. For the selected cases, additional medical information was recorded.

Targeted panel design

We selected 568 candidate genes in TSP as follows: genes marked from 1 to 4 in the ranking categories of the Gene-Scoring (2017) in SFARI Gene (https://gene.sfari.org/), genes predicted by the TADA model with a False discovery rate (FDR) value less than 0.3 (6, 17), and genes reported in large-scale studies (Vorstman et al., 2017; O'Roak et al., 2012; Wang et al., 2016). Genes were grouped and classified into 3 groups: "Group1-Definitive", 66 genes ranked 1 or 2 in SFARI Gene and their FDR value < 0.05; "Group2-Probably", 157 genes ranked 3 in SFARI Gene and their FDR value < 0.3 with more than one genetic study identified loss-of-function mutations that related to ASD; "Group3-Possible", 345 genes ranked 4 in SFARI Gene and their FDR value < 0.3 with no loss-of-function mutation founding that had possible relationship with ASD. There were 110 genes in TSP correlated with ID (from JuniorDoc Database, http://drwang. top/) and 51 genes correlated with epilepsy (from EpilepsyGene Database, http://www.wzgenomics.cn/EpilepsyGene/).

Targeted capture, sequencing, variants filtering and calling

Genomic DNA of participants was isolated from blood samples according to standard procedures by a QIAamp DNA Blood Midi Kit. Two hundred nanograms of genomic DNA from each individual was sheared by a Biorupter (Diagenode, Belgium) to acquire 150–200 bp fragments. The ends of the DNA fragments were repaired, and Illumina Adaptor was added (Fast Library Prep Kit, iGeneTech, Beijing, China). After the sequencing library was constructed, the whole exons were hybridized with costumed probes designed and synthesized by iGeneTech as mentioned above. Captured libraries were mixed in equal molar amounts and sequenced on an Illumina HiSeq2000 platform (Illumina, San Diego, CA) with 150 base paired-end reads. The average on-target sequencing rate was 98.7%, and the target bases covered at >=20X and >=10X were 97.7% and 97.6%, respectively. Raw reads were filtered to remove low-quality reads by using FastQC. Then, clean reads were mapped to the reference genome GRCh37/Hg19 by using BWA. After removing duplications, SNVs and InDels were called and annotated by using GATK. The variants were interpreted according to ACMG guidelines (Richards, et al. Genetics in Medicine (2015) 17, 405) and patient phenotypes and were classified as pathogenic (P), likely pathogenic (LP), variants of

TABLE 1 Clinical characteristics and the results of ADOS/GMDS of ASD patients in the cohort.

Variables	Number (%)	Summary
Age (months)		
Males[a]	125 (78.12%)	34.00 (27.00, 50.00)
Females[a]	35 (21.88%)	34.00 (27.00, 41.00)
ADOS-2	94 (58.75%)	
Score of SA[a]		17.00 (14.00, 19.00)
Score of RRB[a]		2.00 (1.00, 3.00)
Total Score[a]		7.00 (6.00, 8.00)
Calibrated Severity Score[a]		19.00 (16.00, 21.00)
GMDS	75 (46.88%)	
DQ of Lm[b]		70.76 ± 16.88
DQ of P/S[a]		52.00 (44.50, 68.75)
DQ of H/Sp[a]		38.00 (30.00, 56.50)
DQ of E/Hd[b]		59.80 ± 22.90
DQ of Pf[a]		63.00 (52.00, 84.50)
Total DQ[b]		60.44 ± 18.36

SD, standard deviation; **ADOS**, autism diagnostic observation schedule; **SA,** social affect; **RRB,** restricted repetitive patterns of behavior; **DQ,** developmental quotient; **GMDS,** griffiths mental development scales; **Lm,** Locomotor; **P/S,** personal and social; **H/Sp,** Hearing and Speech; **E/Hd,** Eye and Hand; **Pf**, Performance.
[a]Median (IQR).
[b]Means ± SD.

unknown significance (VUS), likely benign (LB) or benign (B). A CNV kit was used to call the large copy number variations (CNVs), and the default parameters were used. To identify CNVs, part of the sequencing library was sequenced directly, and each sample yielded 1G raw data. CNVs were called by using CNVseq, and the controls were the healthy parents. For the diagnostic SNVs of patients and parents, Sanger sequencing was used for variant confirmation. For diagnostic CNVs, qPCR/MLPA was performed.

Statistical analysis

Conventional descriptive statistical methods were used for presenting characteristics of the study cohort. We used unpaired t-test or Mann–Whitney *U* test depending on normality for the comparisons of ADOS scores and DQs of the GMDS in subgroups with positive and negative genetic findings in DD/ID subgroup. For categorical variables, the sex and subgroup differences of detection yields were compared by chi-squared tests. Data were presented as the mean ± standard deviation (SD) or medians and interquartile ranges (IQR) for continuous variables according to whether the data were normally distributed. Data were presented as percentages for categorical variables. Data analysis was performed using SPSS 22.0 (IBM, Armonk, NY, United States).

Results

Cohort description and detection yields

A total of 160 children who were diagnosed with ASD were included in the cohort (125 males and 35 females). The mean age of the patients was 3.24 ± 1.27 years. Ninety-four children completed the ADOS-2, and 75 children were assessed using the GMDS, with 71 children having both ADOS-2 and GMDS assessments (Table 1).

The overall detection yield of TSP was 51.3% (82/160) for analyzing both SNVs and CNVs, of which 57 were male and 25 were female. Although the number of males was higher than that of females, the detection rate of disease-associated variants in females (71.4%) was significantly higher than that in males (45.6%, $\chi 2 = 7.30$, $p = 0.007$). The "pathogenic/likely pathogenic (P/LP)" rate was 16.9% (27/160), including 16 males and 11 females. For SNVs, 73 children had positive results (24 females), accounting for a detection rate of 45.6%, of which "P" variants were found in 4.4% of cases (7/160), "LP" in 8.1% of cases (13/160), and "VUS" in 33.1% of cases (53/160). We identified a total of 90 SNVs, of which 74 were missense mutations, 5 were frameshift mutations, and 11 were splicing mutations. The most common variants were *DLGAP2, SHANK3,* and *KMT2A*, which were present in 3 probands for each variant. Of 73 patients with SNVs, 68 patients underwent parental testing (both father and mother), and 3 patients had variant confirmation only by mother. We found 11 cases carried *de novo* variants, including *ASXL3, KMT2A,* and *MECP2*, which accounted for 16.2% (11/68) of the analyzed trios. Of the other 74 variants, 42 were of maternal origin, and 30 were of paternal origin, with 2 variants of non-maternal origin (lack of paternal samples) (Table 2). CNVs were found in 13 patients (3 females), which accounted for 8.1% (13/160), whereas 4 children had dual SNV and CNV. The percentage of pathogenic CNVs was 15.4% (2/13), "LP" was 46.2% (6/13) and "VUS" was 38.5% (5/13). A total of 23.1% (3/13) were duplication variants, and 76.9% (10/13) were heterozygous deletions. 17p11.2 had the greatest number of reportable CNVs, accounting for 46.2% (6/13) (Table 3).

Comparison of language competence in children with and without genetic abnormalities in DD subgroup

Among 71 children, the average DQ of the GMDS was 61.26 ± 17.43, and the calibrated severity score of the ADOS-2 was 7.14 ± 1.45. The detection yield of these 71 children was 54.9% (39/71), with P/LP variants reached 19.7% (14/71). The detection rate of this subgroup was not statistically different from that of general ASD cohort ($\chi 2 = 0.77$, $p = 0.774$). There were 51 patients (71.8%, 51/71) with a total DQ under 70. In this subgroup of ASD children combined DD, 30 patients

TABLE 2 SNVs identified from TSP.

patient	Sex	Gene	Variant segregation	Position	Mutation	Inheritance pattern	Zygosity
P							
1	F	*MECP2*	*de novo*	ChrX: 153296806	NM_004992.3:exon4:c.473C>T:p.T158M	XL	Het
2	F	*MECP2*	*de novo*	ChrX: 153296362	NM_004992.3:exon4:c.917G>A:p.R306H	XL	Het
3	F	*PTEN* P)	maternal	Chr10:89720857	NM_000314.7:exon8:c.1008C>G:p.Y336X	AD	Het
		CUL9 (VUS)	—	Chr6:43154146	NM_015089.4:exon4:c.1204G>A:p.D402N	--	Het
		NRXN2 (VUS)	—	Chr11:64434827	NM_138732.3:exon8:c.1600C>A:p.L534I	--	Het
4	M	*ASXL3* P)	*de novo*	Chr18:31324172	NM_030632.3:exon12:c.4360C>T:p.Q1454X	AD	Het
		KMT2A (VUS)	paternal	Chr11: 118348825	NM_001197104.1:exon5:c.3478G>A: p.G1160S	AD	Het
5	M	*ASXL3*	*de novo*	Chr18:31324212	NM_030632:exon12:c.4400_4403dup: p.P1470Nfs*4	AD	Het
6	F	*SHANK3*	*de novo*	Chr22:51160241	NM_001372044.2:exon24:c.4209del:p.S1404fs	AD	Het
7	F	*TRIP12*	*de novo*	Chr2:230744795	NM_004238.3:exon2:c.1A>G:p.M1V	AD	Het
LP							
8	F	*CHD4*	not maternal	Chr12:6697033	NM_001273.5:exon24:c.3548G>A:p.R1183H	AD	Mosaic (25%)
9*	F	*CHD1* (LP)	paternal	Chr5:98228317	NM_001270.2:exon14:c.2092G>A:p.V698I	AD	Het
		CTNND2 (VUS)	maternal	Chr5:11411688	NM_001332.4:exon5:c.399A>C:p.E133D	--	Het
		DLGAP2 (VUS)	maternal	Chr8:1616837	NM_001346810.2:exon9:c.2153G>A:p.G718E	--	Het
10	F	*DDX53*	maternal	ChrX:23018700	NM_182699.4:exon1:c.530_549del:p.N177fs	--	Het
11	M	*TMLHE*	maternal	ChrX: 154741452	NM_018196.4:exon5:c.640G>T:p.E214X	XL	Hem
12	M	*KIRREL3*	maternal	Chr11: 126396583	NM_032531.4:intron2:c.134-1G>A	--	Het
13	M	*SCN8A* (LP)	paternal	Chr12: 52167979	NM_014191.4: exon20: c.3652G>T: p. E1218X	AD	Het
		FOXP2 (VUS)	paternal	Chr7:114284820	NM_014491.4: exon8: c.1070G>A: p.C357Y	AD	Het
14	M	*KIRREL3*	paternal	Chr11: 126310421	NM_032531.4:exon11:c.1276C>T:p.Q426X		Het
15	M	*KMT2A*	*de novo*	Chr11: 118392670	NM_001197104.1:exon36:c.11702A>C: p.H3901P	AD	Het
16	M	*NLGN4X* (LP)	*de novo*	ChrX:5821448	NM_020742.3:exon5:c.1271A>C:p.Y424S	Mu/XL	Het
		MAST1 (VUS)	maternal	Chr19:12949464	NM_014975.3: exon1: c.79_80del: p. K27fs	AD	Het
17	M	*KMT2A*	*de novo*	Chr11: 118392670	NM_001197104.1:exon36:c.11702A>C: p.H3901P	AD	Het
18	M	*KMT2C*	*de novo*	Chr7:151927409	NM_170606.3:intron16:c.2770-4dup	AD	Het
19	M	*SND1*	not maternal	Chr7:127724827	NM_014390.4:exon19:c.2168del:p.P723fs	--	Het
20	F	*GABRB3* (LP)	*de novo*	Chr15:26874148	NM_001191321.3:exon1:c.3G>A:p.M1I	AD	Het
		SLC4A8 (VUS)	maternal	Chr12:51847363	NM_001039960.3: exon5: c.454C>T: p.R152C	--	Het
VUS							
21*	M	*SCN3A*	paternal	Chr2:165946956	NM_006922.4:exon28:c.5707T>A:p.S1903T	AD	Het
22	F	*CNTNAP5*	maternal	Chr2:125262049	NM_130773.4:exon8:c.1240G>C:p.G414R	--	Het
23	F	*CDH8*	maternal	Chr16:61854979	NM_001796.5:exon6:c.874G>A:p.G292S	--	Het
24	F	*SLC6A4*	paternal	Chr17:28536176	NM_001045.6:exon12:c.1534G>C:p.V512L	AD	Het
25	F	*CNTNAP5*	paternal	Chr2:125669071	NM_130773.4:exon23:c.3680A>T:p.E1227V	--	Het
26	F	*USP15*	—	Chr12:62696710	NM_001252078.2:exon3:c.348 + 9T>C	--	Het
		CACNA1G	—	Chr17:48685339	NM_018896.5:exon25:c.4664G>A:p.R1555Q	AD	Het
27	F	*RERE*	maternal	Chr1:8418649	NM_012102.4:exon21:c.3946G>A:p.E1316K	AD	Het
28	M	*MYH10*	maternal	Chr17:8452042	NM_001256012.2:exon10:c.983C>T:p.P328L	--	Het
29	F	*RELN*	paternal	Chr7:103629592	NM_005045.4:exon1:c.212G>T:p.G71V	AD/AR	Het
30	F	*POLRMT*	paternal	Chr19:619653	NM_005035.4:exon13:c.2999G>C:p.G1000A	--	Het
		MYO9B	paternal	Chr19:17265185	NM_001130065.2:exon6:c.1159G>A:p.A387T	--	Het
31	F	*ADCY9*	—	Chr16:4029173	NM_001116.4:exon8:c.2623C>T:p.L875F	--	Het
32	F	*PHF10*	paternal	Chr6:170114835	NM_018288.4:exon7:c.797A>G:p.Y266C	--	Het
33	F	*AFF2*	paternal	ChrX: 148037716	NM_002025.4:exon11:c.2141A>C:p.D714A	XL	Het

(Continued on following page)

TABLE 2 (*Continued*) SNVs identified from TSP.

patient	Sex	Gene	Variant segregation	Position	Mutation	Inheritance pattern	Zygosity
34	F	*NR3C2*	maternal	Chr4:149035254	NM_000901.5:intron8:c.2799 + 1G>A	AD	Het
		SLC6A8	paternal	ChrX: 152955824	NM_005629.4:exon2:c.263–6C>T	XL	Het
35	M	*ARVCF*	paternal	Chr22:19965558	NM_001670.3:exon8:c.1621C>T:p.R541W	--	Het
		DAAM2	maternal	Chr6:39832252	NM_001201427.2:exon4:c.302A>G:p.Y101C	--	Het
36	M	*NINL*	maternal	Chr20:25450631	NM_025176.6:exon18:c.3349C>T:p.Q1117X	--	Het
37	M	*DLGAP2*	maternal	Chr8:1513907	NM_001346810.2:exon6:c.1289G>T:p.C430F	--	Het
38	M	*TRPM5*	maternal	Chr11:2436135	NM_014555.3:exon10:c.1620 + 2T>C	--	Het
39	M	*KMT2C*	maternal	Chr7:151851399	NM_170606.3:exon47:c.12092C>G:p.P4031R	AD	Het
40	M	*DDX3X*	maternal	ChrX:41196733	NM_001193416.3:intron2:c.103 + 15T>C	XL	Hem
41	M	*NSD1*	maternal	Chr5:176707762	NM_022455.4:exon18:c.5819A>C:p.Q1940P	AD	Het
42	M	*PRODH*	maternal	Chr22:18900719	NM_016335.5:exon15:c.1772G>C:p.R591P	AD/AR	Het
		PRODH	paternal	Chr22:18908862	NM_016335.5:exon9:c.1004A>G:p.N335S	AD/AR	Het
43	M	*AGO1*	paternal	Chr1:36358887	NM_012199.5:intron4:c.512 + 8G>A	--	Het
44	M	*TNRC6B*	paternal	Chr22:40662956	NM_001162501.2:exon5:c.2722A>T:p.N908Y	AD	Het
45	M	*SHANK3*	maternal	Chr22:51137156	NM_033517.1:exon12:c.1495G>A:p.V499M	AD	Het
46	M	*CHD7*	maternal	Chr8:61734352	NM_017780.4:exon10:c.2701G>A:p.V901M	AD	Het
47	M	*NRXN3*	paternal	Chr14:79432509	NM_004796.6:exon9:c.1418T>A:p.I473N	--	Het
48	M	*CHD8*	maternal	Chr14:21871792	NM_001170629.2:exon17:c.3338G>A: p.R1113H	AD	Het
49	M	*PTPRM*	maternal	Chr18:7926611	NM_001105244.1:exon5:c.593C>G:p.A198G	--	Het
50	M	*NRXN2*	maternal	Chr11:64453401	NM_138732.3:exon5:c.797C>T:p.A266V	--	Het
51	M	*CACNA1H*	maternal	Chr16:1257363	NM_021098.3:exon14:c.2996T>C:p.M999T	AD	Het
52	M	*SOX5*	maternal	Chr12:23908608	NM_006940.6:exon4:c.532C>T:p.L178F	AD	Het
53	M	*SHANK3*	maternal	Chr22:51159239	NM_033517.1:exon21:c.2936G>T:p.R979L	AD	Het
54	M	*NRXN1*	maternal	Chr2:50149270	NM_001135659.2:exon24:c.4456C>A: p.L1486I	AR	Het
		NRXN1	paternal	Chr2:50280420	NM_001135659.2:exon22:c.4237C>T: p.P1413S	AR	Het
		SCN8A	paternal	Chr12:52159495	NM_014191.4:exon16:c.2585A>G:p.N862S	AD	Het
55	M	*SCN2A*	paternal	Chr2:166210993	NM_021007.3:exon17:c.3211G>A:p.G1071R	AD	Het
56	M	*SOS1*	paternal	Chr2:39213067	NM_005633.3:exon23:c.3900A>T:p.Q1300H	AD	Het
57	M	*DDX3X*	maternal	ChrX:41205889	NM_001193416.3:intron14:c.1615 + 14T>C	XL	Hem
58*	M	*ASH1L*	paternal	Chr1:155491209	NM_018489.3:exon2:c.102G>C:p.K34N	AD	Het
59	M	*EP400*	maternal	Chr12: 132446252	NM_015409.5:exon2:c.1088A>C:p.Q363P	AD	Het
60	M	*EPB41L3*	maternal	Chr18:5478269	NM_012307.4:exon3:c.352G>C:p.D118H	--	Het
61	M	*SIN3A*	maternal	Chr15:75688840	NM_001145358.2:intron13:c.1855–3C>G	AD	Het
62	M	*RELN*	paternal	Chr7:103143520	NM_005045.4:exon52:c.8432T>C:p.F2811S	AD/AR	Het
63*	M	*DPP6*	maternal	Chr7:154561214	NM_001936.5:exon9:c.785C>G:p.P262R	AD	Het
		LZTR1	paternal	Chr22:21342407	NM_006767.4:exon5:c.509G>A:p.R170Q	AD/AR	Het
64	M	*SCN3A*	maternal	Chr2:166011041	NM_006922.4:exon11:c.1301C>A:p.T434N	AD	Het
65	M	*SEMA5A*	paternal	Chr5:9108299	NM_003966.3:exon16:c.2026C>T:p.R676C	--	Het
66	M	*SLC6A8*	maternal	ChrX: 152959811	NM_005629.4:exon10:c.1405G>C:p.V469L	XL	Hem
67	M	*SKI*	paternal	Chr1:2237536	NM_003036.4:exon6:c.1845G>T:p.E615D	AD	Het
68	M	*SCN1A*	maternal	Chr2:166912967	NM_001165963.3:exon6:c.427G>A:p.V143M	AD	Het
69	M	*SOS1*	paternal	Chr2:39285930	NM_005633.3:exon3:c.229A>T:p.S77C	AD	Het
70	M	*DLGAP2*	maternal	Chr8:1496851	NM_001346810.2:exon5:c.232C>T:p.P78S	--	Het
71	F	*CHD8*	maternal	Chr14:21894278	NM_001170629.2:exon5:c.1716 + 9A>T	AD	Het
72	M	*LRRC1*	maternal	Chr6:53767467	NM_018214.5:exon9:c.828T>A:p.N276K	--	Het
73	F	*EP400*	paternal	Chr12: 132446354	NM_015409.5:exon2:c.1190A>G:p.Q397R	--	Het
		SRCAP	maternal	Chr16:30735196	NM_006662.3:exon25:c.4451T>A:p.V1484D	AD	Het

SNV, single nucleotide variations; **P,** pathogenic**; LP,** likely pathogenic**; VUS,** variants of unknown significance; **M**, male; **F**, female; **AD**, autosomal dominant; **AR**, autosomal recessive; **XL**, X-linked; **Het**, heterozygous; **Hem**, Hemizygous. *, patients with both SNVs, and CNVs.

had positive genetic variants (58.8%, 30/51), with P/LP rate reaching 21.6% (11/51). Children with genetic abnormalities had lower language competence than children without positive genetic findings (Z = -2.20, p = 0.028). There were no correlations between ASD symptoms and the detection of genetic abnormalities in this DD subgroup (Table 4).

TABLE 3 CNVs in ASD patients from TSP.

patient	Sex	Chromosome location	Position	Size	Deletion/duplication
P					
1	F	15q13.3	chr15:29346088–32460659	3.11 Mb	deletion
2	M	22q13.3	chr22:49895953–51135096	1.24 Mb	deletion
LP					
3	M	17q11.2	chr17:29483001–29687721	204.72 Kb	deletion
4	M	17q11.2	chr17:29483001–29687721	204.72 Kb	deletion
5	M	Xp11.2	chrX:47435744–47473973	38.23 Kb	deletion
6	F	6q27	chr6:164539952–170155049	5.62 Mb	deletion
7	M	17q11.2	chr17:29483001–29657516	174.52 Kb	deletion
8*	F	17q11.2	chr17:29483001–29665823	182.82 Kb	deletion
VUS					
9*	M	8q22.2	chr8:100844597–100887894	43.3 Kb	duplication
10	M	7q36.1	chr7:151833917–151960215	126.3 Kb	duplication
11*	M	22q11.2	chr22:19168244–19263353	95.11 Kb	duplication
12	M	17q11.2	chr17:29483001–29664600	181.6 Kb	deletion
13*	M	17q11.2	chr17:29483001–29687721	204.72 Kb	deletion

*: patients with both SNV and CNV (patient 8, 9, 11, 13 were patient 9,21, 58 and 63 in Table 2); **CNV,** copy number variations; **P,** pathogenic**; LP,** likely pathogenic**; VUS,** variants of unknown significance**; M**, Male; **F**, Female.

De novo variants of *ASXL3* in two patients

Patient 4 and Patient 5 had *de novo* variants of *ASXL3* (Figure 1). Patient 4 was referred to our clinic at 19 months for delayed development. He had poor eye contact as well as response to names. Repetitive behaviors included stamping and shanking head/hands. Tracing the developmental milestones, the patient was unable to crawl and pull up to stand at that time and he learned to sit without support until the age of 10 months. He could only make repeated single-syllable sounds. His birthweight was normal, but feeding seemed very difficult in the early stage, resulting in poor postnatal growth (2 SD below the mean). Physical examination showed that he had a prominent forehead, wildly spaced eyes, strabismus and malformation of external auditory canals. When he had reexamination at 6 years old, he still had language delay. An oral examination revealed that he had dental overcrowding. The Wechsler Preschool and Primary Scale of Intelligence (WPPSI) (Wechsler, 2012) showed that his intelligence quotient (IQ) was 69. Patient 5 was a 2.7-year-old boy. He displayed repetitive behaviors such as throwing and biting objects, turning the wheels and sometimes squinting. He had obvious delayed speech and language development because he was non-verbal at the time of referral. Feeding difficulty also happened to him. Walking independently was at the age of 20 months. His total DQ of the GMDS was 55.2 (the DQs of all the subscales were less than 70). Facial dysmorphism was prominent forehead but there was no obvious deformity in other parts. He had febrile convulsions twice, while electroencephalogram (EEG) and magnetic resonance imaging (MRI) were normal. Two patients shared the common characteristics of *ASXL3* variants, but they had only mild ID/DD, which was noteworthy.

Discussion

In this study, we investigated the detection yields and novel variants through TSP of 568 ASD-associated genes in an ASD cohort. The detection yield was 51.3% in TSP, with the rate of "P/LP" reaching 16.9%. With the falling costs of sequencing, more patients with neurodevelopmental disorders are allowed to receive genetic testing whose positive results give them better access to new treatments. CMA was considered the appropriate initial test for the etiologic evaluation of ASD children (Hyman et al., 2020). There is increasing evidence that NGS, whole-exome sequencing (WES) and whole-genome sequencing (WGS) offer diagnostic advantages over CMA (22). Sirvstava et al.'s review (Srivastava et al., 2019) revealed a yield in the range of 30%–40% for exome sequencing, which exceeds the 10%–20% yield for CMA. Feliciano et al. (2019) conducted WES in 457 ASD families with genetic identification in 15.2% multiplex families and 10.1% simplex families. According to Ghralaigh's study (Ni Ghralaigh et al., 2020), the diagnostic yield in ASD was 31% using WES and 42.4% using WGS, but the cost estimates were €79.33 and €1239.5 for choosing different technologies. For panel sequencing, a meta-analysis by Stefanski et al. (2021) showed that the identification of genetic defects accounted for 22.6%, compared to 27.2% for WES. Speak frankly, WES and WGS have higher diagnostic yields of ASD than panel sequencing; however, the benefits do not outweigh their drawbacks. WES and WGS offer higher costs than panel sequencing; on the other hand, due to the larger amount of data, more time is required for analysis and processing. Therefore, an affordable sequencing panel that can capture relevant genes may be a good compromise. It can not only achieve molecular diagnosis and detection efficiency in less cost and time but also avoid the waste of resources. The most important factor in ASD families' decision about genetic testing is cost. Sequencing panel is still the most cost-effective choice. Ghralaigh et al.'s report (Ni Ghralaigh et al., 2022) demonstrated 0.22%–10.02% diagnostic yields of gene panels to derive the conclusion that gene panels marketed for use in ASD are currently of limited clinical utility. However, gene selection and numbers for inclusion of gene panels are the key factors for results. A well-defined/comprehensive gene set is required in gene panels. We selected genes with the most promising diagnostic purpose of ASD. The most frequent variants in our cohort were *SHANK3, KMT2A,* and

TABLE 4 Comparison of ASD symptoms and developmental scores between children with positive and negative genetic variants in DD/ID subgroup.

	Genetic findings		$\chi 2$/t/Z	*p*-value
	Positive (n = 30)	Negative (n = 21)		
Sex[a]			2.71	0.100
Male (%)	22 (43.1%)	20 (39.2%)		
Female (%)	8 (15.7%)	1 (2.0%)		
Age[b]	41.50 (27.00, 53.00)	40.00 (28.00, 59.00)	0.15	0.878
ADOS				
Score of SA[b]	17.50 (16.00, 19.00)	17.00 (13.00, 18.00)	1.40	0.162
Score of RRB[b]	2.50 (1.00, 3.00)	2.00 (1.00, 4.00)	0.15	0.878
Total score[b]	7.00 (6.25, 8.00)	7.00 (6.00, 8.00)	0.81	0.419
Calibrated severity score[b]	20.00 (17.00, 21.00)	18.00 (15.00, 22.00)	0.88	0.377
GMDS				
DQ of Lm[c]	63.83 ± 13.32	69.10 ± 8.64	1.59	0.118
DQ of P/S[c]	47.27 ± 14.52	54.43 ± 13.76	1.77	0.083
DQ of H/Sp[b]	30.50 (23.00, 40.25)	35.00 (32.00, 48.00)	2.20	**0.028**[d]
DQ of E/Hd[c]	49.33 ± 16.39	54.95 ± 10.24	1.39	0.139
DQ of Pf[b]	61.00 (40.25, 66.75)	56.00 (49.00, 60.00)	0.55	0.585
Total DQ[c]	51.33 ± 13.44	55.59 ± 7.52	1.31	0.155

DD/ID, developmental delay/intellectual disability; **ADOS**, autism diagnostic observation schedule; **SA, s**ocial affect; **RRB,** restricted repetitive patterns of behavior; **GMDS,** griffiths mental development scales; **Lm,** Locomotor; **P/S,** personal and social; **H/Sp,** Hearing and Speech; **E/Hd,** Eye and Hand; **Pf**, Performance; **DQ**, developmental quotient.

[a]Categorical variables were compared with a Chi-square test.

[b]The differences of skewed distributed continuous variables (shown as medians and interquartile ranges) are tested by the Mann-Whitney U tests.

[c]The differences of normally distributed continuous variables (shown as means ± SD) are tested by unpaired t tests.

[d]$p < 0.05$.

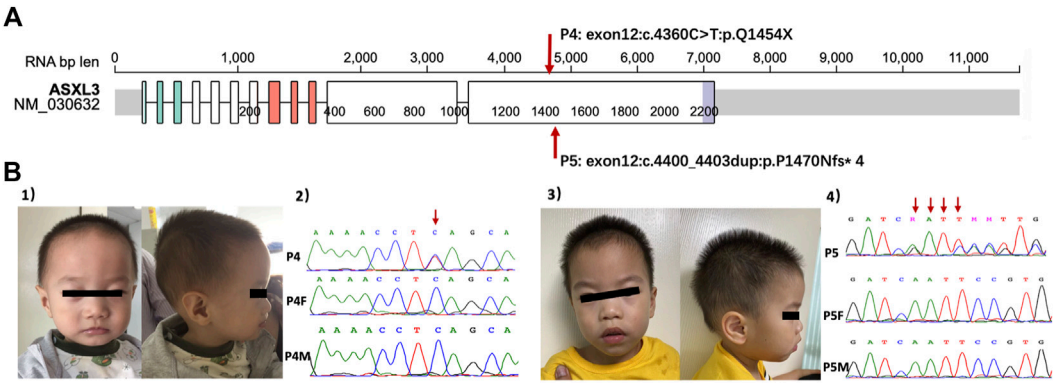

FIGURE 1
(A) The location of *ASXL3* variants in patients based on Protein Paint (https://proteinpaint.stjude.org, access in September 29th). The numbers of patients correspond with Table 2. **(B) (1)** The facial features of P4. **(2)** Sanger sequence of P4 and his parents with *ASXL3* genetic locus. The red arrow showed the mutation stie of P4. **(3)** The facial features of P5. **(4)** Sanger sequence of P5 and his parents with *ASXL3* genetic locus. The red arrows showed the duplication sties of P5. P4, patient 4; P4F, father of patient 4; P4M, mother of patient 4; P5, patient 5; P5F, father of patient 5; P5M, mother of patient 5.

DLGAP2, which was a slightly different from the previous ASD cohort studies (Satterstrom et al., 2020; Fu et al., 2022). ASD frequent genes like *SCN2A, CHD8, PTEN* and so on were identified in our cohort whereas we did not find *SYNGAP1, ADNP* variants according to our sample size. For 72 genes associated with ASD at FDR value <=0.001 in Fu et al.' s study (Fu et al., 2022), we have 51genes overlapped in our panel. Of identified 102 risk gene in Satterstrom's study (Satterstrom et al., 2020), 66 of them overlapped with our TSP. Our designed TSP including most of the ASD frequent genes and whose detection yield reached 51.3%, is specialized for ASD patients, and can be considered a success for panel sequencing and potential for the clinical utility of ASD.

Although the reported prevalence sex ratio is four times higher in males than in females (Brugha et al., 2016), we observed that the detection rate of genetic variants was 1.5 times higher in females than males. Sex differences were also observed in other genetic studies (De Rubeis et al., 2014; Satterstrom et al., 2020). The possible reasons were that cognitive defects and autistic traits in females are less severe than those in males. Conversely, females may need clearer autistic characteristics and comorbid DD/ID to receive a diagnosis of ASD.

It is believed that sex differences are consistent with the female protective effect model, which assumes that women need an increased genetic load to reach the threshold for ASD diagnosis (Werling, 2016). Thus, more prominent phenotypes demonstrate a higher risk for genetic variants in females than males with ASD.

Language plays a major part in the outcomes of ASD. ASD children whose language is impaired, could have a large impact on the social interaction and general wellbeing of individuals (Nudel et al., 2021). Improvements in the language of ASD children before 5 years old may result in catching up to overall average levels in developmental trajectories, whereas the remainders may develop ID (Pickles et al., 2014). Furthermore, patients who have lower cognitive abilities are more likely to obtain an identifiable genetic risk variant than those with a higher IQ (Sanders et al., 2015). Interestingly, our results showed that in the subgroup of ASD children with DD, children with genetic variants had lower language competence. In other words, children with lower language competence had a greater chance of finding genetic variants. Nudel et al. (2021) considered it as pleiotropy between language impairment and ASD. They observed a significant genetic overlap between specific language impairment and childhood autism (which excluded Asperger's syndrome). Another hypothesis is that children with genetic conditions are more likely to display delays in early developmental milestones, especially in language and motor functions. Compared with idiopathic ASD, children with *PPP2R5D, ADNP*, *ASXL3, DYRK1A, MED13L* variants and so on were marked by extensive delays, 2.7 times for single words and 5.7 times for combined words (Wickstrom et al., 2021). Thus, ASD children with DD or ID, especially those with lower language competence, are recommended for genetic testing.

In our subjects, 2 patients had *de novo AXSL3* variants. It is a transcriptional regulator that belongs to a group of vertebrate asx-like proteins. The *ASXL3* gene is highly expressed in the cerebral cortex as an epigenetic regulator that plays a role in regulating and controlling gene expression through chromatin remodeling (Katoh and Katoh, 2004; Katoh, 2015). Most *ASXL3* variants are *de novo*, placing it among the top 10 neurodevelopmental genes with the highest frequency of *de novo* variants (Wright et al., 2015). The characteristics of *ASXL3*-related syndrome (also called Bainbridge-Ropers syndrome) are DD/ID (moderate to severe), language impairment or absent speech, hypotonia and dysmorphic facial features. Our patients had typical phenotypic characteristics, such as feeding difficulties and delayed motor and language abilities. However, they had only mild developmental delay with IQ/DQ higher than 55, and no obvious signs of hypotonia or epilepsy compared with other patients with *ASXL3* variants (Katoh and Katoh, 2004; Katoh, 2015). Although most *ASXL3*-related syndromes rely on molecular confirmation, many individuals with pathogenic variants of *ASXL3* can be identified by a combination of clinical symptoms and unique phenotypes and do not omit those with mild developmental delays.

Conclusion

Our work shows the utility of TSP, which has lower cost and more efficient genetic diagnosis and confirms the effectiveness of the test strategy. TSP should be offered to ASD patients in the expectation of preventative guidance and early detection of comorbidities. Subtypes of ASD children, especially those with language deficits, are recommended for testing to help families develop better intervention strategies.

Data availability statement

The data presented in the study are deposited in the GSA-Human repository, accession number HRA003901.

Ethics statement

The studies involving human participants were reviewed and approved by Ethics Committee of the Children's Hospital of Fudan University. Written informed consent to participate in this study was provided by the participants and legal guardian/next of kin. Written informed consent was obtained from the individual(s), and minor(s)' legal guardian/next of kin, for the publication of any potentially identifiable images or data included in this article.

Author contributions

QX, XX, YL, YW, and CH designed the study. CH, CL, YW, BZ, DL, HL, QX, and XX collected the study samples. YW, LM performed the sequencing experiments. QX, CH, and YW analyzed the data. CH drafted the manuscript, and XX and XQ modified the manuscript. All authors have agreed to the published version of the manuscript.

Funding

This study was supported in part by the National Natural Science Foundation of China (2021NSFC, 82171540), the National Key Research and Development Program of China (No. 2016YFC1306205), and the Key Subject Construction Project of Shanghai Municipal Health Commission (shslczdzk02903).

Acknowledgments

We thank children and their families from the Department of Child Healthcare, Children's Hospital of Fudan University for participation. We thank Xia Wang and Yaping Yang from Ailife Diagnostics (United States) for their help. We also thank Yonghui Jiang from Yale university for his comments.

Conflict of interest

The authors declare that the research was conducted in the absence of any commercial or financial relationships that could be construed as a potential conflict of interest.

Publisher's note

References

American Psychiatric Association (2013). *Diagnostic and statistical manual of mental disorders*. 5th ed. Washington, DC: American Psychiatric Association.

Brugha, T. S., Spiers, N., Bankart, J., Cooper, S. A., McManus, S., Scott, F. J., et al. (2016). Epidemiology of autism in adults across age groups and ability levels. *Br. J. Psychiatry* 209 (6), 498–503. doi:10.1192/bjp.bp.115.174649

De Rubeis, S., He, X., Goldberg, A. P., Poultney, C. S., Samocha, K., Cicek, A. E., et al. (2014). Synaptic, transcriptional and chromatin genes disrupted in autism. *Nature* 515 (7526), 209–215. doi:10.1038/nature13772

Feliciano, P., Zhou, X., Astrovskaya, I., Turner, T. N., Wang, T., Brueggeman, L., et al. (2019). Exome sequencing of 457 autism families recruited online provides evidence for autism risk genes. *NPJ Genom Med.* 4, 19. doi:10.1038/s41525-019-0093-8

Fu, J. M., Satterstrom, F. K., Peng, M., Brand, H., Collins, R. L., Dong, S., et al. (2022). Rare coding variation provides insight into the genetic architecture and phenotypic context of autism. *Nat. Genet.* 54, 1320–1331. doi:10.1038/s41588-022-01104-0

Griffiths, R. (1984). *The abilities of young children. High Wycombe*. UK: The Test Agency Ltd.

He, X., Sanders, S. J., Liu, L., De Rubeis, S., Lim, E. T., Sutcliffe, J. S., et al. (2013). Integrated model of de novo and inherited genetic variants yields greater power to identify risk genes. *PLoS Genet.* 9 (8), e1003671. doi:10.1371/journal.pgen.1003671

Huntley, M. (1996). *The Griffiths mental developmental scales manual from birth to two years*. Oxford, UK: The Test Agency.

Husson, T., Lecoquierre, F., Cassinari, K., Charbonnier, C., Quenez, O., Goldenberg, A., et al. (2020). Rare genetic susceptibility variants assessment in autism spectrum disorder: Detection rate and practical use. *Transl. Psychiatry* 10 (1), 77. doi:10.1038/s41398-020-0760-7

Hyman, S. L., Levy, S. E., and Myers, S. M. (2020). Executive summary: Identification, evaluation, and management of children with autism spectrum disorder. *Pediatrics* 145 (1), e20193448. doi:10.1542/peds.2019-3448

Iossifov, I., O'Roak, B. J., Sanders, S. J., Ronemus, M., Krumm, N., Levy, D., et al. (2014). The contribution of de novo coding mutations to autism spectrum disorder. *Nature* 515 (7526), 216–221. doi:10.1038/nature13908

Katoh, M. (2015). Functional proteomics of the epigenetic regulators ASXL1, ASXL2 and ASXL3: A convergence of proteomics and epigenetics for translational medicine. *Expert Rev. Proteomics* 12 (3), 317–328. doi:10.1586/14789450.2015.1033409

Katoh, M., and Katoh, M. (2004). Identification and characterization of ASXL3 gene *in silico*. *Int. J. Oncol.* 24 (6), 1617–1622.

Lord, C., Brugha, T. S., Charman, T., Cusack, J., Dumas, G., Frazier, T., et al. (2020). Autism spectrum disorder. *Nat. Rev. Dis. Prim.* 6 (1), 5. doi:10.1038/s41572-019-0138-4

Lord C, M., Rutter, P. D., Labore, S., Risi, K., Gotham, S., and Bishop, S. L. (2012). *Autism diagnostic observation schedule*. second edition. Los Angeles, CA: Western Pschological Services. ADOS-2.

Miller, D. T., Adam, M. P., Aradhya, S., Biesecker, L. G., Brothman, A. R., Carter, N. P., et al. (2010). Consensus statement: Chromosomal microarray is a first-tier clinical diagnostic test for individuals with developmental disabilities or congenital anomalies. *Am. J. Hum. Genet.* 86 (5), 749–764. doi:10.1016/j.ajhg.2010.04.006

Ni Ghralaigh, F., Gallagher, L., and Lopez, L. M. (2020). Autism spectrum disorder genomics: The progress and potential of genomic technologies. *Genomics* 112 (6), 5136–5142. doi:10.1016/j.ygeno.2020.09.022

Ni Ghralaigh, F., McCarthy, E., Murphy, D. N., Gallagher, L., and Lopez, L. M. (2022). Brief report: Evaluating the diagnostic yield of commercial gene panels in autism. *J. Autism Dev. Disord* [Epub ahead of print]. doi:10.1007/s10803-021-05417-7

Nudel, R., Appadurai, V., Buil, A., Nordentoft, M., and Werge, T. (2021). Pleiotropy between language impairment and broader behavioral disorders-an investigation of both common and rare genetic variants. *J. Neurodev. Disord.* 13 (1), 54. doi:10.1186/s11689-021-09403-z

O'Roak, B. J., Vives, L., Fu, W., Egertson, J. D., Stanaway, I. B., Phelps, I. G., et al. (2012). Multiplex targeted sequencing identifies recurrently mutated genes in autism spectrum disorders. *Science* 338 (6114), 1619–1622. doi:10.1126/science.1227764

Pickles, A., Anderson, D. K., and Lord, C. (2014). Heterogeneity and plasticity in the development of language: A 17-year follow-up of children referred early for possible autism. *J. Child. Psychol. Psychiatry* 55 (12), 1354–1362. doi:10.1111/jcpp.12269

Sanders, S. J., He, X., Willsey, A. J., Ercan-Sencicek, A. G., Samocha, K. E., Cicek, A. E., et al. (2015). Insights into autism spectrum disorder genomic architecture and biology from 71 risk loci. *Neuron* 87 (6), 1215–1233. doi:10.1016/j.neuron.2015.09.016

Satterstrom, F. K., Kosmicki, J. A., Wang, J., Breen, M. S., De Rubeis, S., An, J. Y., et al. (2020). Large-scale exome sequencing study implicates both developmental and functional changes in the neurobiology of autism. *Cell* 180 (3), 568–584. doi:10.1016/j.cell.2019.12.036

Shaw, K. A., Maenner, M. J., Bakian, A. V., Bilder, D. A., Durkin, M. S., Furnier, S. M., et al. (2021). Early identification of autism spectrum disorder among children aged 4 Years - autism and developmental disabilities monitoring network, 11 sites, United States, 2018. *MMWR Surveill. Summ.* 70 (10), 1–14. doi:10.15585/mmwr.ss7010a1

Srivastava, S., Love-Nichols, J. A., Dies, K. A., Ledbetter, D. H., Martin, C. L., Chung, W. K., et al. (2019). Meta-analysis and multidisciplinary consensus statement: Exome sequencing is a first-tier clinical diagnostic test for individuals with neurodevelopmental disorders. *Genet. Med.* 21 (11), 2413–2421. doi:10.1038/s41436-019-0554-6

Stefanski, A., Calle-Lopez, Y., Leu, C., Perez-Palma, E., Pestana-Knight, E., and Lal, D. (2021). Clinical sequencing yield in epilepsy, autism spectrum disorder, and intellectual disability: A systematic review and meta-analysis. *Epilepsia* 62 (1), 143–151. doi:10.1111/epi.16755

Tammimies, K., Marshall, C. R., Walker, S., Kaur, G., Thiruvahindrapuram, B., Lionel, A. C., et al. (2015). Molecular diagnostic yield of chromosomal microarray analysis and whole-exome sequencing in children with autism spectrum disorder. *JAMA* 314 (9), 895–903. doi:10.1001/jama.2015.10078

Vorstman, J. A. S., Parr, J. R., Moreno-De-Luca, D., Anney, R. J. L., Nurnberger, J. I., Jr., and Hallmayer, J. F. (2017). Autism genetics: Opportunities and challenges for clinical translation. *Nat. Rev. Genet.* 18 (6), 362–376. doi:10.1038/nrg.2017.4

Wang, T., Guo, H., Xiong, B., Stessman, H. A., Wu, H., Coe, B. P., et al. (2016). De novo genic mutations among a Chinese autism spectrum disorder cohort. *Nat. Commun.* 7, 13316. doi:10.1038/ncomms13316

Wechsler, D. (2012). *Wechsler Preschool and primary scale of intelligence*. Fourth Edition. San Antonio, TX: The Psychological Corporation.

Werling, D. M. (2016). The role of sex-differential biology in risk for autism spectrum disorder. *Biol. Sex. Differ.* 7, 58. doi:10.1186/s13293-016-0112-8

Wickstrom, J., Farmer, C., Green Snyder, L., Mitz, A. R., Sanders, S. J., Bishop, S., et al. (2021). Patterns of delay in early gross motor and expressive language milestone attainment in probands with genetic conditions versus idiopathic ASD from SFARI registries. *J. Child. Psychol. Psychiatry* 62 (11), 1297–1307. doi:10.1111/jcpp.13492

Wright, C. F., Fitzgerald, T. W., Jones, W. D., Clayton, S., McRae, J. F., van Kogelenberg, M., et al. (2015). Genetic diagnosis of developmental disorders in the DDD study: A scalable analysis of genome-wide research data. *Lancet* 385 (9975), 1305–1314. doi:10.1016/S0140-6736(14)61705-0

Zhou, X., Feliciano, P., Shu, C., Wang, T., Astrovskaya, I., Hall, J. B., et al. (2022). Integrating de novo and inherited variants in 42, 607 autism cases identifies mutations in new moderate-risk genes. *Nat. Genet.* 54, 1305–1319. doi:10.1038/s41588-022-01148-2

Frontiers in Genetics

Highlights genetic and genomic inquiry relating to all domains of life

The most cited genetics and heredity journal, which advances our understanding of genes from humans to plants and other model organisms. It highlights developments in the function and variability of the genome, and the use of genomic tools.

Discover the latest Research Topics

See more →

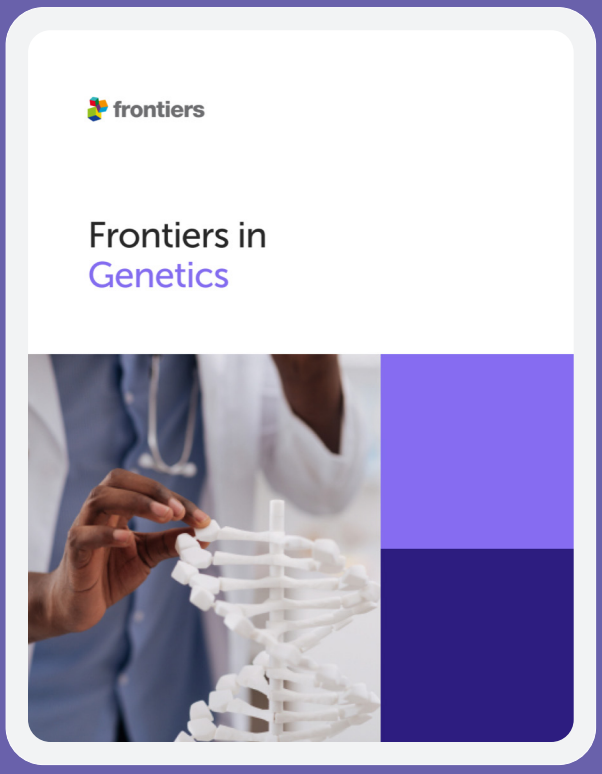

Frontiers

Avenue du Tribunal-Fédéral 34
1005 Lausanne, Switzerland
frontiersin.org

Contact us

+41 (0)21 510 17 00
frontiersin.org/about/contact